

Ph.D. Thesis

*REFLECTION AND RADIATION OF
CAPILLARY-GRAVITY WATER WAVES*

Thesis Submitted For The Degree Of Doctor Of Philosophy

DELJOO MAHDMINA

Department Of Mathematics

University College London

1991

ProQuest Number: 10797685

All rights reserved

INFORMATION TO ALL USERS

The quality of this reproduction is dependent upon the quality of the copy submitted.

In the unlikely event that the author did not send a complete manuscript and there are missing pages, these will be noted. Also, if material had to be removed, a note will indicate the deletion.



ProQuest 10797685

Published by ProQuest LLC (2018). Copyright of the Dissertation is held by the Author.

All rights reserved.

This work is protected against unauthorized copying under Title 17, United States Code
Microform Edition © ProQuest LLC.

ProQuest LLC.
789 East Eisenhower Parkway
P.O. Box 1346
Ann Arbor, MI 48106 – 1346

ABSTRACT

The necessary edge condition, which is used here, includes both dynamic variation of the contact angle and contact angle hysteresis. It is given by making the slope of the free surface at contact proportional to its velocity, however, viscosity has been ignored throughout.

Six problems are studied. The first one is the damping of capillary-gravity waves inside a vertical and axisymmetric cylinder, where the frequency of these waves are calculated.

The second problem is concerned with the study of the waves produced by a vertically oscillating cylinder, and determining the surface elevation, at both on and large distances away from the cylinder.

The third problem is the horizontal oscillation of a cylinder partially immersed in the fluid, such that the cylinder and the fluid are both of infinite or finite depth, where again the surface elevation from the free surface at large distances and on the edge of the cylinder are evaluated.

The fourth problem studies the scattering of a capillary-gravity wave by a surface-piercing circular cylinder, and the depending condition applied at the contact line between the fluid and the obstacle. Using a model for this condition that incorporates the effect of dynamic contact-angle variation, the wave field close to the obstacle and at large distances away are determined.

The fifth problem studied, concerns the vertical and horizontal oscillation of a vertical cylinder, as well as the scattering of waves made by it, in shallow water. When the depth of the fluid is small compared with the

wavelength, the simplifications of shallow-water theory can be applied and the results arrived at more readily than by the methods used for arbitrary depths. In each case, the surface elevation of the radiated waves at large distances away from the cylinder is obtained, as well as some special cases (when some of the parameters have extreme values).

The sixth problem studied is the waves produced by a vertical plate, when it is forced to oscillate horizontally. The length of the plate is considered to be finite and the fluid is either of infinite depth or of the same depth as the length of the plate. Both the steady-state and the transient motion are studied. However, when the depth of the fluid is small, the simplifications of shallow-water theory can be applied. The surface elevation at large distances away and the amplitude of these waves are calculated for the cases of vertically moving boundary and for the reflection of an incident wave.

CONTENTS

Abstract	2
Acknowledgements	8

CHAPTER I INTRODUCTION

1.1 - Surface Waves	9
1.2 - Present Work	13

CHAPTER II NON-DIMENSIONALIZATION AND FORMULATION

2.1 - Introduction	16
2.2 - Cylinders	18
2.3 - Plates	21

CHAPTER III DAMPING OF WAVES AT CYLINDRICAL BOUNDARIES

3.1 - Introduction	25
3.2 - Three-dimensional Standing Waves	28
3.3 - Axisymmetric Waves	34
3.4 - Numerical Approach	34
Figures	37

CHAPTER IV VERTICALLY OSCILLATING CYLINDERS

4.1 - Introduction	39
4.2 - Surface Elevation	40
4.3 - Away From The Cylinder	44
4.4 - On The Cylinder	47

4.5 - Numerical Approach	48
Figures	50

CHAPTER V

WAVES PRODUCED BY HORIZONTAL OSCILLATION OF A CYLINDER

5.1 - Introduction	56
5.2 - Surface Elevation	57
5.3 - Finite Depth	59
5.4 - Infinite Depth	63
5.5 - Surface Elevation On The Cylinder	65
5.6 - Numerical Approach	66
Figures	69

CHAPTER VI

SCATTERING OF WAVES BY A VERTICAL CYLINDER

6.1 - Introduction	85
6.2 - Formulation	88
6.3 - Orthogonal Contact	91
6.4 - Finite λ	93
6.5 - Numerical Approach	100
Figures	103

CHAPTER VII

CYLINDERS IN SHALLOW WATER

7.1 - Introduction	108
7.2 - Horizontal Oscillation	109
7.3 - Limiting Cases Of The Horizontal Oscillation	111
7.4 - Vertical Oscillation	116
7.5 - Limiting Cases Of The Vertical Oscillation	118
7.6 - Scattering Of Waves In Shallow Water	119
7.7 - Limiting Cases Of The Scattering Problem	122

CHAPTER VIII
HORIZONTAL OSCILLATION OF PLATES

8.1 - Finite Length Plate And Infinite Depth Fluid	125
8.2 - Numerical Approach	131
8.3 - Waves Produced By A Wavemaker In A Channel	134
8.4 - Finite Depth	139
8.5 - Infinite Depth	143
8.6 - Small Depth	145
Figures	151

CHAPTER IX
CONCLUSION

	159
List Of References	165

(In the name of God, the compassionate, the merciful)

Dedicated to my parents Jahangir Mahdmina and Nooshindokht Dowlatshahi, whom I have no way of thanking for their love, sacrifice, support and encouragement throughout my life.

ACKNOWLEDGEMENTS

I would like to thank Professor Leslie Hocking for his fine supervision, invaluable advice, encouragement, and patience, throughout the whole of this study.

I am also very grateful to Professor Susan Brown for offering her kind suggestions and criticisms during our many discussions. I am indebted to Professor Frank Smith too for his help and arrangement of financial support. In addition, I would like to express my appreciation to my friend and colleague Ahmad Farid Khorrami, for his untiring efforts during the final stages of preparing this thesis. My appreciation also goes to other members of the UCL Mathematics Department, in particular Rowena Hurst-Bowles and Robert Bowles.

I would like to thank my parents too for their ever lasting love and devotion as well as their endless sacrifices throughout the whole of my academic career, and for providing me with a much better start in life than I could have ever wished or hoped for.

Finally, this thesis would not have been initiated nor completed, without persistent encouragement, support, criticism and general assistance of my dearest husband Jamshid. I cannot thank him enough. The patience shown by my son Ehhsan, in view of the many occasions in which my study resulted in his neglect, is also appreciated.

Deljoo Mahdmina, February 1991.

CHAPTER I

INTRODUCTION

1.1 - Surface Waves

Wave phenomena is observed every day in our normal life at home (e.g. in the bath). When water is disturbed, waves are produced which are due to gravity and on a small scale surface tension, where both of these factors try to restore the surface to its original level. For gravity waves which are sufficiently long, surface tension is unimportant. However, short waves are dominated by capillarity, capillary-gravity waves, and produced by the effect of surface tension as well as gravity.

When the container or obstacle is large (e.g. in oceans, lakes and large basins), the surface tension can be ignored, and the waves are treated as gravity waves only. However, when gravity is reduced or when very short waves are important, both forces of gravity and capillarity must be considered. For precise experimental studies on a laboratory scale, the effects of surface tension need to be taken into account. In experimental tanks, wavemakers are used to produce waves. They are very important for ship and sea defense designers. Most of the research done on capillary-gravity waves has concentrated on the propagation of waves. It is also well-known that in unbounded regions capillary-gravity waves behave in much the same way as pure gravity waves, but with a different wave velocity. If the wavemaker oscillates with a given amplitude and frequency, the steady state at large distance from it (the wavemaker) shall consist of a plane wave and the amplitude and phase of this wave are the quantities to be determined. This calculation was performed first by Havelock (1929) for a vertical infinite plane and a vertical circular cylinder.

When capillarity is present, there is an extra term in the free-surface pressure condition which is proportional to the curvature of the free surface. For propagating waves in unbounded regions, the only effect of capillarity is the change in the dispersion relation. When there is a boundary (or boundaries) which intersects the free surface, the increase in the order of the pressure condition (the dispersion relation) requires extra conditions to be imposed at the line of contact between the free surface and the boundary. Therefore when surface tension is included, at the intersection of ^{the} free surface of the fluid with the boundary, the order of the dynamic boundary condition shall be increased at the interface and a term proportional to the curvature of the free surface would be included, and hence a further condition would be required. The need for this extra condition was first pointed out by Evans (1968) in his discussion of the reflection of capillary-gravity waves by a vertical barrier. Although he recognized the importance of the edge condition, he assumed that the slope of the free surface at the edge had a harmonic oscillation with a prescribed amplitude. He made no attempt to relate this amplitude with the wave motion (and it cannot be chosen independently), and his solution contains an arbitrary parameter. The wavemaker problem with the surface tension included was discussed by Rhodes-Robinson (1971) who also made a similar assumption. He assumed that the slope of the free surface at the edge could be prescribed and varied in phase with the horizontal motion of the wavemaker.

If the microscopic-scale physics of the processes involved near the contact line is considered, it would be justifiable in some contexts, to postulate that their macroscopic effect can be accounted for by a contact angle that exhibits both a dynamic variation with the speed of the contact line and contact-angle hysteresis. Figure 1.1 shows the typical behaviour of the contact angle for an

air-fluid-solid contact.

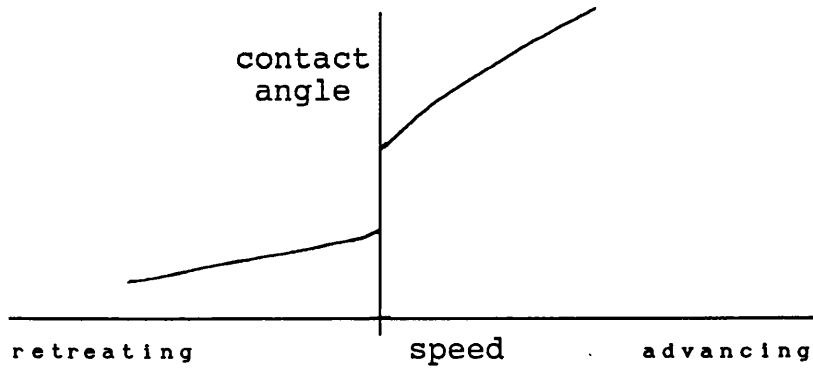


Figure 1.1. Dynamic contact angle with hysteresis.

In the fluid, the contact angle increases when the speed of advance of the fluid into the air increases and decreases when the fluid retreats. There is also a discontinuity between the minimum advancing angle and the maximum retreating angle. Therefore, there is a range of possible static angles, and not just a single static contact angle. It follows that this behaviour of the contact line shall produce an oscillatory motion on the free surface. If the hysteresis is sufficiently large (for example for waves of small amplitude) then the contact line will remain at rest throughout the oscillation, which is the edge condition used by Benjamin & Scott (1979). However, in general the contact line remains at rest until the slope increases sufficiently for it to move up the boundary. When the speed decreases, the contact line will stop moving and remains at rest until the slope decreases far enough for it to begin to move down again, and again remains at rest for a while and starts moving up and so on.

For the first time, Benjamin & Scott (1979) discussed the need to impose edge conditions. They argue that the contact line must remain fixed throughout the motion (the pinned-end condition). In brimful channel, which was their main interest, the fixed contact line is appropriate, but

they also argued that the same condition can be used on a solid surface when the contact angle between the fluid and the solid exhibits hysteresis. Therefore, when there is a range of possible static contact angles, the edge remains stationary. Surface roughness on the solid boundary, appears to have effects on the range of possible static contact angles (Jansons 1985) and can be reduced by careful preparation of the material. It is possible that the wave amplitude may be so large (but still small enough, so that the linear theory still holds) that the static range of contact angle is exceeded, leading to dynamic behaviour becoming more significant. In a different context, Davis (1980) suggested that, a more profitable alternative is to discuss the situation when the static range of angle is very small. In this case the dynamic behaviour becomes the significant feature.

The edge condition used by Benjamin & Scott (1979) was also used by Graham-Eagle (1984) in his study of determination of the frequencies of capillary-gravity waves in a full circular cylinder. The edge condition used by them is the extreme case in which the contact line remains fixed throughout the motion. The other extreme case is when the contact line can move freely up and down the boundary. As well as these two extreme cases, there are also some intermediate possibilities. An edge condition that incorporates the dynamic variation, but not the hysteresis, was used by Hocking (1987a) to calculate the frequency and damping of standing waves between two parallel vertical walls. The contribution to the damping from the edge condition is sometimes much larger than that produced by viscosity. Young and Davis (1987) studied the motion of a vertically oscillating plate partially immersed in fluid with both the dynamic variation and the hysteresis of the contact angle included in their analysis. There was no coupling between the fluid motion induced and the position of the contact line, to the leading order, with the range of parameter chosen. With an increase in the size of the surface tension parameter, the

fluid motion and the contact-line motion have to be determined simultaneously and this problem has been solved by Hocking (1987c). In this edge condition proposed by Hocking, the mean static contact angle is taken to be 90° for simplicity, so that the free surface is horizontal in equilibrium. For small amplitude waves, the linear dynamic variation of the contact angle has the form:

$$\frac{\partial \eta}{\partial t} = \lambda \frac{\partial \eta}{\partial x}, \quad (1.1)$$

where x is the horizontal distance from the plate, t is the time and $\eta(x,t)$ is the elevation of the free surface. The constant λ measures the strength of the dynamic variation; $\lambda = 0$ corresponds to a fixed contact line (that is large hysteresis) and with $\lambda = \infty$ the contact line can move freely along the plate with the contact line fixed at 90° . Therefore the proposed edge condition not only includes the free-end ($\lambda = \infty$) edge condition, but also the pinned-end ($\lambda = 0$) condition which was used by Benjamin & Scott (1979) and Graham-Eagle (1984). Hocking (1987c) has used this condition to determine the amplitude of capillary-gravity waves generated by the vertical motion of a plate. This condition takes into account some of the wetting properties of the fluid and can be referred to as the "wetting" condition.

1.2 - Present Work

In chapter II, the general formulation for the following chapters is given, using the wetting edge condition explained in section 1.1.

Damping of surface waves has been studied by Benjamin & Ursell (1954), Case & Parkinson (1957) and Keulegan (1959) for containers of different shapes. Hocking (1987a) has solved the problem for capillary-gravity waves between two vertical walls. In chapter III, the problem solved by Hocking has been extended for water inside circular cylinder.

Many investigations have been done on the interaction between surface waves and partially immersed bodies. These bodies may be fixed or moving. Wehausen (1971) and Evans (1981) have contributions on wave-body interactions. Hogan (1979) and Vanden-Broeck (1984) have discussed the capillary-gravity waves in horizontally unbounded regions. Since surface tension is included, an extra edge condition would be needed. Using the edge condition (1.1) discussed in section 1.1, the problem of vertical and horizontal oscillation of a cylinder in water has been investigated in chapters IV and V respectively, where the surface elevation of the waves at a large distance away and on the cylinder have been obtained.

One of the interesting problems of wave motion is the scattering of a gravity wave on the surface of a fluid by a solid obstacle. Thomson (1871), Hogan (1979) and Vanden-Broeck (1984) have extensively studied the effect of surface tension on the propagation of surface waves in unbounded regions. The reflection of capillary gravity waves by an obstacle of the shape of a vertical plate is studied by Hocking (1987b). In chapter VI, however, a full account of the paper by Mahdmina and Hocking (1990) is given, in which the problem of scattering of capillary-gravity waves by a cylindrical shaped obstacle is investigated. The surface elevation both at large distance and on the cylinder have been obtained.

When the depth of the fluid is small compared with the wavelength, the shallow-water approximation can be used to simplify the analysis considerably. With shallow water, the limiting value of the quantities calculated in chapters VI (for large time), V and IV, for small depth can be solved easily using the shallow water theory. These problems are investigated in chapter VII for circular cylinder wavemakers and obstacles.

So far, the steady state's problem was mentioned.

Now, if the time expands, the problem would become harder because of the singularity which should be removed. In determining the transient motion after an impulsive start, there is always a difficulty, since an initial singularity in the slope of the free surface at the wavemaker would be predicted. This phenomenon was described in an unpublished note by Peregrine (1972), and is treated at length by Roberts (1988). He considered the transient motion for power-law motions of the wavemaker and concluded that the singularity could only be removed by starting the motion sufficiently smoothly. The solutions so far described have ignored the presence of surface tension, which also acts to provide a restoring force on the free surface. In chapter VIII, the wavemaker problems for capillary-gravity waves are studied, in which the edge condition of 1.1 has been used. More importantly, the examination of the small-time solution shows that, when the postulated edge condition is employed, there is no singularity in the free-surface elevation or the slope at the wavemaker, even when it is started impulsively. It is not necessary to include nonlinear terms in the free-surface condition to arrive at an acceptable solution. The particular case of a plane vertical wavemaker which is impulsively brought into a harmonic oscillation of small amplitude is considered. There are two special cases which have been concentrated on: fluid of finite depth with the wavemaker extending from top to bottom of the fluid, and fluid of infinite depth with only the top portion of the vertical boundary of the fluid brought into motion. The amplitude of the steady-state wave train is obtained, generalizing the results of Havelock (1929). In this chapter, the problem of a horizontally oscillating plate in fluid of infinite depth is also studied, using the source-sink approach to find the surface elevation of surface waves at large distances away from the plate.

Finally in chapter IX, conclusions and possible suggestions on the previous chapters are made.

NON-DIMENSIONALIZATION AND FORMULATION

2.1- Introduction

For an inviscid and incompressible fluid (which is a good assumption for fluids in general, specially water waves), moving with the velocity \mathbf{v} , the equation of continuity is

$$\nabla \cdot (\mathbf{v}) = 0, \quad (2.1)$$

and the Euler's equation is

$$\frac{D\mathbf{v}}{Dt} = - \frac{1}{\rho} \nabla p + \mathbf{g}, \quad (2.2)$$

where, ρ is the uniform density, p is the pressure, \mathbf{g} is the acceleration due to gravity and D/Dt is the conventional notation for differentiation. Furthermore, since the waves amplitude are small, the fluid motion is irrotational and the velocity vector can be expressed in terms of a scalar velocity potential ϕ as

$$\mathbf{v} = \nabla \phi, \quad (2.3)$$

and consequently the equation of continuity becomes a Laplace's equation

$$\text{div}(\nabla \phi) \equiv \nabla^2 \phi = 0, \quad (2.4)$$

which is solved with appropriate boundary conditions to determine the behaviour of small amplitude surface waves for different conditions.

Consider unbounded fluid of depth D' , with angular

frequency σ' and wavelength $2\pi/k'$. The velocity potential for waves progressing in the horizontal x' -direction is given by

$$\phi = A \exp[i(k'x' - \sigma't')] \cosh[k'(z' + D')], \quad (2.5)$$

where z' is measured vertically upwards from the free surface.

The horizontal and vertical components of velocity in terms of the velocity potential are respectively

$$u = \frac{\partial \phi}{\partial x'}, \quad v = \frac{\partial \phi}{\partial z'}, \quad (2.6)$$

and furthermore the horizontal component of velocity is expressed as (using equation 2.2)

$$\frac{\partial u}{\partial t} = - \frac{1}{\rho} \frac{\partial p}{\partial x'}. \quad (2.7)$$

The kinematic and dynamic boundary conditions for small amplitude waves are

$$\frac{\partial \eta'}{\partial t'} = \frac{\partial \phi}{\partial z'}, \quad \rho g \eta' - \gamma \frac{\partial^2 \eta'}{\partial x'^2} = p, \quad (2.8)$$

where η' corresponds to the disturbance of the free surface.

The scaling quantity k' can be determined (using equation 2.8) from the kinematic condition for capillary-gravity waves of the given frequency at $z' = 0$ such that

$$\sigma'^2 = \left(gk' + \frac{\gamma k'^3}{\rho} \right) \tanh(k'D'). \quad (2.9)$$

where γ is the surface tension at the fluid/air interface, however, if the fluid has of infinite depth, then

$$\sigma'^2 = \left(gk' + \frac{\gamma k'^3}{\rho} \right), \quad (2.10)$$

noting that depth of the fluid also affects the boundary condition on the bottom end of the fluid along the z-axis.

Below, the problem of surface waves in the presence of vertical barriers (planes or cylinders) is discussed, with the fluid either outside the barriers or confined between them. The barriers themselves can be of planes or cylinders.

2.2- Cylinders

Here, it is assumed that the fluid is bounded by a circular cylinder of radius a . Cylindrical polar coordinates (ar, ϑ, az) with the upward vertical z-axis along the axis of the cylinder. The radius of the cylinder is chosen as the non-dimensionalization factor. The fluid occupies the region $r \geq 1$ if it is outside the cylinder, and $r \leq 1$ if it is inside.

The gravity acceleration g can be used in conjunction with the length scale a to provide a time scale. Thus time is measured by $(a/g)^{1/2}t$. The dynamic pressure is $\rho g a$, the velocity components are $(g a)^{1/2}(u, v, w)$ and the free surface elevation is $\eta(r, \vartheta, t)$. Euler's equations are (using scaled variables),

$$\begin{aligned} \frac{\partial u}{\partial t} &= - \frac{\partial p}{\partial r} & , & \quad \frac{\partial v}{\partial t} = - \frac{1}{r} \frac{\partial p}{\partial \vartheta} & , \\ \frac{\partial w}{\partial t} &= - \frac{\partial p}{\partial z} & , & & \end{aligned} \quad (2.11)$$

the equation of continuity is,

$$\frac{\partial u}{\partial r} + \frac{u}{r} + \frac{1}{r} \frac{\partial v}{\partial \vartheta} + \frac{\partial w}{\partial z} = 0, \quad (2.12)$$

and Laplace's equation for the pressure p is

$$\frac{\partial^2 p}{\partial r^2} + \frac{1}{r} \cdot \frac{\partial p}{\partial r} + \frac{1}{r^2} \cdot \frac{\partial^2 p}{\partial \vartheta^2} + \frac{\partial^2 p}{\partial z^2} = 0. \quad (2.13)$$

The time factor $\exp(i\sigma t)$ (or $\exp(-i\sigma t)$) can be removed from all the dependent variables, u , v , w , p and η , by considering waves of non-dimensional frequency σ .

We also need to know the conditions on the cylinder as well as the conditions at the bottom of the fluid to solve the problem.

The edge condition is (from equation 1.1, as was justified in chapter 1 for a stationary boundary)

$$\frac{\partial \eta}{\partial t} = \lambda \frac{\partial \eta}{\partial r} \quad \text{at} \quad r = 1, \quad (2.14)$$

and it includes the effect of contact-angle variation with the speed of the contact line. If $\lambda \rightarrow \infty$, the free surface meets the cylinder orthogonally and if $\lambda = 0$ the contact line does not move. If the cylinder has a vertical motion $u \exp(i\sigma t)$, the edge condition (2.14) becomes

$$\frac{\partial \eta}{\partial t} - u = \lambda \frac{\partial \eta}{\partial r}, \quad (2.15)$$

since it is the motion of the edge relative to the boundary that is required.

Finally the behaviour of the vertical component of velocity should be considered as the bottom of the fluid is approached, that is $-h$ (when the fluid is of finite depth h) or $-\infty$ when the fluid is of infinite depth. However, the radiation condition is needed only when the fluid is outside the cylinder, which gives the behaviour of waves at large distances away from the cylinder.

At the free surface, the kinematic and dynamic boundary conditions (in equation 2.8) are used. The dynamic condition balances the disturbance to the dynamic and

hydrostatic parts of the pressure by the capillary pressure, which is proportional to the local curvature of the surface. For a cylinder, this condition is (in non-dimensionalization form),

$$K \left[\frac{\partial^2 \eta}{\partial r^2} + \frac{\partial \eta}{r \partial r} + \frac{1}{r^2} \frac{\partial^2 \eta}{\partial \vartheta^2} \right] - \eta = - p, \quad (2.16)$$

where the capillarity coefficient K is the inverse of the Bond number and is defined as

$$K = \frac{\gamma}{\rho g a^2}. \quad (2.17)$$

The capillarity coefficient measures the relative importance of the two restoring forces, capillarity and gravity.

On the free-surface,

$$\frac{\partial \eta}{\partial t} = w \quad \text{at } z = 0, \quad (2.18)$$

which can be compared with equation 2.16 to investigate the propagation of surface waves in different cases.

The solution of the Laplace's equation in the cylindrical polar coordinates leads to Bessel functions, and if the centre of the cylinder is included (that is when the fluid is inside the cylinder) the Y-Bessel functions should be excluded from the solutions, because they are singular at $z = 0$ (and example of which is the problem in chapter 3, where the damping of capillary-gravity waves inside a vertical cylinder is studied). However, if the fluid is outside the cylinder, the Y-Bessel functions as well as J-Bessel functions should be included in the solutions.

The shallow water approximation can be used for the fluid with the small depth ($h \ll 1$) outside a cylindrical

wavemaker oscillating horizontally and consequently simplifying the problem. The variables can be expressed in terms of powers of h if $w = hW$ and $z = h\zeta$, and the relationship between frequency and wavenumber is

$$\sigma^2 = k'^2 h (1 + Kk'^2). \quad (2.19)$$

2.3- Plates

The general approach for plane wavemaker is similar to the cylindrical one (as discussed in section 2.2). There are only two major differences. One is the system of coordinates and the other is the scaling factor.

For plates, the Cartesian coordinates is used with the x -axis perpendicular to the plate, along the undisturbed free surface, and the z -axis in the upward vertical direction. It is assumed that a thin plate is oscillating with a frequency σ' , then the motion is entirely two-dimensional, and the chosen lengthscale for the non-dimensionalization is proportional to the wavelength $2\pi/k'$ of the surface waves, which has the same frequency as the plate's oscillation. The coordinates of a point in the fluid are denoted by $(x,z)/k'$. The corresponding velocity components are $V'(u,w)$, time is measured by $(gk')^{-1/2}t$, pressure by $\rho V'(g/k')^{1/2}p$ and the free-surface elevation by $V'(gk')^{-1/2}\eta$, where ρ is the uniform density of the fluid and g is the gravitational acceleration.

Then linearized Euler's equations for the inviscid fluid is,

$$u = \frac{\partial \phi}{\partial x}, \quad \frac{\partial u}{\partial t} = - \frac{\partial p}{\partial x}, \quad \frac{\partial w}{\partial t} = - \frac{\partial p}{\partial z}, \quad (2.20)$$

the continuity equation is

$$\frac{\partial u}{\partial x} + \frac{\partial w}{\partial z} = 0, \quad (2.21)$$

and Laplace's equation for the pressure is

$$\frac{\partial^2 p}{\partial x^2} + \frac{\partial^2 p}{\partial z^2} = 0, \quad (2.22)$$

where factor $\exp(i\sigma t)$ is removed from all the dependent variables, u, v, w, p and η , if the non dimensional waves frequency is σ . Furthermore, the conditions on the plate and at the bottom of the fluid are needed to solve the problem. For the edge condition, the condition in equation 1.1 is used (which was justified in chapter 1 for a stationary boundary)

$$\frac{\partial \eta}{\partial t} = \lambda \frac{\partial \eta}{\partial x} \quad \text{at} \quad x = 0, \quad (2.23)$$

however, if the plate has a vertical motion u.e $e^{i\sigma t}$, this condition becomes

$$\frac{\partial \eta}{\partial t} - u = \lambda \frac{\partial \eta}{\partial x}, \quad (2.24)$$

since it is the motion of the edge relative to the boundary which is required, and at $x = 0$, the velocity u is zero or non-zero if the plate oscillates vertically or horizontally respectively.

Finally, w approaches zero towards the bottom of the fluid, that is at $-h$ or $-\infty$ (when the fluid is of finite or infinite depth) respectively, where the radiation condition should also be satisfied.

The conditions on the free surface which should be considered, are

$$\frac{\partial \eta}{\partial t} = w \quad \text{at} \quad z = 0, \quad (2.25)$$

and

$$K \frac{\partial^2 \eta}{\partial x^2} - \eta = -p, \quad (2.26)$$

where the capillarity coefficient K is

$$K = \frac{\gamma k'^2}{\rho g}, \quad (2.27)$$

and the equation for η can be obtained by comparing equation 2.25 and 2.26.

The non-dimensional form of σ' the frequency, that is σ is

$$\sigma^2 = (1 + K) \tanh(d), \quad (2.28)$$

$$\sigma^2 = (1 + K), \quad (2.29)$$

when the fluid has finite or infinite depth respectively.

If the problem of plane wavemaker which is considered to be the oscillation of a wavemaker at one end of a channel with inviscid fluid inside it, then since the analysis takes different forms for finite and infinite fluid depth, we can treat the two cases separately. In case of the finite depth, where the depth of the fluid d , and the channel h , are the same, the channel's end position (at $x = 0$) is shifted forward. When the fluid is of infinite depth, with a boundary at $x = 0$ of which the top portion, of depth h , is the wavemaker, the analysis can proceed in a similar fashion to that for a finite depth of fluid. If the depth of the channel is small compared with the wavelength, the simplifications of shallow-water theory can be applied and the results arrived at more readily than by the methods used for arbitrary depths. In this case, the relationship for the frequency is,

$$\sigma^2 = (1 + K) d. \quad (2.30)$$

It is possible to find the transient solution of the shallow-water equations by taking a Laplace transform. However, this does not give the correct result for the short-time behaviour because the limits h and t do not commute in their limits approaching zero. The impulsive

initial motion of the wavemaker creates waves of all wavelengths, including those that are short compared with the fluid depth. but the shallow-water approximation assumes that all variations in the x-direction are small compared with those in the z-direction and this assumption is not valid for t small.

DAMPING OF WAVES AT CYLINDRICAL BOUNDARIES

3.1 - Introduction

Most research on capillary-gravity waves on a free liquid surface has concentrated on their propagation. Lamb (1932) introduced methods for determining the frequencies of standing gravity waves for vertical boundaries. When the horizontal dimension of the container is large, as in harbours and lakes, capillarity can be ignored and only gravity waves need to be considered, but this is not so when the container is small, such as in basins used in the laboratories. Even then, the effect of capillarity introduces only a quantitative change except for very small containers, high frequency modes or low-gravity environments.

The free surface must intersect the vertical walls orthogonally in absence of surface tension, however with surface tension present, the free-surface condition has an extra term, which is proportional to the curvature of the free surface, and for progressive waves, produces a change in the frequency of the waves for a given wavenumber. However, the increase in the order of the pressure condition, requires that extra conditions to be imposed. These conditions control the position of the free surface at its intersection with the boundary of the container. If the orthogonality condition of the free surface at the walls is imposed when capillarity is present, the frequency of the standing waves in the container shall alter in a similar way to the change produced in progressive waves. But it is not clear that the condition of orthogonal intersection of free surface and boundary is the appropriate one for standing capillary-gravity waves.

The pinned-end edge condition (one in which the edge remains stationary) was introduced (as explained in chapter 1) by Benjamin & Scott (1979) and Graham-Eagle (1984) independently. They argue that the surface elevation at the edge of the free surface stays in its equilibrium position, and furthermore this is the appropriate condition for a rim-full container and determined the frequencies for progressive waves along a channel with sidewalls, two-dimensional standing waves between two vertical boundaries and standing waves in a circular cylinder. Furthermore, Benjamin & Scott (1979) argue that the pinned-end edge condition may also be appropriate when the container is not brimful.

When the gravity-wave condition of an orthogonal intersection with the free-end edge condition, is extended to waves with capillarity, the contact angle needs to remain fixed at 90° without any dynamic behaviour, and the contact line can move freely across the solid boundary.

There are two questions of major importance in the study of standing waves. One is the determination of their possible frequencies and the rate of which they are damped. The damping of gravity waves has been examined theoretically by Ursell (1952). He showed that the major contribution came from the action of viscosity at the sidewalls, except when the container is very wide or very shallow. In his study of damping in closed basins, Miles (1967) included the effects of capillary hysteresis. He assumed that the contact angle is a constant with different values (depending on the direction of motion of the contact line), and deduced the dissipation from the rate of working of the capillary forces. He ignored the fraction of the time period during which the contact angle changes and the contact line is at rest. Without any reference to the edge conditions (i.e. assuming the free-end value) the frequency of the wave is determined. Mei & Liu (1973) have demonstrated the importance of the

edge region in the calculation of the viscous damping of surface waves. In the absence of surface tension, such as in the analysis of Mei & Liu (1973), the surface elevation is also unbounded at the edge, however, when surface tension is present, the pressure is balanced by the free-surface curvature, and the elevation is uniformly small. Benjamin & Ursell (1954), Case & Parkinson (1957) and Keulegan (1959) independently have measured the damping of surface waves for containers of various shapes. The degree of agreement between these observations and the predicted values of the damping rate based on the action of viscosity is variable and seems to depend on the properties of the materials used and the preparation of the solid boundaries. They suggest that the neglected capillary effects, particularly when associated with the behaviour of the interface near the edge, may have caused the discrepancy between theory and observation. The free-end edge condition used by these authors and the pinned-end condition suggested by Benjamin & Scott (1979) show that the gap between theory and experiment is not likely to be improved. The damping rate when the pinned-end edge condition is used is probably less than that for the free-end condition because of the reduction in the movement of the interface at the contact line and hence of the fluid near to it. The observed damping rates are often considerably greater than the theoretical predictions. The wetting boundary condition implies the dissipation of energy at the contact line which may be equal to or greater than that produced by viscosity.

However, the wetting edge condition, used by Hocking (1987a) is applied here. This condition (explained in chapter 1) includes the free- and the pinned-end conditions as special cases. It relates the speed of the contact line to the change in the contact angle. Hocking (1987a) applied the wetting condition to the problem of standing capillary-gravity waves between two parallel vertical walls. The frequencies of these waves, and their damping both by wetting and viscosity, are determined. He

showed that the dissipation associated with the surface forces can exceed of that produced by viscosity.

Below, the problem of standing waves inside an upright fixed circular cylinder is studied with inviscid fluid, and the waves of small amplitude. The axis of the cylinder is perpendicular to the free-surface of the fluid and the depth of the fluid is sufficiently large for the effect of the bottom to be ignored, in comparison to the radius of the cylinder. The static contact angle is 90° . The waves are three-dimensional and the elevation of the waves from the free surface in the presence of capillarity is studied.

3.2 - Three-dimensional Standing Waves

An inviscid fluid of infinite depth is confined inside a vertical cylinder of radius a . Cylindrical polar coordinates (r, ϑ, z) is used with the origin at the centre of the cylinder. The non-dimensionalization factor is the radius of the cylinder (as discussed in chapter 2), and the waves can be linearized due to their small amplitude. The linearized equations of motion are:

$$\frac{\partial u}{\partial t} = - \frac{\partial p}{\partial r}, \quad (3.1)$$

$$\frac{\partial v}{\partial t} = - \frac{1}{r} \frac{\partial p}{\partial \vartheta}, \quad \frac{\partial w}{\partial t} = - \frac{\partial p}{\partial z}, \quad (3.2)$$

$$\frac{1}{r} \frac{\partial v}{\partial \vartheta} + \frac{\partial u}{\partial r} + \frac{u}{r} + \frac{\partial v}{\partial z} = 0, \quad (3.3)$$

where p is the pressure and u & v are the components of the velocity. The boundary conditions are :

$$\frac{\partial p}{\partial r} = 0 \quad \text{at } r = 1, \quad (3.4)$$

and

$$\frac{\partial p}{\partial z} \rightarrow 0 \quad \text{as } z \rightarrow -\infty. \quad (3.5)$$

If η is the free-surface elevation above its

equilibrium position at $z = 0$, the kinematic and pressure conditions in the linearized form, are

$$w = \frac{\partial \eta}{\partial t}, \quad (3.6)$$

$$\eta - K \left(\frac{\partial^2 \eta}{\partial r^2} + \frac{1}{r} \frac{\partial \eta}{\partial r} + \frac{1}{r^2} \frac{\partial^2 \eta}{\partial \vartheta^2} \right) = p, \quad (3.7)$$

where K is the capillarity coefficient. Finally, the wetting edge condition (explained in chapter 1) is

$$\frac{\partial \eta}{\partial t} = -\lambda \frac{\partial \eta}{\partial r} \quad \text{on} \quad r = 1. \quad (3.8)$$

The pressure p , depends on the distance from the centre of the cylinder r , the vertical distance from the free surface of the fluid z , and ϑ . The z -dependence is

$$Z(z) = \sum_{n=1}^{\infty} P_n \exp(k_n z) + Q_n \exp(-k_n z). \quad (3.9)$$

The radial-dependence $R(r)$, is a combination of Bessel functions ($J_m(k_n r)$ and $Y_m(k_n r)$), where m is the mode number which is the order of the Bessel functions, and n is the number of terms in the series, and the arguments of the Bessel and the exponential functions k_n , are determined later using the frequency equation (when $\lambda = \infty$ which shall be explained in section 3.4)

$$\sigma_n^2 = Kk_n^3 + k_n, \quad (3.10)$$

where equation 3.10 is obtained (as discussed in chapter 2) from equation 3.7, and the coefficient P_n is found later (in equation 3.27). The ϑ -dependence $\Theta(\vartheta)$, satisfies the following differential equation :

$$\frac{1}{\Theta} \frac{\partial^2 \Theta}{\partial \vartheta^2} = -m^2, \quad (3.11)$$

which gives,

$$\Theta(\vartheta) = A \cos(m\vartheta), \quad (3.12)$$

when $J_m(k_n r)$ should be used to avoid singularity at $r = 0$. The time factor $\exp(i\omega t)$ is omitted from each term.

The following conditions are obtained (by satisfying the equations 3.4 & 3.5)

$$J_m'(k_n) = 0, \quad Q_n = 0. \quad (3.13)$$

Therefore, the pressure can be written as

$$p = \sigma \cos(m\vartheta) \sum_{n=1}^{\infty} J_m(k_n r) P_n \exp(k_n z), \quad (3.14)$$

and (using equations 3.1 & 3.2)

$$u = i \cos(m\vartheta) \sum_{n=1}^{\infty} P_n k_n J_m'(k_n r) \exp(k_n z), \quad (3.15)$$

$$w = i \cos(m\vartheta) \sum_{n=1}^{\infty} P_n k_n J_m(k_n r) \exp(k_n z). \quad (3.16)$$

Therefore, the surface elevation η (using equations 3.6 & 3.16) is

$$\begin{aligned} \eta &= \frac{1}{\sigma^2} \frac{\partial p}{\partial z} \\ &= \frac{\cos(m\vartheta)}{\sigma} \sum_{n=1}^{\infty} P_n k_n J_m(k_n r). \end{aligned} \quad (3.17)$$

On the free surface, the exponential term is unity, then surface elevation is a function of r and ϑ only.

The complementary solution of equation 3.7 is

$$\eta = A \omega^m J_m \left(r i K^{-1/2} \right) = A i^m I_m \left(r K^{-1/2} \right) \omega^m \quad (3.18)$$

and since I_m produces inward moving waves, as is required. In order to compare the solution of equations 3.17 and 3.7, surface elevation η , should be

$$\eta = \sum_{n=1}^{\infty} C_n J_m(k_n r) \cos(m\theta), \quad (3.19)$$

where C_n is (using equations 3.14 & 3.7 and equating the coefficients of $J_m(k_n r)$)

$$C_n = \frac{\sigma}{Kk_n^2 + 1} P_n. \quad (3.20)$$

Since $J_m(k_n r)$ is a Bessel function, it satisfies the following differential equation

$$\frac{\partial^2 J_m(k_n r)}{\partial r^2} + \frac{1}{r} \frac{\partial J_m(k_n r)}{\partial r} + k_n^2 J_m(k_n r) = \frac{m^2}{r^2} J_m(k_n r) \quad (3.21)$$

hence the solution to the differential equation of 3.7 is

$$\begin{aligned} \eta &= A i^m I_m \left(r K^{-1/2} \right) \cos(m\theta) \\ &+ \sigma \cos(m\theta) \sum_{n=1}^{\infty} \frac{P_n}{1 + Kk_n^2} J_m(k_n r). \end{aligned} \quad (3.22)$$

In order to compare the two expressions for η (in equations 3.22 and 3.19), the first term of the above equation (3.22) should be written as an infinite series of $J_m(k_n r)$. Therefore let

$$I_m \left(r K^{-1/2} \right) = \cos(m\theta) \sum_{n=1}^{\infty} B_n J_m(k_n r), \quad (3.23)$$

and hence

$$\int_0^1 r I_m \left(r K^{-1/2} \right) J_m(k_n r) dr = B_n \int_0^1 r J_m(k_n r) J_m(k_n r) dr, \quad (3.24)$$

where the right-hand side of the equation 3.24 becomes

$(k_n^2 - m^2)$
 $B_n \wedge J_m^2(k_n) / 2k_n^2$ (by using the first condition in equation 3.13 and the l'Hopital's rule), and its left-hand side gives

$$\frac{i K^{1/2} J_m' \left(i K^{-1/2} \right) J_m(k_n)}{\left(K k_n^2 + 1 \right)} e^{-m\vartheta}, \quad (3.25)$$

and hence the coefficient B_n is obtained. Therefore η becomes (by using equations 3.23 and 3.22)

$$\eta = \cos(m\vartheta) \sum_{n=1}^{\infty} \left[\frac{-2Ai K^{1/2} k_n^2 J_m' \left(i K^{-1/2} \right)}{\left(K k_n^2 + 1 \right) \left(m^2 - k_n^2 \right) J_m(k_n)} + \sigma \frac{P_n}{1 + K k_n^2} \right] J_m(k_n r). \quad (3.26)$$

By equating the coefficients of $J_m(k_n r)$ in equations 3.26 and 3.17, the following expression for P_n in terms of A is

$$P_n = \frac{-2Ai\sigma K^{1/2} k_n^2 J_m' \left(i K^{-1/2} \right)}{\left(-K k_n^3 - k_n - \sigma^2 \right) J_m(k_n) \left(m^2 - k_n^2 \right)}. \quad (3.27)$$

Therefore the edge condition in equation 3.8 can be written as

$$\sum_{n=1}^{\infty} J_m(k_n) k_n \frac{2A \sigma k_n^2 K^{1/2} J_m' \left(i K^{-1/2} \right) \cos(m\vartheta)}{\left(+K k_n^3 + k_n - \sigma^2 \right) J_m(k_n) \left(m^2 - k_n^2 \right)} = -\lambda Ai K^{-1/2} J_m' \left(i K^{-1/2} \right) \cos(m\vartheta), \quad (3.28)$$

and therefore,

$$\lambda = \sum_{n=1}^{\infty} \frac{-2\sigma K i k_n^3}{\left(m^2 - k_n^2 \right) d_n(\sigma)}, \quad (3.29)$$

where

$$d_n(\sigma) = \sigma^2 - K k_n^3 - k_n. \quad (3.30)$$

Here, a theoretical determination of the damping of surface waves by capillary action has been presented. This damping is associated with conditions at the line of contact between the fluid and the container. A significant contribution to the total damping rate, and sometimes a dominant one, is the capillarity, since the wetting edge condition can account partially for the effect of the surface tension in dissipating the wave energy. The important point to remember is that in this chapter, a free-oscillation problem is studied and hence the frequency σ , is unknown (the analytical approach to find the real and the imaginary parts of the frequency is given in the next section). In figures 3.1, 3.2 and 3.3, the imaginary part of σ is drawn against the real part for the first three modes. The imaginary parts give the damping rate associated with capillarity and the edge condition. As predicted this is zero for the free- and the pinned-end cases, but intermediate values of λ give significant damping rates. For each mode, the initial guess for σ is made at $\lambda = \infty$, which corresponds to the free-end case and as λ decreases, the graph goes to its maximum which corresponds to a loss of energy, and then decreases towards the pinned-end case with $\lambda = 0$.

The case of $m = 0$ corresponds to the axisymmetric case with the lowest loss of energy.

In all three cases, the biggest frequency corresponds to the larger mode. For K and m equal to unity (where $m = 1$ corresponds to the splashing mode), the real and the

imaginary parts are of the same order, suggesting a big loss of energy. In this case (i.e. $m = 1$ & $K = 1$), the first part of the curve starting from $\lambda = 0$, before approaching its maximum value at (4.2, 3.01), is vertical. This behaviour is less apparent when $K = 0.1$ and $K = 10$. When the splashing mode is considered and $K = 1$, the real and imaginary part of the maximum frequency are of the same order. When K is 10 they are again of the same order, but if $K = 0.1$ (i.e. small capillarity), they are not of the same order with the maximum at (2.02, 0.56).

3.3 - Axisymmetric waves

This is the special case of the problem discussed in the previous section. Here, the problem is axisymmetric (i.e. independent of ϑ), and $m = 0$. There is an additional term independent of r in the expansion 3.23 (Dini Series) which can be cancelled by including a constant pressure term in equation 3.14. Thus the complete solution of 3.7 satisfies the condition that the volume of the fluid is unchanged by the disturbance. Therefore, the equations for η and λ can be obtained by substituting $m = 0$ into the corresponding equations (i.e. equations 3.22 and 3.29 respectively).

3.4 - Numerical Approach

In this chapter, unlike the other chapters, the frequency is unknown, therefore the real and imaginary parts of σ are to be found. If k_n is known, σ can also be obtained. Therefore, the first step is to determine the root of

$$J'_m(k_n) = 0. \quad (3.32)$$

The Bessel functions J_m and J'_m can be written in terms of lower orders of Bessel functions, using recurrence relations. The values of $J_0(k_n)$ and $J_1(k_n)$ are determined numerically (using NAG library). The initial guess for the root of the equation 3.32 is improved by using Newton's

method in the following form

$$s_n^* = s_n - \frac{J_m'(s_n)}{J_m''(s_n)}, \quad (3.32)$$

where the final updated root (s_n^*) is the root of the equation 3.31. The next root for the given mode is $k_n + \pi$, and therefore this way all the roots of the equation 3.31 are obtained by adding π to the previous root. This procedure is repeated for every mode (here, only three modes of 0, 1 & 2 are considered). For the Newton method, here, numerical results (and comparing them with the available tables of roots of Bessel functions (e.g. Abramovitz's (1970)) show that 20 iterations give sufficient accuracy (up to 10^{-4}).

Once the roots of the equation 3.31 are known, the real and imaginary parts of the frequency are obtained. When $\lambda = \infty$, $d_n(\sigma) = 0$ (according to equation 3.29) and therefore the initial value for the real part of σ (by using equation 3.32) for fixed m and the first root of the equation 3.31 (i.e. for $n = 1$) is

$$\sigma = \left(Kk_1^3 + k_1 \right)^{1/2}. \quad (3.33)$$

When λ is infinite or zero the imaginary part of σ is zero. But for other values of λ (5, 2, 1, 0.5, 0.2, 0.1) between these two extreme values, both the real and the imaginary parts of σ shall be obtained. For each value of λ , the real part of σ is updated using Newton's method in the following way

$$\sigma^* = \sigma - \frac{F(\sigma)}{F'(\sigma)}, \quad (3.34)$$

where

$$F(\sigma) = \lambda i - 2\sigma K \sum_{n=1}^{\infty} \frac{k_n^3}{\left(m^2 - k_n^2 \right) d_n(\sigma)}, \quad (3.35)$$

where the equation for $d_n(\sigma)$ is given in the equation 3.29. For the fixed value of λ , the frequency σ , has an imaginary part, say ε , where (using equation 3.29)

$$\varepsilon = \frac{Kk_1^3}{\lambda (k_1^2 - m^2)}, \quad (3.36)$$

which is a good approximation for the initial guess of the imaginary part of σ . This can be improved, using Newton's method again.

The calculation was repeated for the first five modes. Values chosen for the parameter K are 10, 1, 0.1 and 0.01. The range of λ is taken to be from 0 to 10. There is no need to choose a larger value for λ since increasing the value of λ from 10 to 100 has little effect on the convergence. Therefore the behaviour of the curves at $\lambda = 10$ gives a good idea of their behaviour at the extreme case of the free-end edge condition.

Numerical results shows that the number of terms required in the series depends on the value of K . For a larger K , the number of terms that need be included is smaller. The summation is truncated at $n = 200$ in all cases, since larger values of n (300 and 400) only differ in the third decimal place.

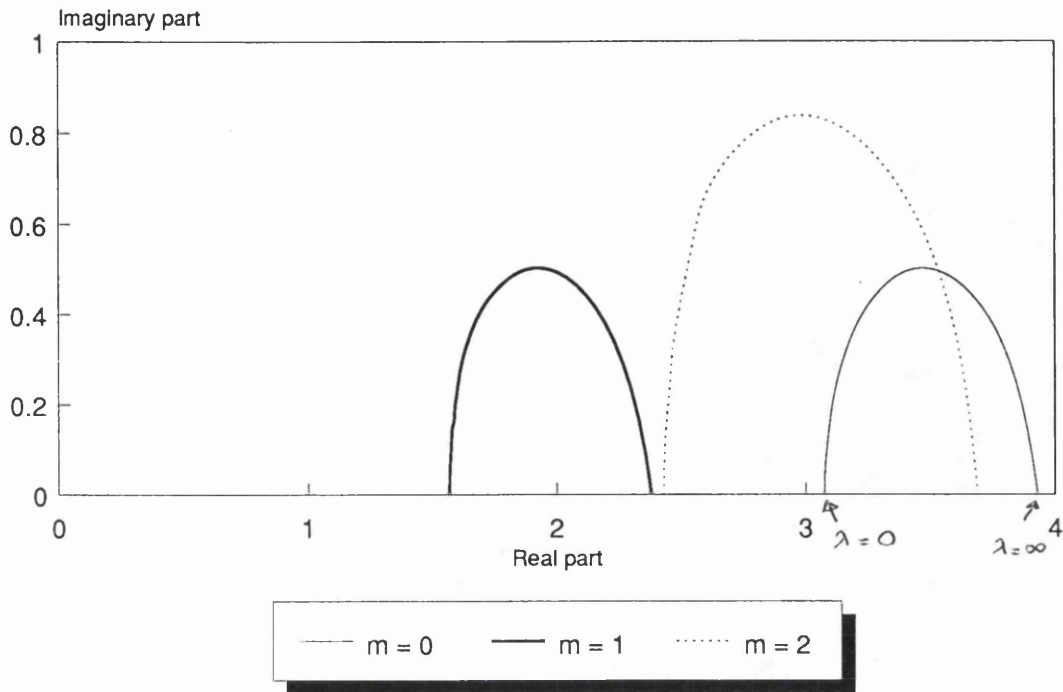


Figure 3.1. Imaginary against real part of frequency with $K = 0.1$.

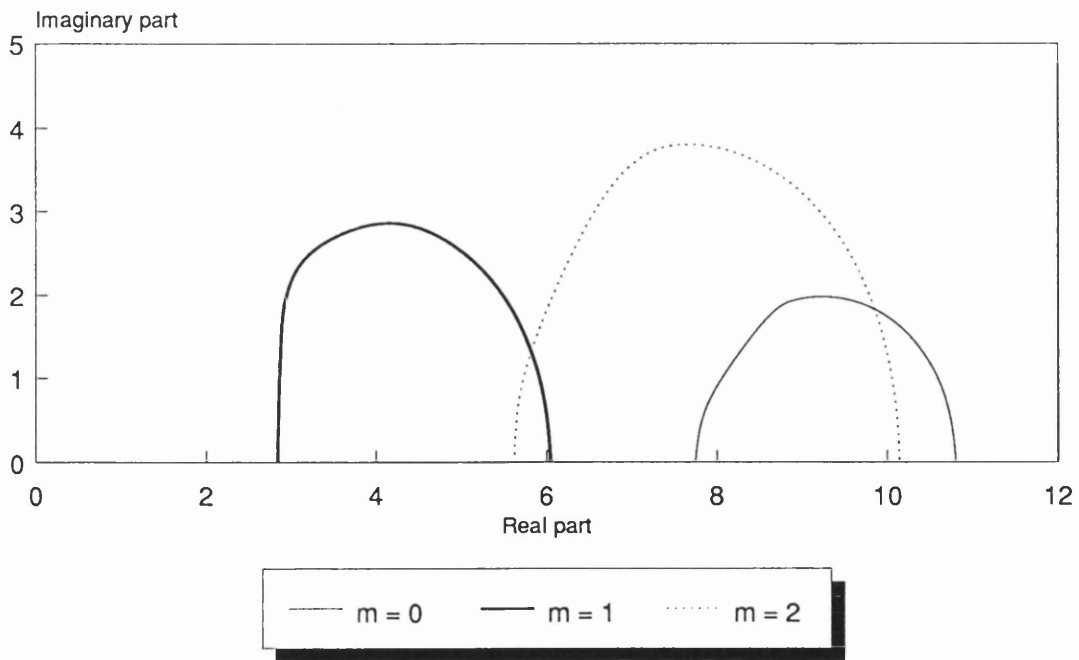


Figure 3.2. Imaginary against real part of frequency with $K = 1$.

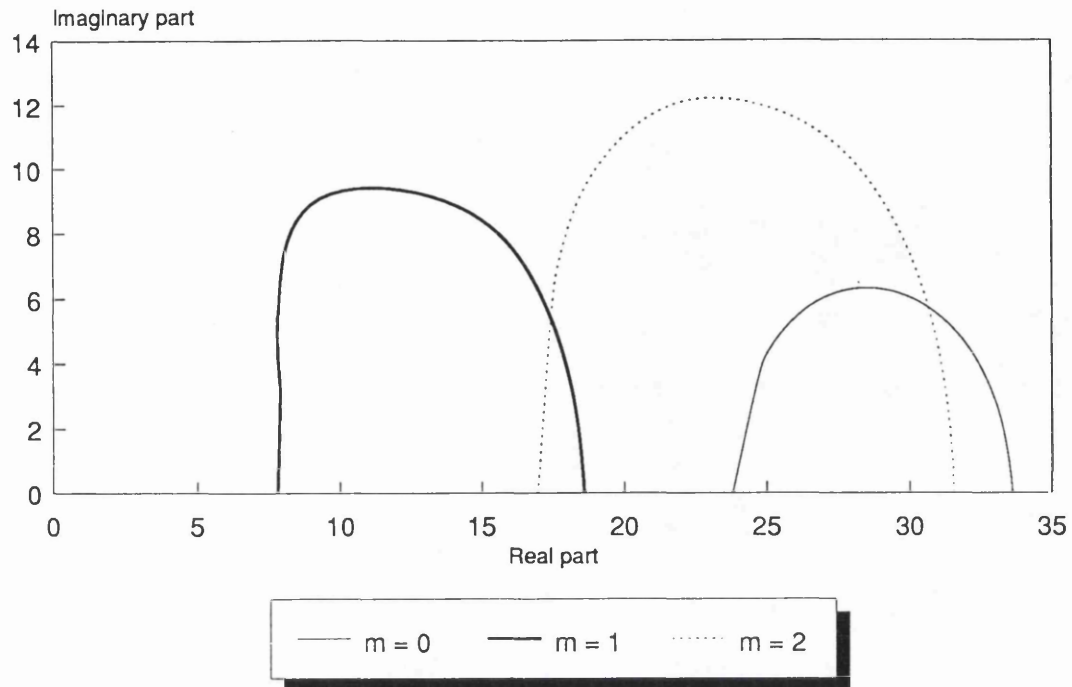


Figure 3.3. Imaginary against real part of frequency with $K = 10$.

VERTICALLY OSCILLATING CYLINDER

4.1- Introduction

The interaction between surface waves and partially immersed bodies (either fixed or floating) has been investigated (see e.g. Wehausen (1971)) before, where in the majority of the applications the gravity waves have been considered only and the effect of the surface tension has been ignored. When gravity is reduced or short waves tend to be important, capillarity cannot be ignored and both restoring forces of gravity and capillarity should be included. Hogan (1979) and Vanden-Broeck (1984) have investigated the capillary-gravity waves in horizontally unbounded regions, but little consideration has been given to the interaction of such waves with vertical boundaries. Hocking (1987c) studied the case of vertical oscillation of a plate partially immersed in a fluid, where both restoring forces, the dynamic variation of the contact angle and contact-angle hysteresis were considered.

Below, it is assumed that a cylinder of radius a is oscillating vertically along its z axis, partially immersed in a fluid with inviscid fluid (with negligible viscosity) of infinite depth with the radial coordinate $a \leq r \leq \infty$, such that the motion is independent of the azimuthal angle ϑ (since the cylinder oscillates parallel to its z axis), and the waves can be linearized due to the small amplitude of the motion. Then the elevation of the surface waves from the free surface of the fluid is determined.

The following notation introduced below shall be

used in the sections of this chapter

$$\bar{J}_0(k, r) = Y_0(kr) J_0'(k) - J_0(kr) Y_0'(k),$$

$$\hat{J}_0(k) = Y_0'^2(k) + J_0'^2(k),$$

$$k_1 = k(Kk^2 + 1), \quad k_2 = k'(Kk'^2 + 1),$$

$$k_3 = k_1 - k_2, \quad k_4 = 3Kk'^2 + 1,$$

$$\bar{e} = e^{i(kr - \pi/4)}, \quad k_5 = k^2K + k'^2K + Kkk' + 1$$

$$\bar{H}_0^{(1)} = \int_0^{\infty} \frac{k}{(k - k') k_5} \frac{H_0^{(1)}(k)}{H_0^{(1)'}(k)} dk$$

$$\bar{H}_0^{(2)} = \int_0^{\infty} \frac{k}{(k - k') k_5} \frac{H_0^{(2)}(k)}{H_0^{(2)'}(k)} dk$$

$$\hat{H}_0^{(1)}(k) = \bar{e} \bar{H}_0^{(1)'}(k), \quad \hat{H}_0^{(2)}(k) = \frac{1}{\bar{e}} \bar{H}_0^{(2)'}(k)$$

where J_0 and Y_0 represent the Bessel functions, H_0 is the Hankel function, K is the capillarity coefficient. The length scale chosen for non-dimensionalization (as explained in chapter 2) is radius of the cylinder. The wavelength $2\pi/k'$ of surface waves have the same frequency as the oscillation of the cylinder, and the angular frequency is σ . It should also be noted that differentiation with respect to the corresponding argument is represented by ' .

4.2- Surface Elevation

The equations of motion and continuity, in the non-dimensional form (as discussed in chapter 2) are respectively

$$\frac{\partial u}{\partial t} = - \frac{\partial p}{\partial r} , \quad (4.1)$$

$$\frac{\partial w}{\partial t} = - \frac{\partial p}{\partial z} , \quad (4.2)$$

$$\frac{\partial u}{\partial r} + \frac{u}{r} + \frac{\partial w}{\partial z} = 0 , \quad (4.3)$$

where the conditions on the free surface are

$$w = \frac{\partial \eta}{\partial t} , \quad (4.4)$$

$$\frac{\partial \eta}{\partial t} - e^{-\sigma t} = \lambda \frac{\partial \eta}{\partial r} \quad \text{at } r = 1 , \quad (4.5)$$

$$p - \eta = - K \left[\frac{\partial^2 \eta}{\partial r^2} + \frac{1}{r} \frac{\partial \eta}{\partial r} \right] , \quad (4.6)$$

and the associated boundary conditions are

$$u = w = 0 \quad \text{as } r \rightarrow \infty , \quad (4.7)$$

$$u \rightarrow 0 , w \rightarrow 0 \quad \text{as } z \rightarrow -\infty , \quad (4.8)$$

$$u = 0 \quad \text{at } r = 1 . \quad (4.9)$$

The pressure, by using a superposition of separable solutions can be expressed as

$$p = e^{-\sigma t} \int_0^{\infty} e^{kz} \left[f_1 J_0(kr) + f_2 Y_0(kr) \right] dk , \quad (4.10)$$

such that ^{by} using equations 4.1, 4.2 & 4.9)

$$f_1 = - \frac{f_2 Y_0'(k)}{J_0'(k)} , \quad (4.11)$$

and since the fluid is outside the cylinder, both Bessel functions are included, that is the singularity at the centre of the cylinder ($r = 0$) does not need to be excluded. Until further notice, the exponential term in t has been omitted since it appears in the right-hand side of all equations.

The relationship between σ and k' (as explained in chapter 2, using the dynamic condition on the free surface) is

$$\sigma^2 = k'(Kk'^2 + 1) = k_2. \quad (4.12)$$

The surface elevation η (using equations 4.6 and 4.10) can be expressed as a non-homogeneous second order ordinary differential equation

$$\frac{\partial^2 \eta}{\partial r^2} + \frac{1}{r} \frac{\partial \eta}{\partial r} - \frac{1}{K} \eta = - \frac{1}{K} \int_0^{\infty} f_3 \bar{J}_0(k, r) dk, \quad (4.13)$$

where

$$f_3 = \frac{f_2}{J_0'(k)}, \quad (4.14)$$

and its solution as the sum of the complementary and principal solutions respectively is (noting that $J_0(r/ K^{1/2})$ and $K_0(r/ K^{1/2})$ are equal)

$$\eta = f_4 K^{1/2} \frac{K_0(r/ K^{1/2})}{K_0'(K^{-1/2})} + \int_0^{\infty} f_2 \frac{k}{k_1} \frac{\bar{J}_0(k, r)}{J_0'(k)} dk, \quad (4.15)$$

where f_2 shall be determined later (when the coefficient f_3 is found by first evaluating f_4 and f_5) by using equation 4.14, as its principal solution should be a linear combination of Bessel functions $J_0(kr)$ and $Y_0(kr)$. Then, using the complementary solution of η (in equation 4.15)

$$\frac{\partial \eta}{\partial r} = f_4 \quad \text{at} \quad r = 1, \quad (4.16)$$

where the coefficient f_4 is determined later (equation 4.32), and finally, the surface elevation can be expressed as (using equations 4.2 and 4.4)

$$\eta = \frac{1}{\sigma^2} \frac{\partial p}{\partial z} = \frac{1}{\sigma^2} \int_0^{\infty} f_3 k \bar{J}_0(k, r) dk. \quad (4.17)$$

The term $K_0(r/\kappa^{1/2})$ of the complementary solution of the surface elevation (in equation 4.15) can be written as an infinite integral of the linear combination of Bessel functions such that

$$K_0\left(\frac{r}{\kappa^{1/2}}\right) = \int_0^{\infty} J_0^*(k) \bar{J}_0(k, r) dk, \quad (4.18)$$

and after multiplying both sides (of equation 4.18) by $rk\bar{J}_0(k, r)$, using the Fourier-Bessel integral theorem's approach (discussed by Sneddon (1951)) and the definition of the Bessel function

$$\lim_{\substack{R \rightarrow \infty \\ k' \rightarrow k}} \int_1^R \int_0^{\infty} rk J_0^*(k) \bar{J}_0(k, r) \bar{J}_0(k', r) dk dr = J_0^*(k) \hat{J}_0(k) \quad (4.19)$$

$$\int_1^{\infty} rk K_0\left(\frac{r}{\kappa^{1/2}}\right) \bar{J}_0(k, r) dr = \frac{-k^2 \kappa^{1/2}}{k_1} \bar{J}_0(k, 1) K_0'(K^{-1/2}) \quad (4.20)$$

respectively, however, since $\bar{J}_0(k, 1)$ is the Wronskian of $Y_0(k)$ and $J_0(k)$ it is equal to $-2/\pi k$, and

$$J_0^*(k) = \frac{2k \kappa^{1/2}}{\pi k_1} \frac{K_0'(K^{-1/2})}{\hat{J}_0(k)}, \quad (4.21)$$

with (using equations 4.18, 4.17 & 4.15)

$$f_3 = \frac{2f_4 \kappa \sigma^2}{\pi k_3 \hat{J}_0(k)} + f_5 \frac{k_2}{k'} \delta(k-k'), \quad (4.22)$$

where f_5 is determined later (from equation 4.32), and δ is the Dirac delta function. Finally, the surface elevation is expressed as (by substituting equation 4.22 in equation 4.17)

$$\eta = \int_0^{\infty} \frac{2f_4 kK}{\pi k_3} \frac{\bar{J}_0(k, r)}{\hat{J}_0(k)} dk + f_5 \bar{J}_0(k', r). \quad (4.23)$$

4.3- Away From The Cylinder

The behaviour of the surface elevation η at a large distance away from the cylinder (that is when the radial distance r approaches infinity) is analyzed here. The Bessel functions are expanded in terms of the Hankel functions as

$$\hat{J}_0(k) = H_0^{(1)'}(k) H_0^{(2)'}(k) \quad (4.24)$$

$$\bar{J}_0(k, r) = \frac{1}{2i} \left\{ H_0^{(1)}(kr) H_0^{(2)'}(k) - H_0^{(2)}(kr) H_0^{(1)'}(k) \right\}, \quad (4.25)$$

where the asymptotic value (as $r \rightarrow \infty$) is

$$\bar{J}_0(k, r) = \frac{1}{2i} \left(\frac{2}{\pi kr} \right)^{1/2} \left\{ \bar{e} H_0^{(2)'}(k) - \frac{1}{\bar{e}} H_0^{(1)'}(k) \right\}, \quad (4.26)$$

and the surface elevation can be expressed as (using equations 4.26, 4.24 and 4.23)

$$\begin{aligned} \eta &= - \int_0^{\infty} \left\{ \frac{if_4 K}{\pi (k-k') k_5} \left[\frac{H_0^{(1)}(k, r)}{H_0^{(1)'}(k)} - \frac{H_0^{(2)}(k, r)}{H_0^{(2)'}(k)} \right] \right\} dk \\ &+ \left[f_5 \bar{J}_0(k', r) \right] \\ &= - \frac{if_4 K}{\pi} \left[\bar{H}_0^{(1)}(k) - \bar{H}_0^{(2)}(k) \right] + \left[f_5 \bar{J}_0(k', r) \right]. \end{aligned} \quad (4.27)$$

In order to avoid singularity as $k \rightarrow k'$, and assuming that $k = i\bar{k}$ and $k = -i\bar{k}$ for $\bar{H}_0^{(1)}(k)$ and $\bar{H}_0^{(2)}(k)$ respectively, as r approaches infinity, for small values of \bar{k} , and noting that

$$\int_0^{\infty} e^{-\bar{k}r} \left(\frac{2i}{\pi\bar{k}r} \right)^{1/2} \left[\frac{\bar{k}}{\sigma^2 - [i\bar{k}(1-K\bar{k}^2) H_0^{(1)'}(i\bar{k})]} - \frac{\bar{k}}{\sigma^2 + [i\bar{k}(1-K\bar{k}^2) H_0^{(2)'}(i\bar{k})]} \right] d\bar{k} \approx \int_0^{\infty} \frac{e^{-\bar{k}r} \bar{k}^{3/2}}{r^{1/2} K_0'(\bar{k})} d\bar{k} \\ = \mathcal{L} \left\{ \bar{k}^{3/2} r^{-1/2} \right\} = \frac{\Gamma(5/2)}{r^3} \rightarrow 0 \quad \text{as } r \rightarrow \infty \quad (4.28)$$

since with \bar{k} is small, $K_0'(\bar{k}) \approx \bar{k}^{-1}$, and (furthermore from Abramowitz (1970))

$$K_0(\bar{k}) = \frac{\pi i}{2} H_0^{(1)}(i\bar{k}) = -\frac{\pi i}{2} H_0^{(2)}(-i\bar{k}) \quad (4.29)$$

$$H_0^{(1)'}(i\bar{k}) = H_0^{(2)'}(-i\bar{k}) = -\frac{2}{\pi} K_0'(\bar{k}), \quad (4.30)$$

then by contour integration

$$\bar{H}_0^{(1)}(k) - \bar{H}_0^{(2)}(k) \approx \frac{i(2\pi k')^{1/2}}{r^{1/2} k_4} \left[\frac{\bar{e}(k')}{H_0^{(1)'}(k')} + \frac{\bar{e}^{-1}(k')}{H_0^{(2)'}(k')} \right]. \quad (4.31)$$

The function f_s , considering the radiation condition and the time dependence $e^{-i\sigma t}$, can be expressed as (using equations 4.30 and 4.27)

$$f_5 = \frac{2ik'K f_4}{k_4 H_0^{(1)'}(k') H_0^{(2)'}(k')}, \quad (4.32)$$

and finally the surface elevation at a large distance away from the cylinder η_∞ , is

$$\eta_\infty = \bar{e}(k') \left(\frac{2}{\pi k' r} \right)^{1/2} \frac{2f_4 K}{k_4 H_0^{(1)'}(k')} \quad \text{as } r \rightarrow \infty, \quad (4.33)$$

noting that the right-hand side should be multiplied by $e^{-i\sigma t}$ term. Then using equation 4.5, f_4 can be determined as

$$f_4 = - \frac{i\pi^2}{4K\sigma f_6}, \quad (4.34)$$

and

$$f_6 = \int_0^\infty \frac{1}{k_3 J_0(k)} dk + \frac{\pi i}{k_4 J_0(k')} + \frac{i\pi^2 \lambda}{4K\sigma}. \quad (4.35)$$

The principal value integral above is evaluated in section 4.5 of this chapter.

Finally, the surface elevation in the transformed coordinate $\bar{\eta} = \eta_\infty r^{1/2}$,

$$\bar{\eta} = \bar{e}(k') \left(\frac{2}{\pi k'} \right)^{1/2} \frac{2f_4 K}{k_4 H_0^{(1)'}(k')}, \quad (4.36)$$

and are presented in Figures 4.1-4.7.

For a given capillarity coefficient K , the value of $\bar{\eta}$ decreases monotonically as λ increases for k' less than unity, as presented in Figures 4.1 and 4.2 (with $K = 10$ and 0.1 respectively). However, the value of surface elevation $\bar{\eta}$, tends to be very small when k' is large (such as 8,4,2,1) for a given K ($= 100$ and 0.1 as presented in Figures 4.3 and 4.4).

The variation of $\bar{\eta}$ with λ for different values of K ($= 0.1, 1$ and 10) for fixed value of k' (of unity) is presented in Figure 4.5. The surface elevation $\bar{\eta}$ for small values of k' , behaves as $K^{1/2}$ and is directly proportional to K for values of $\lambda < 0.5$ and $\lambda \geq 0.5$ respectively, and furthermore for a given value of k' , it ($\bar{\eta}$) decreases as capillarity coefficient increases and λ approaches infinity.

The value of the surface elevation depends on the radius of the cylinder which changes with k' if values of λ and Kk'^2 are zero and constant respectively, such that $\bar{\eta}$ decreases when the radius increases while k' increases. In Figures 4.6 and 4.7 variation of $\bar{\eta}$ with k' (for fixed values of K) and with K (for fixed values of k') are presented respectively.

4.4- On The Cylinder

The surface elevation on the cylinder, that is at $r = 1$, can be expressed as (using equation 4.23)

$$\eta = \int_0^{\infty} \frac{-ik\pi \bar{J}_0(k, r)}{2 \sigma \hat{J}_0(k) k_3 W(K, k')} dk + \frac{k'\pi^2 \bar{J}_0(k', r)}{2\sigma k_4 H_0^{(2)'}(k') H_0^{(1)'}(k') W(K, k')}, \quad (4.37)$$

then

$$\eta|_{r=1} = \frac{\frac{-\pi}{k_4 H_0^{(1)'}(k') H_0^{(2)'}(k')} + i Z(K, k')}{\sigma W(K, k')} \quad (4.38)$$

where

$$W(K, k') = \frac{\pi i}{k_4 H_0^{(1)'}(k') H_0^{(2)'}(k')} + Z(K, k') + \frac{\lambda i \pi^2}{4K\sigma}, \quad (4.39)$$

with $Z(K, k')$ being evaluated in section 4.5.

The value of the surface elevation at different values of K and k' and λ is computed (and presented in Figures 4.8-4.12). Furthermore, as in Figures 4.8 - 4.10, the surface elevation tends to be a constant approaching zero for large values of k' (typically 4 or larger) and $K \geq 1$.

4.5 - Numerical Approach

The principal value integral in equation 4.35 can be expressed as

$$Z(K, k') = I = \int_0^{\infty} \frac{1}{k_3 \hat{J}_0(k)} dk = I_1 - I_2, \quad (4.40)$$

where I_1 and I_2 are

$$I_1 = \frac{1}{\hat{J}_0(k')} \int_0^{\infty} \frac{1}{(k_1 - k_2)} dk = \frac{1}{k_4 \hat{J}_0(k)} \left[\ln \left(\frac{k_2}{Kk'^3} \right)^{1/2} - \frac{3k'K^{1/2}}{(k_4 + 3)^{1/2}} \tan^{-1} \left(\frac{k_4 + 3}{Kk'^2} \right)^{1/2} \right], \quad (4.41)$$

$$I_2 = \int_0^{\infty} \frac{\hat{J}_0(k) - \hat{J}_0(k')}{(k_1 - \sigma^2) \hat{J}_0(k) \hat{J}_0(k')} dk$$

$$= \begin{cases} \frac{1}{k_4} \frac{\hat{J}_0'(k')}{\hat{J}_0^2(k')} & \text{as } k \rightarrow k', \\ -\frac{1}{\hat{J}_0(k') k_2} & \text{as } k \rightarrow 0. \end{cases} \quad (4.42)$$

For other values of k the above principal value integral is integrated numerically by the trapezoidal rule from zero (its lower limit) to a large value of k ($= 200$ with step size of 0.1 , where satisfactory accuracy is obtained according to the computational results), and then analytically to its upper limit infinity (using the asymptotic value, since I_2 tends to be indefinite at large values of k). The computation is performed for different values of the capillarity coefficient K ($= 0.1, 1.0$ and 10.0) and k' ($= 0.1, 0.2, 0.4, 0.6, 0.8, 1, 2, 4$ and 8 for each value of K) with $0 \leq \lambda \rightarrow \infty$ ($= 0.0, 0.1, 0.2, 0.5, 1.0, 2.0, 5.0$ and 10 , where the last value satisfactorily presents the upper limit of λ from numerical point of view).

The step size is taken to be 0.1 since the computed values are accurate to three decimal points with smaller step size such as $0.05, 0.025, 0.0125$ according to the computational results.

The upper value for the trapezoidal rule is taken to be 200 since with larger values, the accuracy is to the second decimal points.

The capillarity coefficient K is taken to be $100, 10, 1, 0.1, 0.01, 0.001$, where the upper value is according to the experimental results.

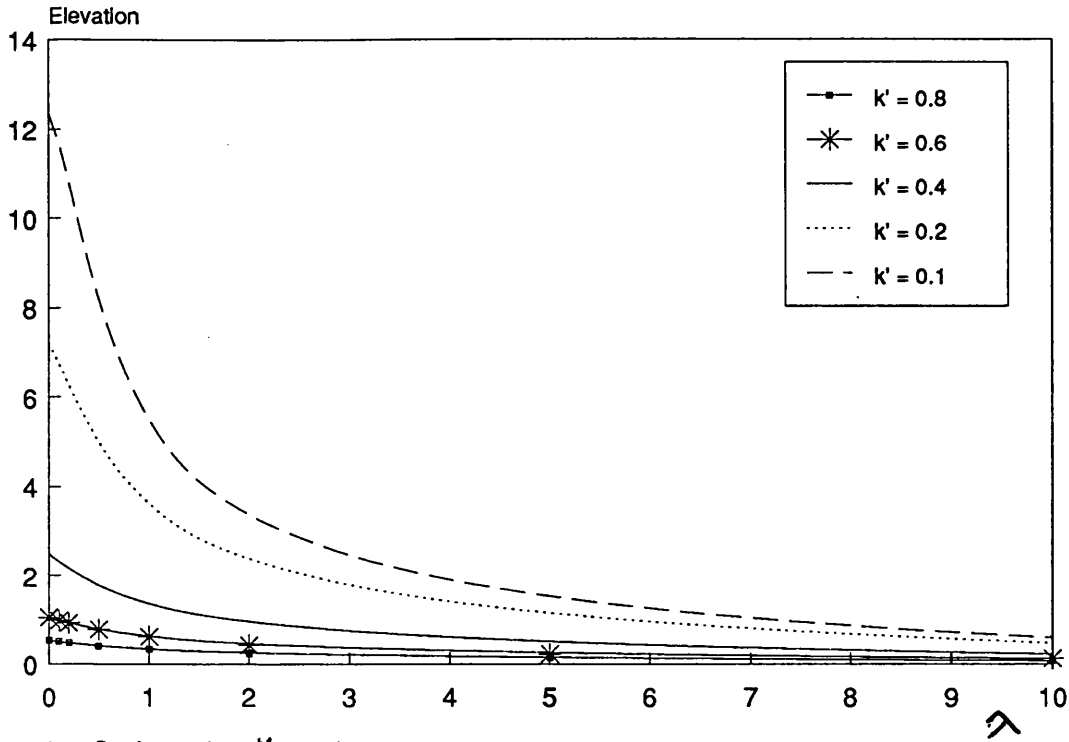


Figure 4.1. Surface elevation at large distance away from the cylinder; $K = 10$.

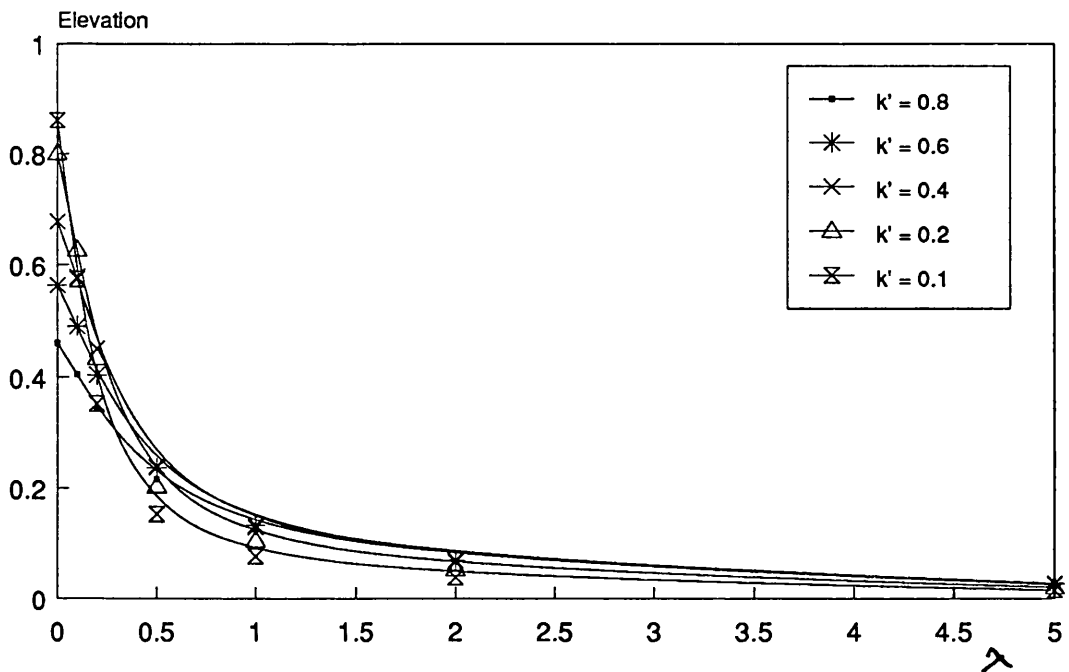


Figure 4.2. Surface elevation at large distance away from the cylinder; $K = 0.1$

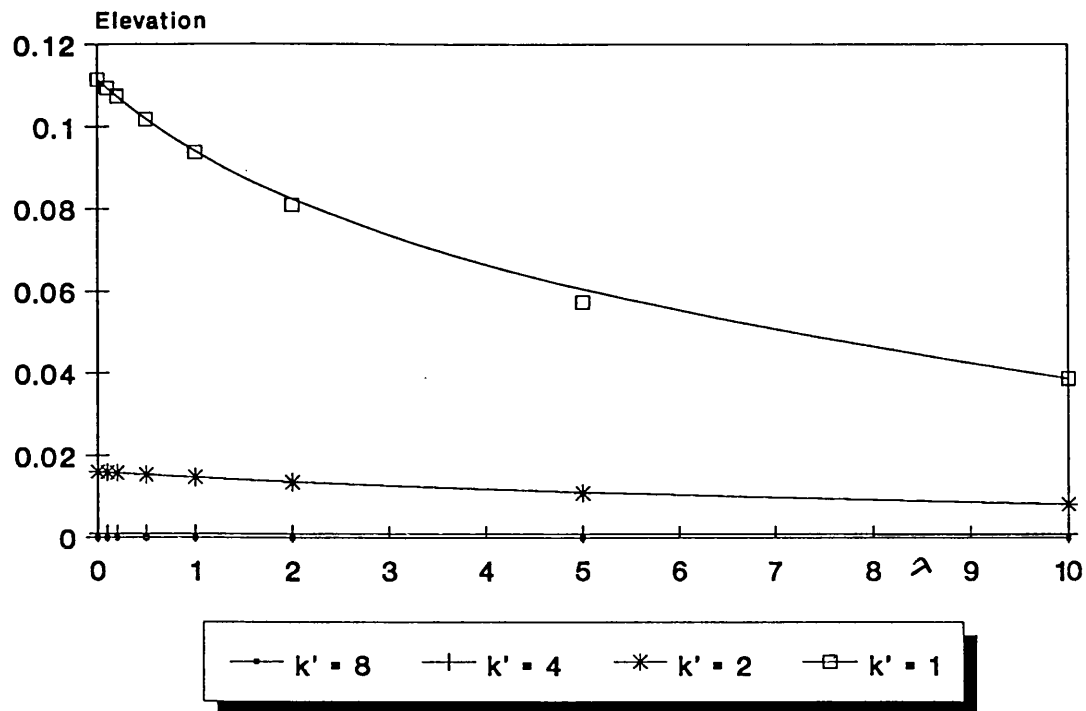


Figure 4.3. Surface elevation at large distance away from the cylinder; $K = 100$

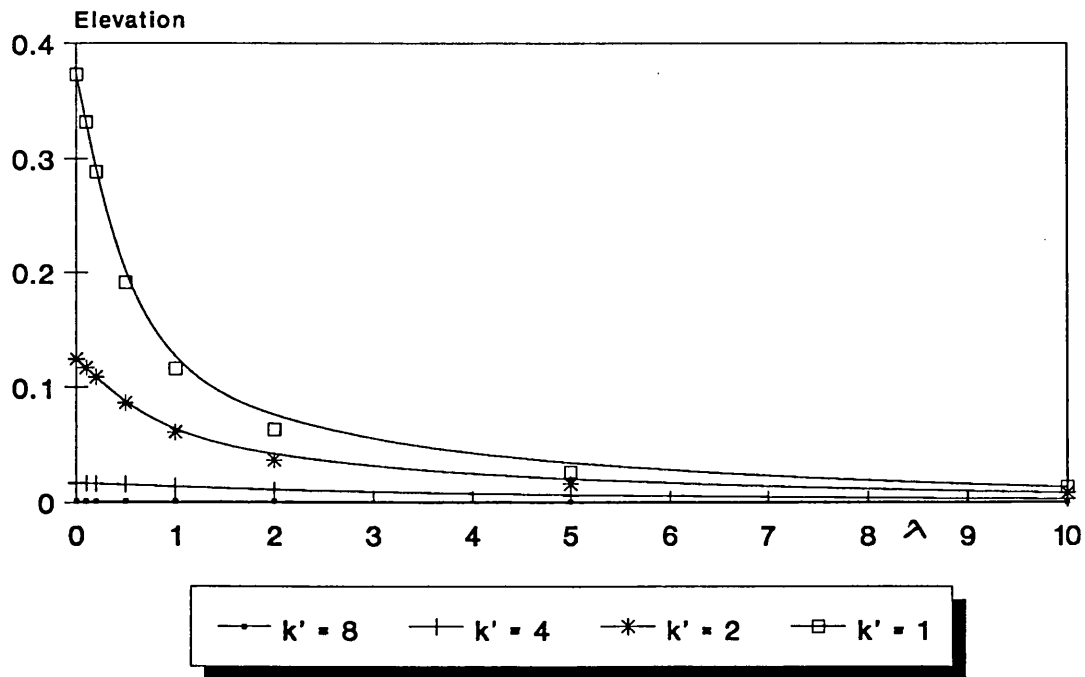


Figure 4.4. Surface elevation at large distance away from the cylinder; $K = 0.1$

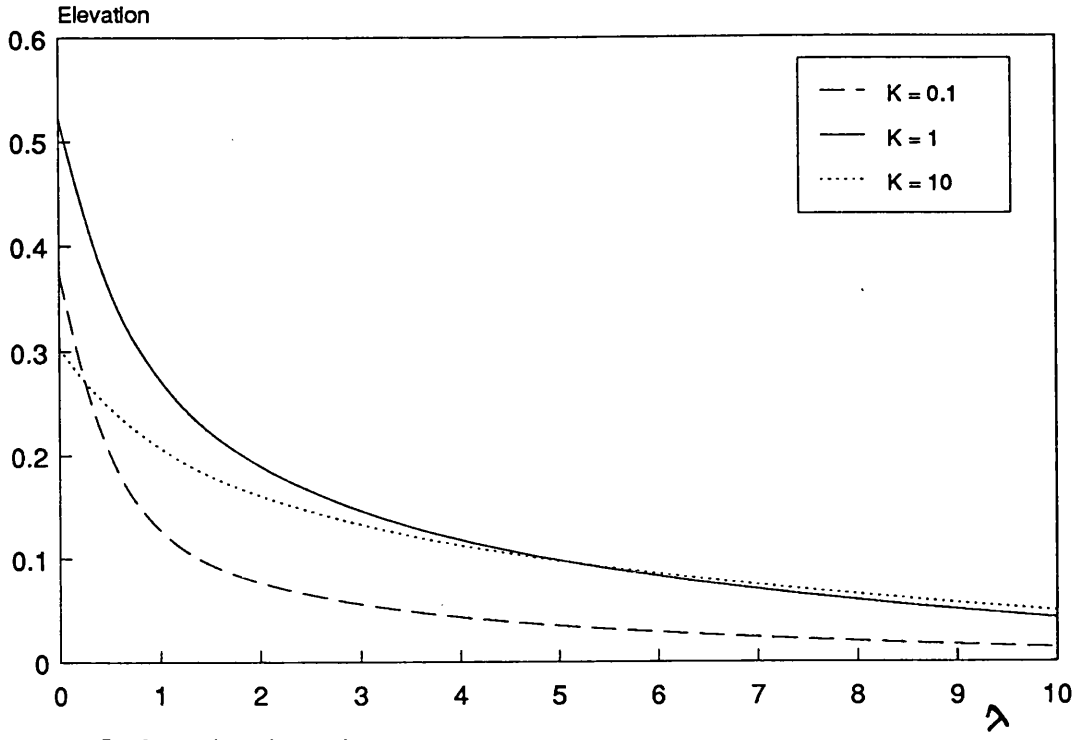


Figure 4.5. Surface elevation at large distance away from the cylinder; $k' = 1$.

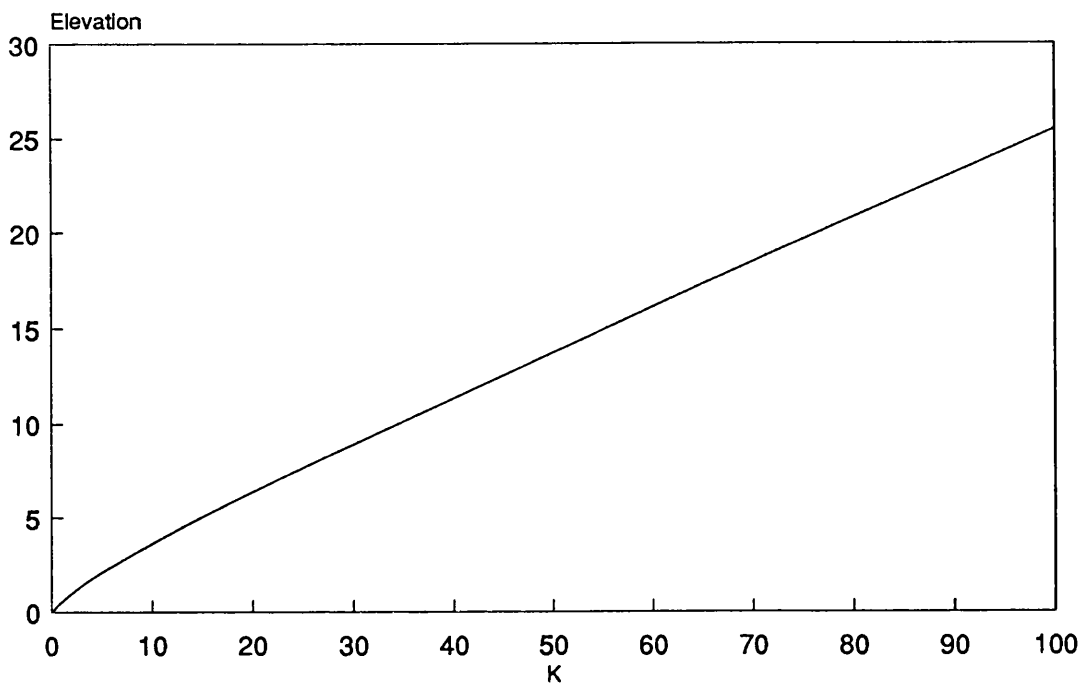


Figure 4.6. Elevation at large distance as a function of K , $\lambda = 0$ & $Kk'^2 = 1$.

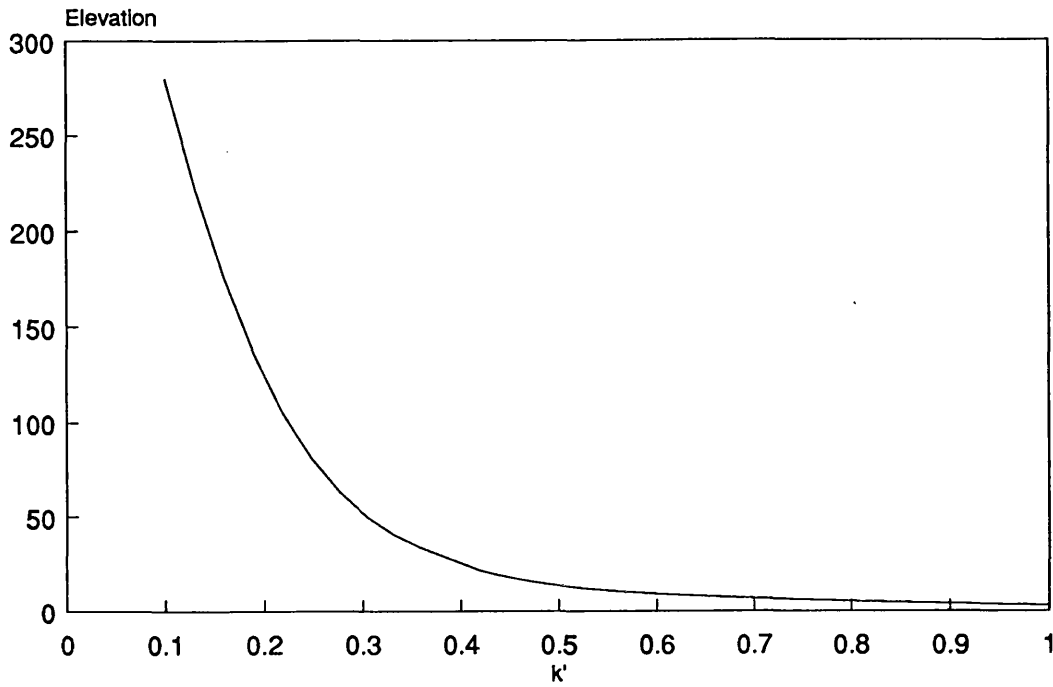


Figure 4.7. Surface elevation at large distance away from the cylinder as a function of k' ; $\lambda = 0$ & $Kk'^2 = 1$.

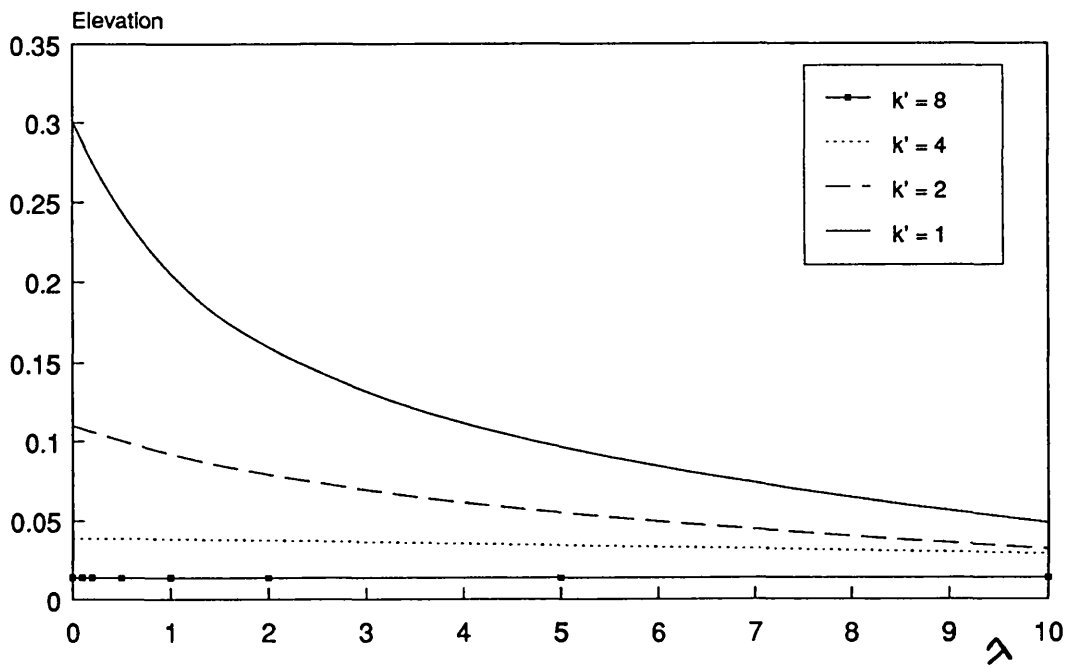


Figure 4.8. Surface elevation on the cylinder; $K = 10$.

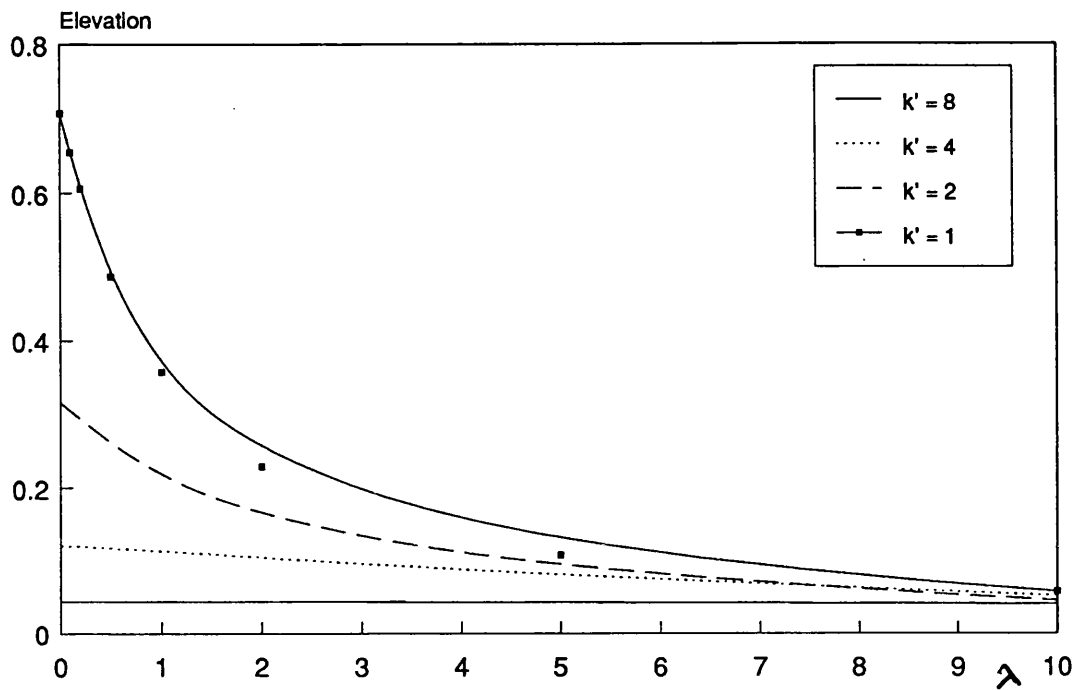


Figure 4.9. Surface elevation on the cylinder; $K = 1$.

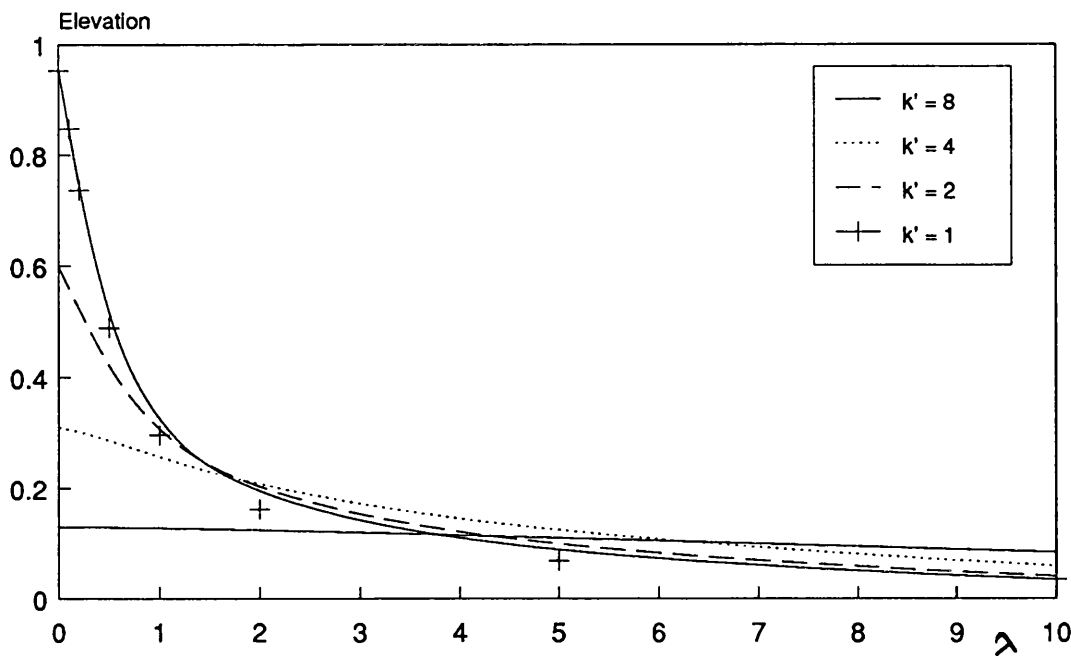


Figure 4.10. Surface elevation on the cylinder; $K = 0.1$.

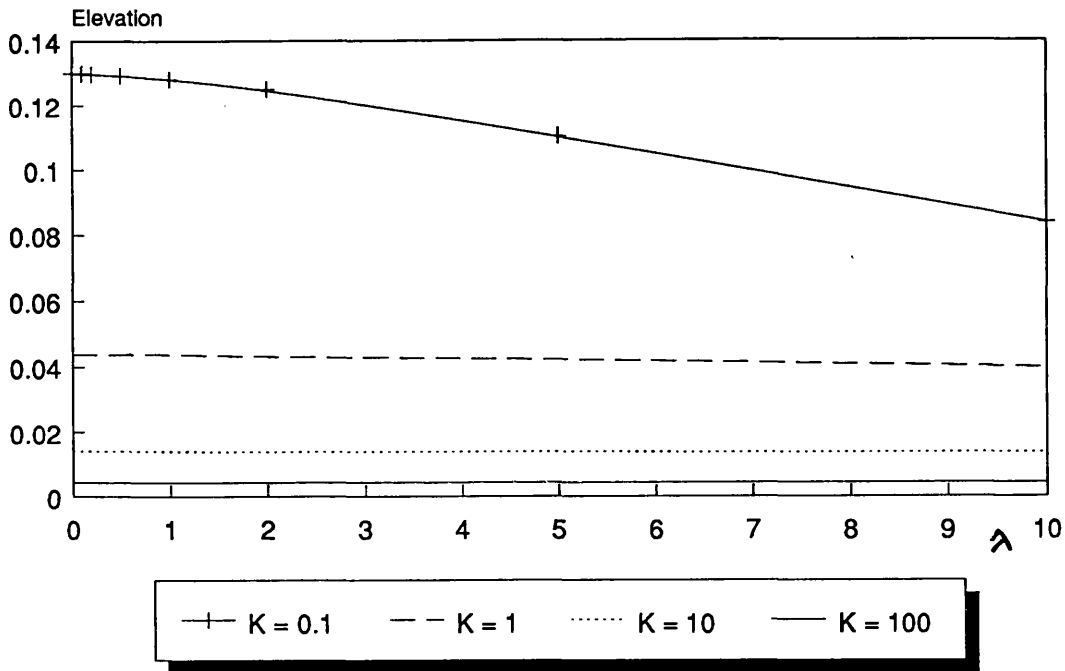


Figure 4.11. Surface elevation on the cylinder; $k' = 8$.

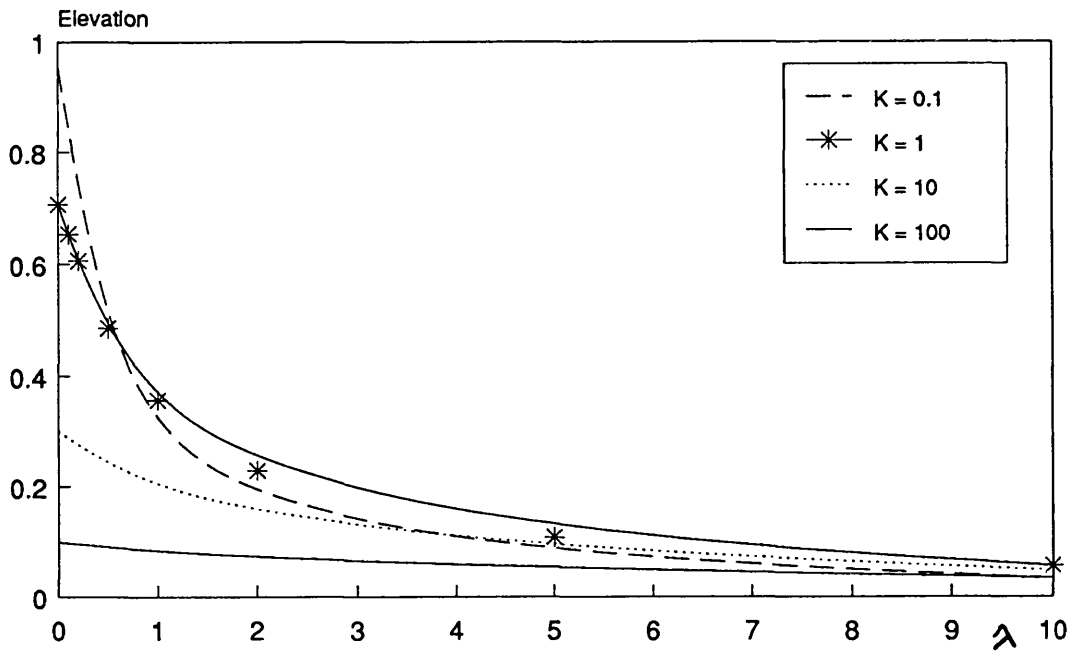


Figure 4.12. Surface elevation on the cylinder; $k' = 1$.

WAVES PRODUCED BY HORIZONTAL OSCILLATION OF A CYLINDER

5.1 - Introduction

Waves on the free surface of a fluid in a gravitational field can be produced by the normal motion of a wavemaker immersed in the fluid. The displacement of the fluid by the wavemaker leads to a deformation of the free surface, which propagates away from the wavemaker. The problem is then to determine the characteristics of this propagating wave train, given the motion of the wavemaker.

There has been a number of investigations and research on the propagation of water wave trains but most of them have ignored the presence of surface tension, which in addition to gravity acts to provide a restoring force on the free surface. There has been some work by Hogan (1979) and Vanden-Broeck (1983) on capillary-gravity waves in horizontally unbounded regions, although the interaction of these waves with the boundaries is not taken into account. The dispersion relation for waves controlled by the combination of gravity and surface tension is well known, and suffices to determine the properties of such capillary-gravity waves in the absence of vertical boundaries. However, since the presence of surface tension increases the order of the dynamic boundary condition on the pressure at the free surface, the problem of capillary-gravity waves in a horizontally unbounded fluid can be solved only when some suitable edge condition is applied where the free surface and the boundary intersect. In this chapter, the edge condition which has been justified in chapter 1, is used.

Here, the elevation of surface waves (both at a large

distance and on the wavemaker) produced by horizontal oscillation of a vertical cylinder, is studied. The surface elevation at large distances away from the cylinder shall be studied both when the fluid is of finite and of infinite depth.

The following notation is introduced which shall be used in the following sections

$$\bar{J}_1(k, r) = Y_1(kr) J_1'(k) - J_1(kr) Y_1'(k),$$

$$\hat{J}_1(k) = Y_1'^2(k) + J_1'^2(k),$$

$$k_1 = 1 + Kk^2,$$

$$k_2 = k(1 + Kk^2) \tanh(kh),$$

$$k_3 = k'(1 + Kk'^2) \tanh(k'h),$$

$$k_4 = 1 + Kk'^2,$$

$$k_5 = 1 + 3Kk'^2,$$

$$\bar{H}_1(k) = H_1^{(1)'}(k) H_1^{(2)'}(k).$$

Consider a vertical cylinder of radius a which is partially immersed in the fluid, and whose axis is the z -axis. If a force is applied to the cylinder in a horizontal direction, the fluid will be displaced which leads to the free surface being deformed. As well as gravity, surface tension acts on the surface to provide a restoring force. The consequence is a propagating wave train whose characteristics are interesting to be determined.

5.2 - Surface Elevation

The velocity potential has two components: the forcing ϕ_1 , and the scattering part ϕ_2 . The total velocity potential ϕ is the sum of ϕ_1 and ϕ_2 . The potential ϕ_1 has

r and ϑ dependence and no z - dependence. However, ϕ_2 is a function of r , ϑ and z . The ϑ - dependence is like $\cos\vartheta$ and time dependence is like $e^{+i\sigma t}$.

The following conditions should be satisfied by the velocity potential and its components

$$\frac{\partial\phi}{\partial r} = e^{+i\sigma t} \cos\vartheta \quad \text{on } r=1, \quad (5.1)$$

$$\frac{\partial\phi_2}{\partial z} \rightarrow 0 \quad \text{at the bottom,} \quad (5.2)$$

$$\phi_1 \rightarrow 0 \quad \text{as } r \rightarrow \infty. \quad (5.3)$$

The edge conditions are (using the non-dimensionalization discussed in chapter 2)

$$\frac{\partial\phi_2}{\partial r} = 0 \quad \text{on } r = 1, \quad (5.4)$$

$$\frac{\partial\eta}{\partial t} = \lambda \frac{\partial\eta}{\partial r} \quad \text{on } r = 1. \quad (5.5)$$

Now, the first component of the velocity potential ϕ_1 , satisfies Laplace's equation and is

$$\phi_1 = (Ar + \frac{B}{r}) \cos\vartheta e^{+i\sigma t}. \quad (5.6)$$

Therefore $A = 0$ (using equation 5.3). Hence ϕ_1 (by applying equations 5.1 and 5.4) becomes

$$\phi_1 = - \frac{e^{+i\sigma t}}{r} \cos\vartheta. \quad (5.7)$$

The second component ϕ_2 , has two different z - components depending on whether the height of the cylinder is finite or infinite.

5.3 - Finite Depth

In this case, the depth of the fluid is h (finite) and therefore the z -dependence of ϕ_2 is $\cosh\{k(z+h)\}$ (satisfying condition 5.2). Since the fluid is outside the cylinder, the radial dependence of ϕ_2 is a combination of the two Bessel functions $J_1(kr)$ and $Y_1(kr)$ and hence

$$\phi_2 = \int_0^{\infty} \left[C J_1(kr) + D Y_1(kr) \right] \frac{\cosh\{k(z+h)\}}{\cosh(kh)} \cos\vartheta \, dk. \quad (5.8)$$

The coefficient C can be written in terms of D (by using equation 5.4) and if $E(k)$ is written as

$$E(k) = \frac{D(k)}{J_1'(k)}, \quad (5.9)$$

then the total velocity potential ϕ is

$$\phi = e^{-i\sigma t} \cos\vartheta \left\{ -\frac{1}{r} + \int_0^{\infty} E(k) \bar{J}_1(k, r) \frac{\cosh\{k(z+h)\}}{\cosh(kh)} \, dk \right\}. \quad (5.10)$$

The time dependence $e^{-i\sigma t}$ can be omitted since it appears in every term. Since

$$u = \frac{\partial\phi}{\partial r} \quad \text{and} \quad \frac{\partial u}{\partial t} = -\frac{\partial p}{\partial r}, \quad (5.11)$$

therefore

$$p = -i\sigma \cos\vartheta \left\{ -\frac{1}{r} + \int_0^{\infty} E(k) \bar{J}_1(k, r) \frac{\cosh\{k(z+h)\}}{\cosh(kh)} \, dk \right\}. \quad (5.12)$$

By noting that

$$w = \frac{\partial\eta}{\partial t} \quad \text{at } z = 0 \quad \text{and} \quad \frac{\partial w}{\partial t} = -\frac{\partial p}{\partial z}, \quad (5.13)$$

We have,

$$\eta = - \frac{i \cos\vartheta}{\sigma} \int_0^{\infty} E(k) k \bar{J}_1(k, r) \tanh(kh) dk. \quad (5.14)$$

At the free surface, the disturbance to the dynamic and hydrostatic parts of the pressure (as mentioned in chapter 2) must be balanced by the capillary pressure, which is proportional to the local curvature of the surface. Hence at $z = 0$,

$$\eta - K \left[\frac{\partial^2 \eta}{\partial r^2} + \frac{1}{r} \frac{\partial \eta}{\partial r} + \frac{1}{r^2} \frac{\partial^2 \eta}{\partial \vartheta^2} \right] = p, \quad (5.15)$$

where the parameter K , an inverse Bond number, is defined as

$$K = \frac{\gamma}{\rho g a^2}, \quad (5.16)$$

but $\frac{\partial^2 \eta}{\partial \vartheta^2} = -\eta$ (from equation 5.14), then

$$\eta = Qi K_1 \left(\frac{r}{K^{1/2}} \right) \cos\vartheta + \frac{i\sigma \cos\vartheta}{r} - \int_0^{\infty} E(k) \frac{i\sigma \cos\vartheta \bar{J}_1(k, r)}{k_1} dk, \quad (5.17)$$

where

$$Q = \frac{K^{1/2} L}{K_1' \left(\frac{1}{K^{1/2}} \right)}, \quad (5.18)$$

and L is some parameter which shall be determined later (in equation 5.24). Writing the first two terms of equation 5.17 as integrals with the same kernel as the third term (following Fourier-Bessel Integral Theorem's approach) gives,

$$\eta = 2KLi \cos\vartheta \int_0^{\infty} \frac{\bar{J}_1(k, r)}{\pi k_1 \hat{J}_1(k)} dk - 2i\sigma \cos\vartheta \int_0^{\infty} \frac{\bar{J}_1(k, r)}{\pi k^2 \hat{J}_1(k)} dk$$

$$- i\sigma \cos\vartheta \int_0^{\infty} \frac{1}{k_1} E(k) \bar{J}_1(k, r) dk. \quad (5.19)$$

Now, by equating the two expressions for η ,

$$E(k) = \frac{2\sigma \left(KLk^2 - \sigma k_1 \right)}{\pi k^2 \hat{J}_1(k) \left(\sigma^2 - k_2 \right)} + D \delta(k-k'), \quad (5.20)$$

where δ is the Dirac delta function and the coefficient D is to be determined later. Therefore the equation for η has the following form (by substituting $E(k)$ into the equation for η),

$$\eta = - \frac{i}{\sigma} \cos\vartheta \int_0^{\infty} \frac{\tanh(kh) \bar{J}_1(k, r) 2\sigma \left(KLk^2 - \sigma k_1 \right)}{\pi \hat{J}_1(k) k \left(\sigma^2 - k_2 \right)} dk$$

$$- \frac{i}{\sigma} \cos\vartheta \int_0^{\infty} k \tanh(kh) \bar{J}_1(k, r) D \delta(k-k') dk. \quad (5.21)$$

To find the surface elevation of the fluid from the free surface at a large distance away from the cylinder, η_{∞} , as in chapter 4, the asymptotic forms of the functions of r should be written. Then the denominator of the first term of the above equation is factorized, followed by k approaching k' . By satisfying the radiation condition, the parameter D can be obtained as

$$D = \frac{2\sigma i \left[KLk'^2 - \sigma k_4 \right]}{k'^2 \bar{H}_1(k')} \cdot \frac{1}{\tanh(k'h) k_5 + k'h k_4 \operatorname{sech}^2(k'h)}, \quad (5.22)$$

and hence

$$\eta_\infty = 2 \left(\frac{2}{\pi k' r} \right)^{1/2} \frac{\cos\vartheta \tanh(k'h) e^{-i(k'r-3\pi/4)}}{H_1^{(2)'}(k')} \cdot \frac{\left[KLk'^2 - \sigma k_4 \right] i}{k' \left[\tanh(k'h) k_5 + k'h k_4 \operatorname{sech}^2(k'h) \right]}. \quad (5.23)$$

Now applying the edge condition 5.5, the parameter L can be determined as

$$L = \frac{G_1(h, k')}{G_2(h, k')} \quad (5.24)$$

where

$$G_1(h, k') = \lambda\sigma + \frac{4\sigma^2 k_4 \tanh(k'h)}{\pi k'^2 \bar{H}_1(k') M(k')} - \frac{4\sigma^2 i}{\pi^2} N_1, \quad (5.25)$$

$$G_2(h, k') = \lambda + \frac{4K\sigma \tanh(k'h)}{\pi \bar{H}_1(k') M(k')} - \frac{4\sigma Ki}{\pi^2} N_2, \quad (5.26)$$

$$M(k') = \tanh(k'h)k_5 + k'hk_4 \operatorname{sech}^2(k'h) \quad (5.27)$$

$$N_1 = \int_0^\infty \frac{k_1 \tanh(kh)}{k^2 J_1(k) (\sigma^2 - k_2)} dk, \quad (5.28)$$

$$N_2 = \int_0^{\infty} \frac{\tanh(kh)}{\bar{J}_1(k) (\sigma^2 - k_2)} dk. \quad (5.29)$$

The principle value integrals shall be evaluated in section 5.7.

The surface elevation at large distances away from the cylinder is obtained for different depths h , namely 0.1 (corresponding to shallow water), 1 and 100 (corresponding to infinite depths). For each of these depths, different values for the parameter k' , namely 10, 5, 2, 1, and 1 to 0.2 with interval of 0.1 have been tried.

Figures 5.1-5.17 show that $|\eta_{\infty}|r^{1/2}$ is a monotonically decreasing function of K . The curves seem to attain their limits when $\lambda \rightarrow 10$, although $\lambda = 10$ is not large enough to be infinite. Another interesting feature about these curves is that when k' changes from 10 to 0.2, the curves first have minima and as k' reduces, they gradually seem to have maxima, although the peaks are rather flat. The behaviour of these curves is the same for different depths, that is when h is 100, 1 or 0.1.

5.4 - Infinite Depth

Here, the depth h is taken to be infinite. The corresponding velocity potential, therefore becomes:

$$\phi = e^{+i\sigma t} \cos\vartheta \left\{ -\frac{1}{r} + \int_0^{\infty} E(k) \bar{J}_1(k, r) e^{kz} dk \right\}, \quad (5.30)$$

which satisfies the boundary conditions 5.1, 5.2 and 5.3. The pressure and the surface elevation are

$$p = i\sigma \cos\vartheta \left\{ -\frac{1}{r} + \int_0^{\infty} E(k) \bar{J}_1(k, r) e^{kz} dk \right\}, \quad (5.31)$$

$$\eta = Qi K_1 \left(\frac{r}{K^{1/2}} \right) \cos\vartheta + \frac{i\sigma \cos\vartheta}{r} + \int_0^{\infty} E(k) \frac{-i\sigma \cos\vartheta \bar{J}_1(k, r)}{k_1} dk, \quad (5.32)$$

respectively.

An identical procedure to the one in the previous section for finite depth will lead to the following form for surface elevation from the free surface η_{∞} , when the depth h is infinite at large distances away from the cylinder,

$$|\eta_{\infty}| r^{1/2} = 2 \left(\frac{2}{\pi k' r} \right)^{1/2} \left| \frac{\cos\vartheta (KLk'^2 - \sigma k_4)}{k' k_5 H_1^{(2)'}(k')} \right|. \quad (5.33)$$

The parameter L is (by using the edge condition 5.5)

$$L = \frac{G_1(h, k')}{G_2(h, k')} \quad (5.34)$$

where

$$G_1(h, k') = \lambda\sigma + \frac{4\sigma^2 k_4}{\pi k'^2 \bar{H}_1(k') M(k')} - \frac{4\sigma^2 i}{\pi^2} N_3, \quad (5.35)$$

$$G_2(h, k') = \lambda + \frac{4K\sigma}{\pi \bar{H}_1(k') M(k')} - \frac{4\sigma Ki}{\pi^2} N_4, \quad (5.36)$$

with

$$N_3 = \int_0^{\infty} \frac{k_1}{k^2 J_1(k) (\sigma^2 - kk_1)} dk, \quad (5.37)$$

$$N_4 = \int_0^{\infty} \frac{1}{J_1(k) (\sigma^2 - kk_1)} dk, \quad (5.38)$$

and $M(k') = k_5$.

Comparing the surface elevation of infinite depth and finite depth, it can be noticed that when the finite depth problem for large depth is solved an identical answer to the infinite depth problem is obtained proving the validity of the expression for the finite depth.

Figures 5.7-5.12 (which correspond to the large depth) show that the surface elevation of the surface waves at large distances monotonically increases as K decreases. When k' changes from 10 to 1, the curves appear to find minima, whereas in the interval of 1 to 0.2, the minima gradually change to maxima (this behaviour is more apparent in the case of smallest capillarity coefficient).

5.5 - Surface Elevation On The Cylinder

In the previous sections, the elevation of water waves above the free surface at large distance away from the cylinder, was determined. In this section, the elevation of the waves above the free surface on the outer surface of the cylinder is studied.

In equation 5.14, if r is given the value of 1, which is the radius of the cylinder, the surface elevation on the cylinder becomes

$$\begin{aligned}
|\eta|_{r=1} &= -\frac{i \cos\vartheta}{\sigma} \int_0^{\infty} E(k) k \bar{J}_1(k,1) \tanh(kh) dk \\
&= \frac{2i \cos\vartheta}{\pi\sigma} \int_0^{\infty} E(k) \tanh(kh) dk \\
&= \frac{2i \cos\vartheta}{\pi\sigma} \int_0^{\infty} \frac{\tanh(kh) 2\sigma \left(KLk^2 + \sigma k_1 \right)}{\pi k^2 \hat{J}_1(k) \left(\sigma^2 - k_2 \right)} dk \\
&+ \frac{2i \cos\vartheta}{\pi\sigma} \tanh(k'h) D = \left| \lambda \cos\vartheta \left(\frac{L - \sigma}{\sigma} \right) \right|. \quad (5.39)
\end{aligned}$$

The surface elevation on the cylinder is a monotonic decreasing function of K , regardless of the value of h . The bigger k' , the smoother the curves. For smaller k' , the curves tend to their limits faster as λ grows, and the steeper are the curves. Generally, λ as 10 is large enough for our calculations, although it is not infinite. $|\eta|_{r=1}$ is a monotonically increasing function of λ (Figures 5.18-5.32). This behaviour is repeated when the depth is changed to 100 or 0.1 although they are the two extremes for the depth. The smaller the height, the sooner the corresponding curves tend to their limits.

5.6 - Numerical Approach

The two principal value integrals, N_2 and N_5 should be evaluated, where

$$N_5 = \int_0^{\infty} \frac{\tanh(kh)}{k^2 \hat{J}_1(k) \left(\sigma^2 - k_2 \right)} dk, \quad (5.40)$$

and

$$N_2 = \int_0^{\infty} \frac{\tanh(kh)}{\hat{J}_1(k) (\sigma^2 - k_2)} dk. \quad (5.41)$$

From these two N_1 (in equation 5.28) can also be obtained, which is $N_5 + K N_2$.

$$\text{When } k \rightarrow 0, \begin{cases} \tanh(kh) \cong kh, \\ \hat{J}_1(k) \cong \frac{1}{k^4}, \end{cases} \quad \text{and hence } N_3 \rightarrow 0.$$

$$\text{When } k \text{ is large, } \begin{cases} \tanh(kh) \rightarrow 1, \\ \hat{J}_1(k) \cong \frac{2}{\pi k}, \end{cases} \quad \text{and therefore}$$

$$\int_X^{\infty} \frac{\tanh(kh)}{k^2 \hat{J}_1(k) (\sigma^2 - k_2)} dk \cong -\frac{\pi}{6KX^3}, \quad (5.42)$$

where X is some large number, which is taken to be 20 in the numerical calculations.

Now, for other values of k , the limits of integration can be divided into smaller divisions ; 0 to $k' - \zeta$, $k' - \zeta$ to $k' - \varepsilon$, $k' + \varepsilon$ to $k' + \zeta$, $k' + \zeta$ to X and X to ∞ , where ζ is the step size of the integration using the trapezium rule, and ε is a small number which gives the smallest interval near k' . Therefore

$$N_3 = \left\{ \frac{1}{2} (\zeta - \varepsilon) \left[f(k' + \zeta) + f(k' + \varepsilon) + f(k' - \varepsilon) + f(k' - \zeta) \right] \right\} - \frac{\pi}{6KX^3} + \int_0^{k' - \zeta} f(k) dk + \int_{k' - \zeta}^X f(k) dk, \quad (5.43)$$

where

$$f(k) = \frac{\tanh(kh)}{k^2 \hat{J}_1(k) (\sigma^2 - k_2)} dk. \quad (5.44)$$

The integrand above between the two different sets of limits can be evaluated numerically using the trapezium rule. The step size for the integration is taken to be 0.1, and ε is 0.01. Halving the step size from 0.1 to 0.05 and reducing ε by a factor of 10 from 0.01 to 0.001, improves the results only in the 7th decimal place. Therefore in these calculations ζ is taken to be 0.1 and ε is 0.01.

The integrand in equation 5.29 approaches zero, when $k \rightarrow 0$. When $k \gg 1$, $N_2(k) \cong -\frac{\pi}{2KX}$, and because of the pole at $k = k'$,

$$N_2(k) = \int_0^{k' - \zeta} \frac{\tanh(kh)}{\hat{J}_1(k) (\sigma^2 - k_2)} dk + \int_{k' + \zeta}^X \frac{\tanh(kh)}{\hat{J}_1(k) (\sigma^2 - k_2)} dk$$

$$+ \left\{ \frac{1}{2} (\zeta - \varepsilon) [g(k' + \zeta) + g(k' + \varepsilon) + g(k' - \varepsilon) + g(k' - \zeta)] \right\} - \frac{\pi}{2KX}, \quad (5.45)$$

where, here

$$g(k) = \frac{\tanh(kh)}{\hat{J}_1(k) (\sigma^2 - k_2)}. \quad (5.46)$$

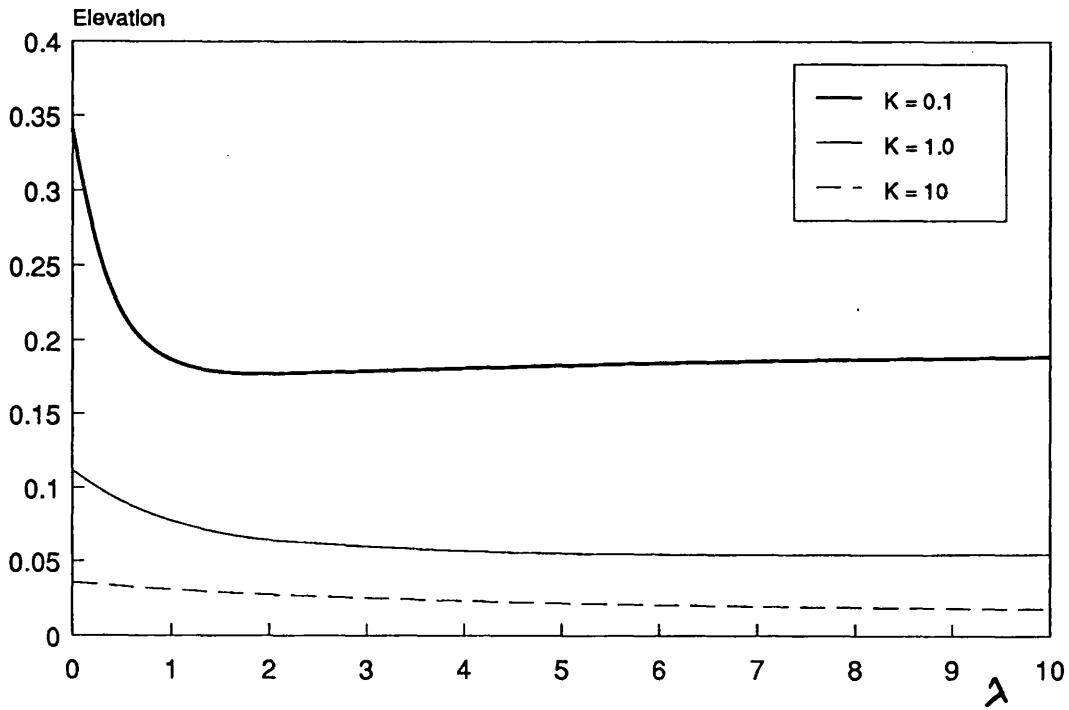


Figure 5.1. Elevation as a function of λ at a large distance from the cylinder; $k' = 5$ and height = 1.

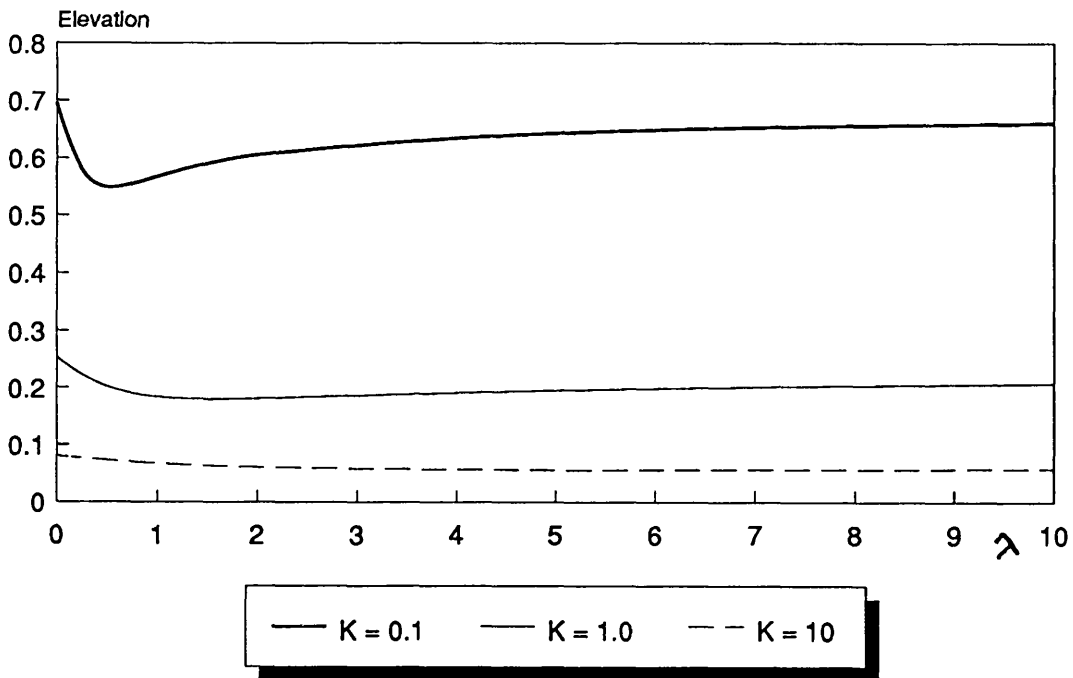


Figure 5.2. Elevation as a function of λ at large distance; $k' = 2$ & height = 1.

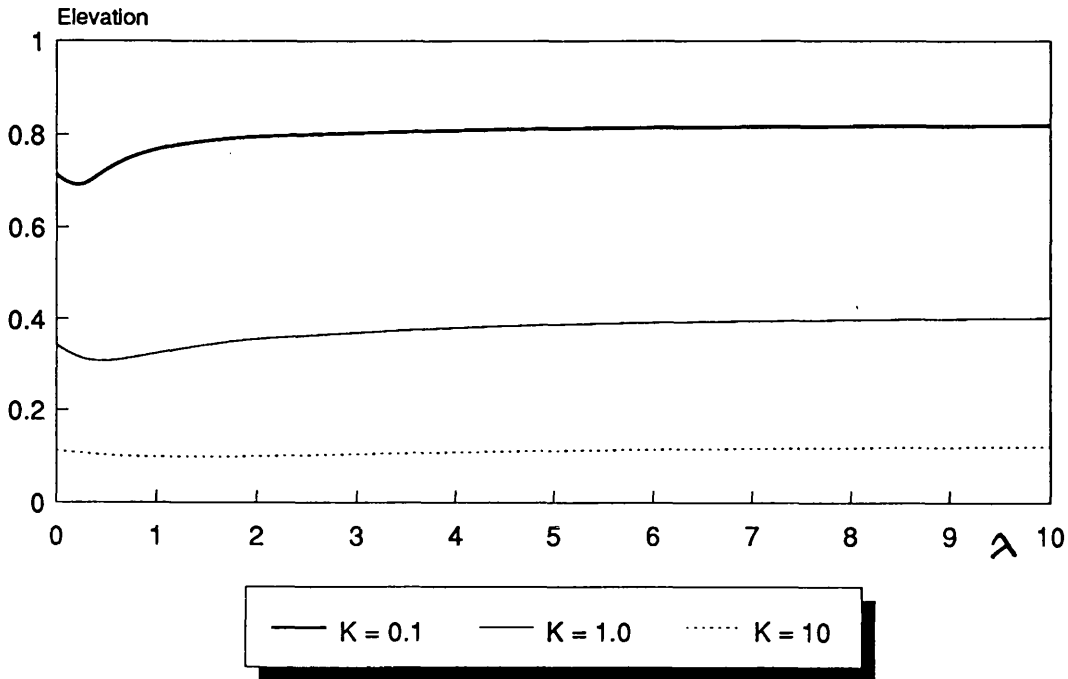


Figure 5.3. Elevation as a function of λ at a large distance from the cylinder; $k' = 1$, height = 1.

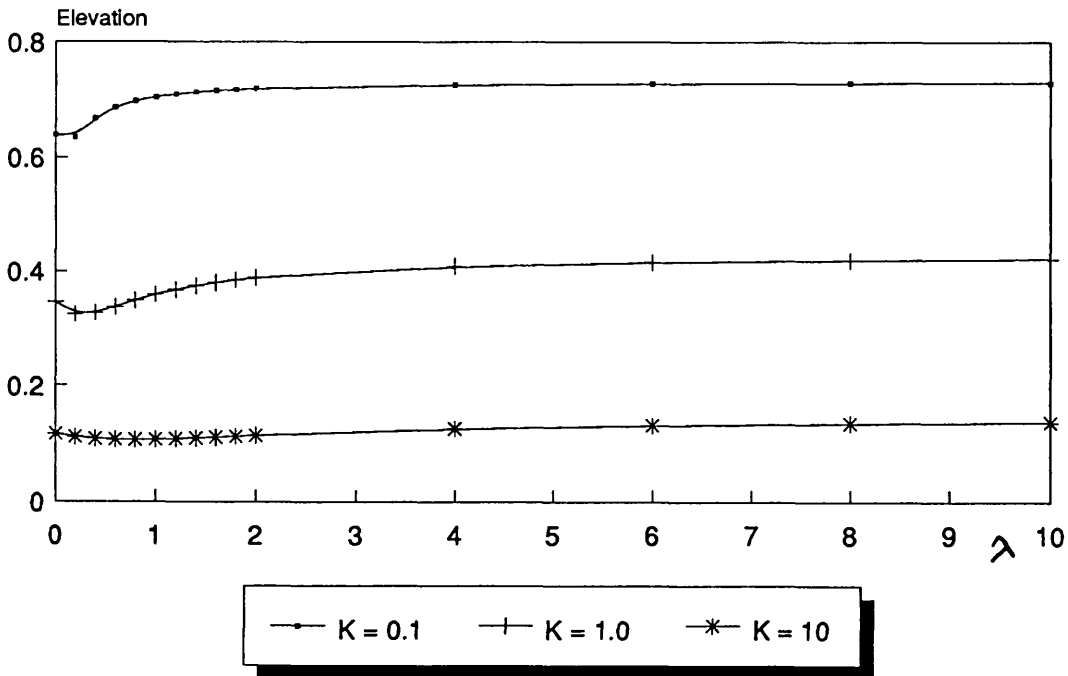


Figure 5.4. Elevation as a function of λ at large distance; $k' = 0.8$, height = 1.

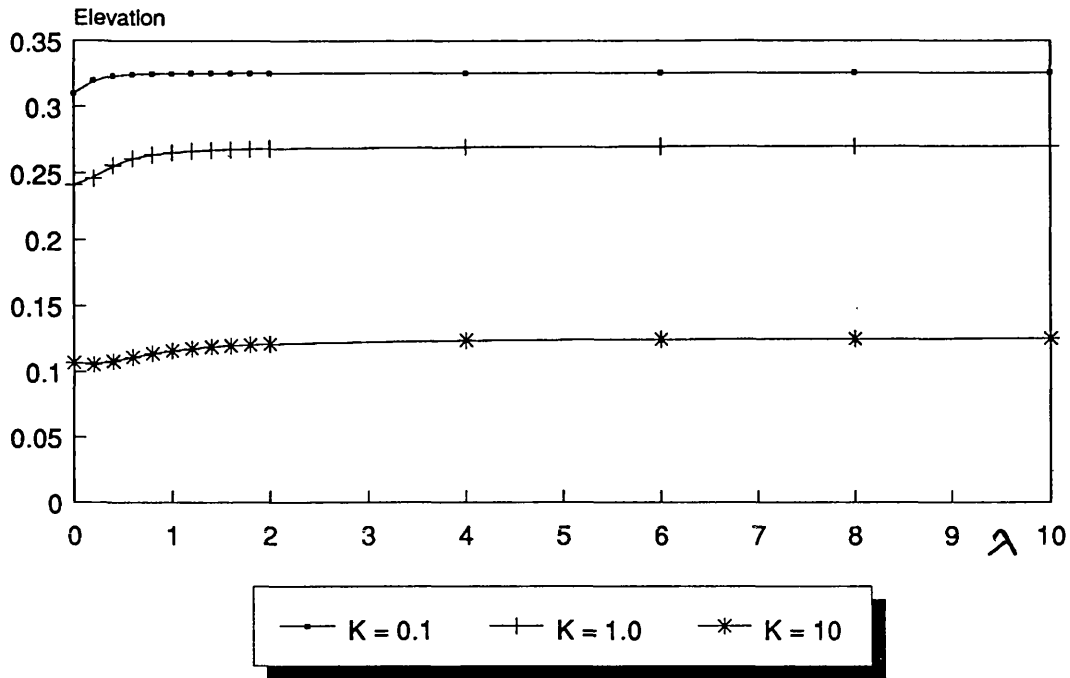


Figure 5.5. Elevation as a function of λ at a large distance from the cylinder; $k' = 0.4$, height = 1.

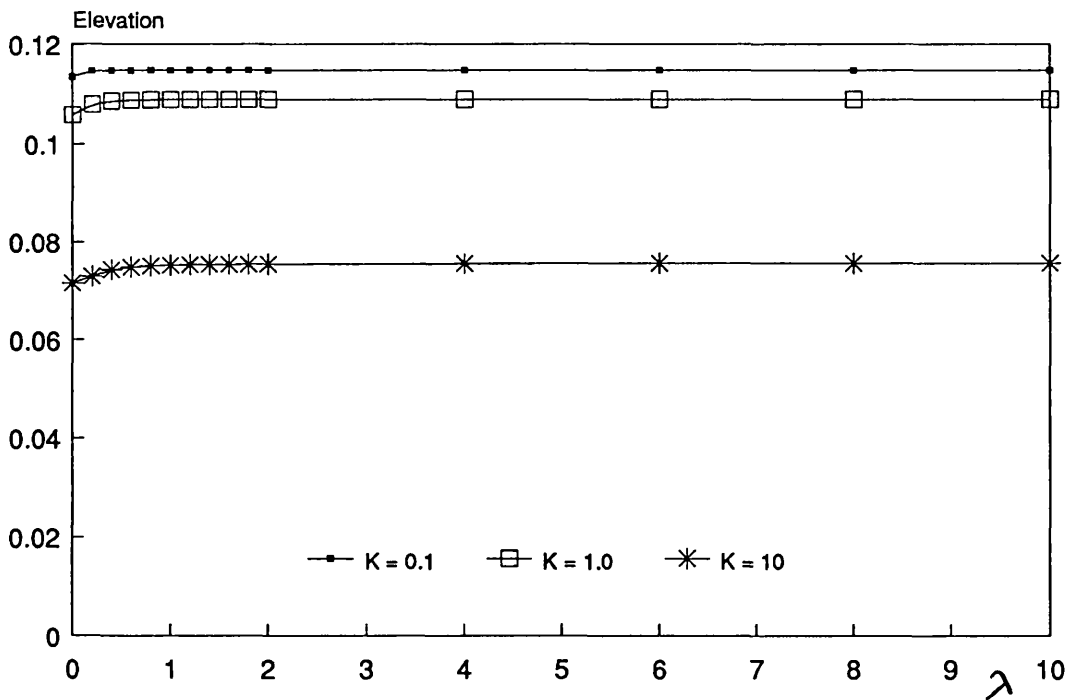


Figure 5.6. Elevation as a function of λ at large distance; $k' = 0.2$, height = 1.

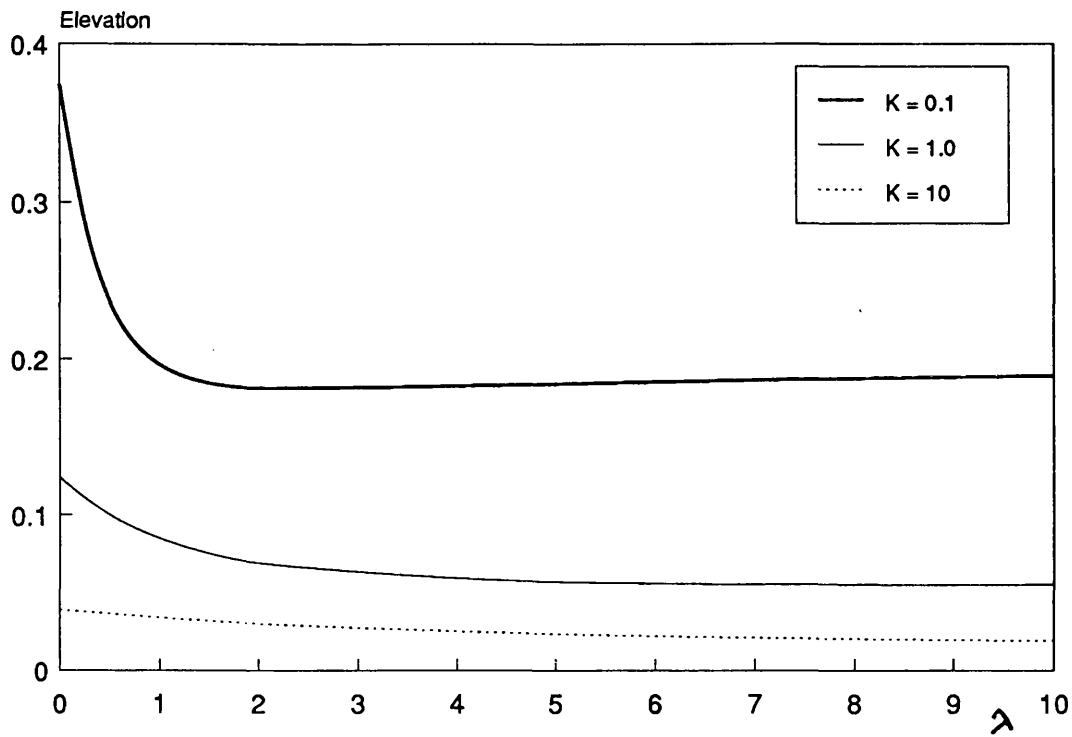


Figure 5.7. Elevation as a function of λ at large distance; $k'=5$, infinite height.

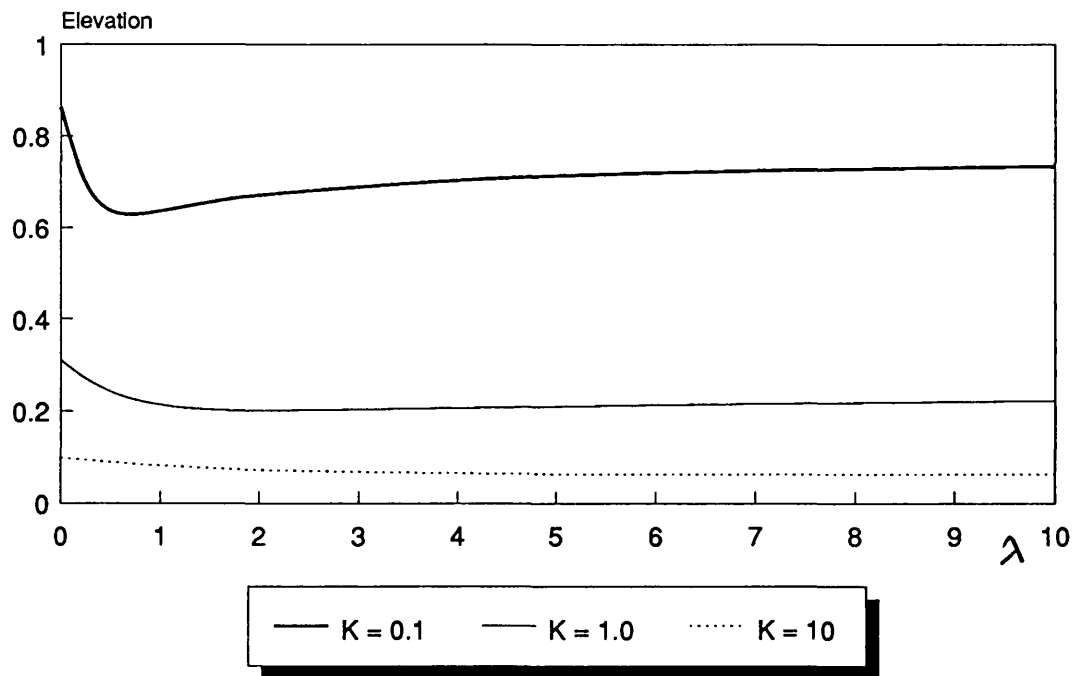


Figure 5.8. Elevation as a function of λ at large distance; $k'=2$, infinite height.

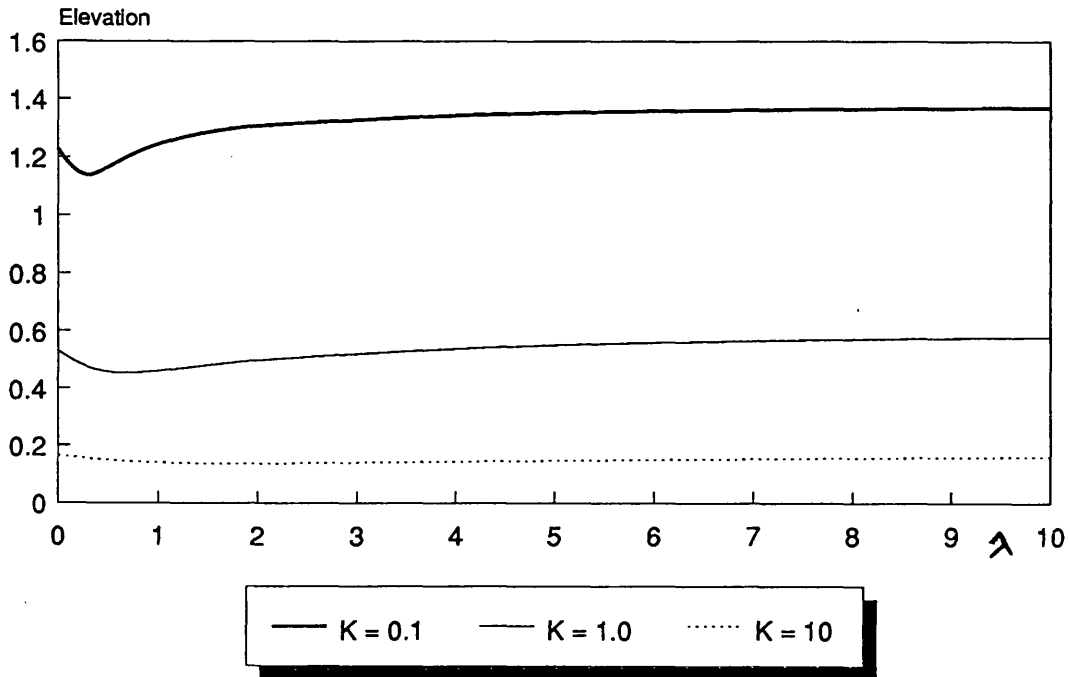


Figure 5.9. Elevation as a function of λ at a large distance from the cylinder; $k' = 1$, infinite height.

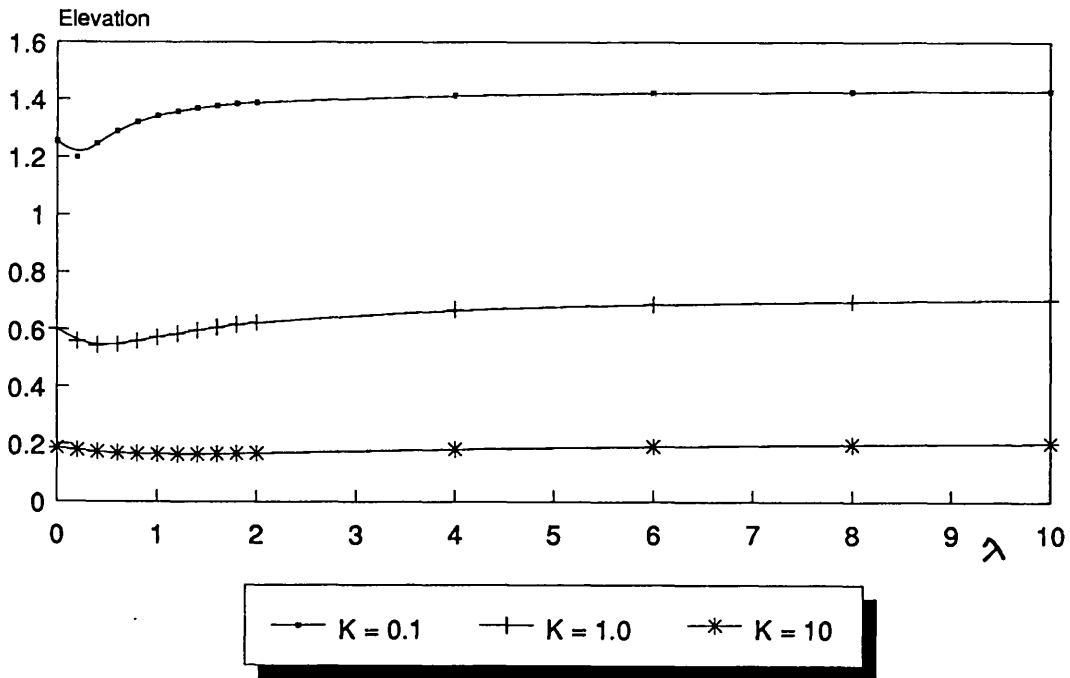


Figure 5.10. Elevation as a function of λ at large distance; $k'=0.8$, inf. height.

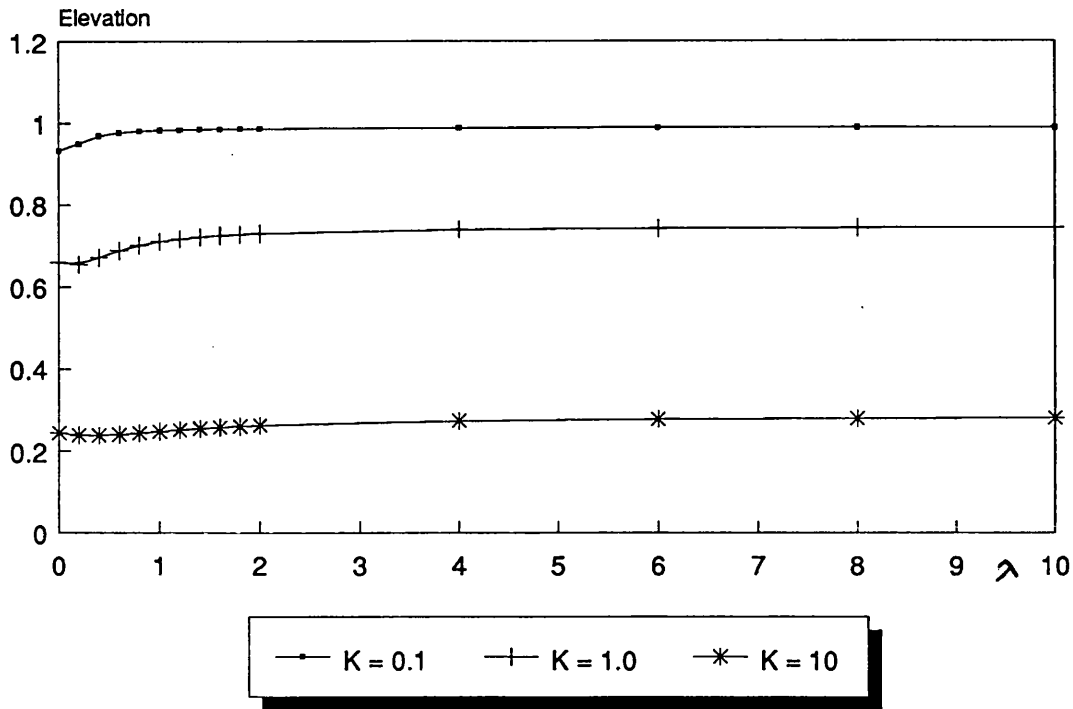


Figure 5.11. Elevation as a function of λ at large distance; $k' = 0.4$, inf. height

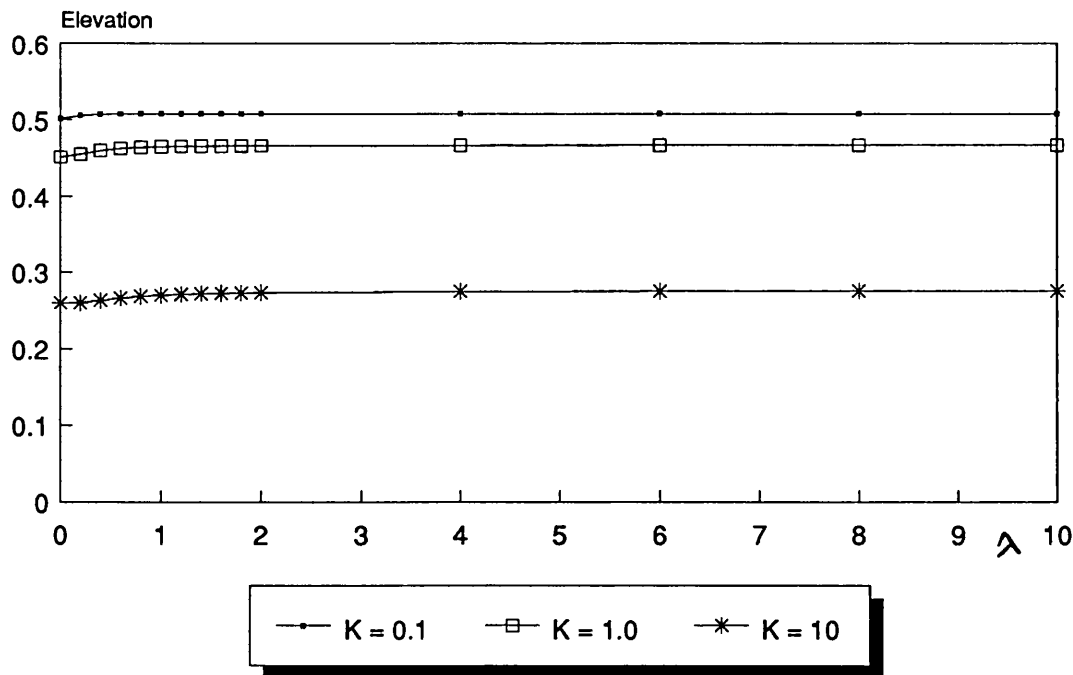
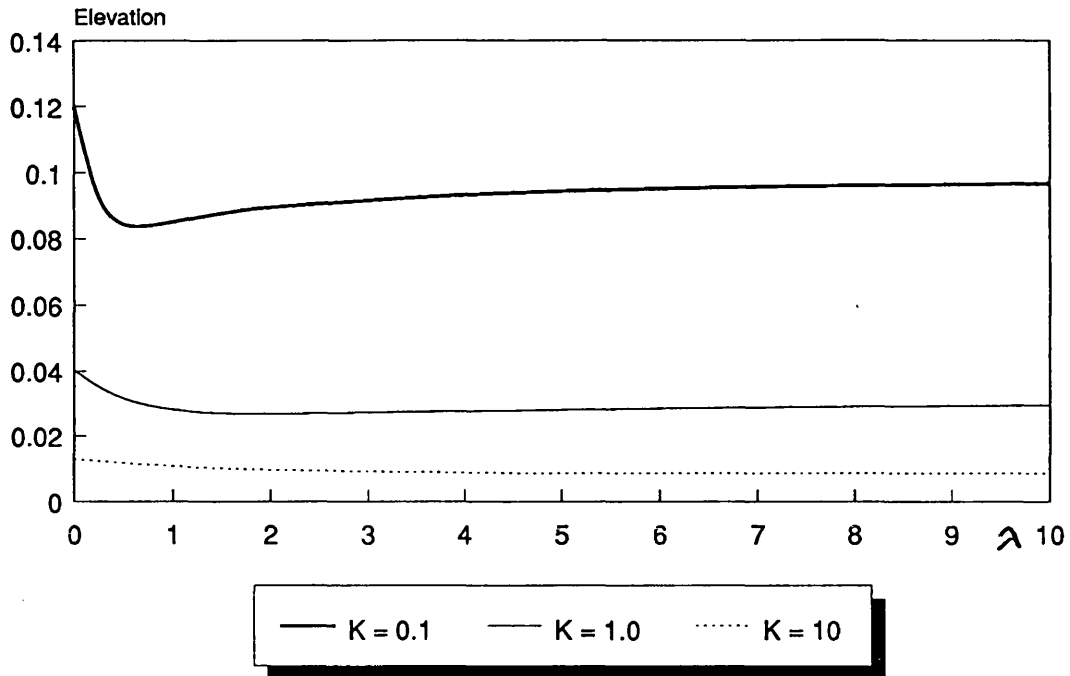


Figure 5.12. Elevation as a function of λ at large distance; $k' = 0.2$, inf. height



5.13. Elevation as a function of λ at a large distance from the cylinder; $k' = 5$, small depth (0.1).

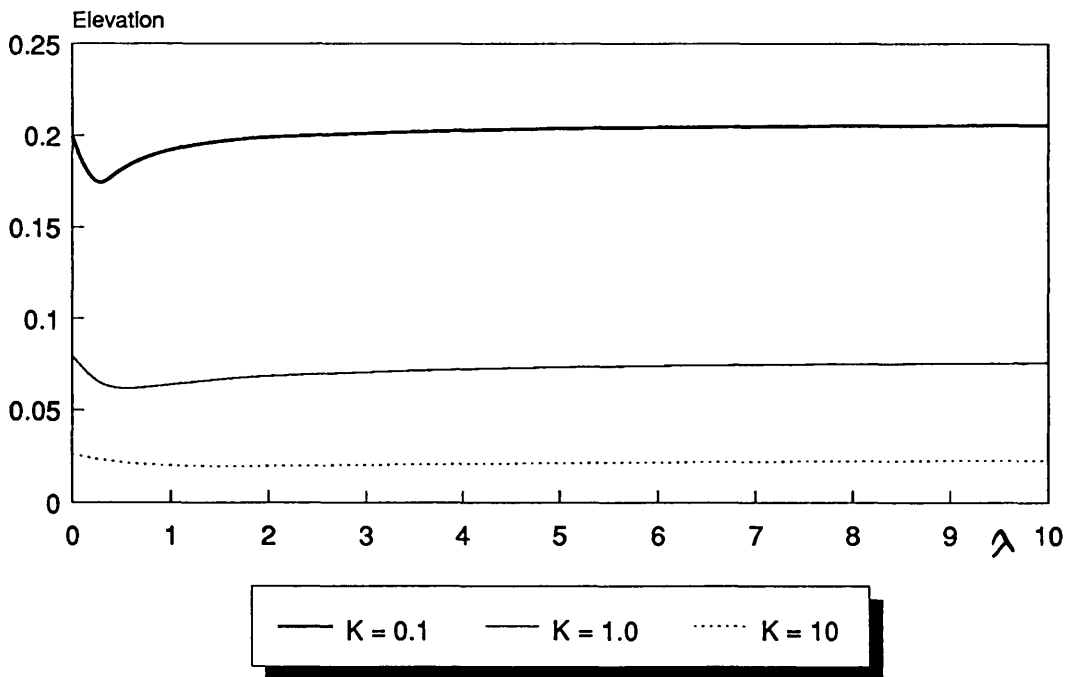


Figure 5.14. Elevation as a function of λ at large distance; $k'=2$, small depth (0.1).

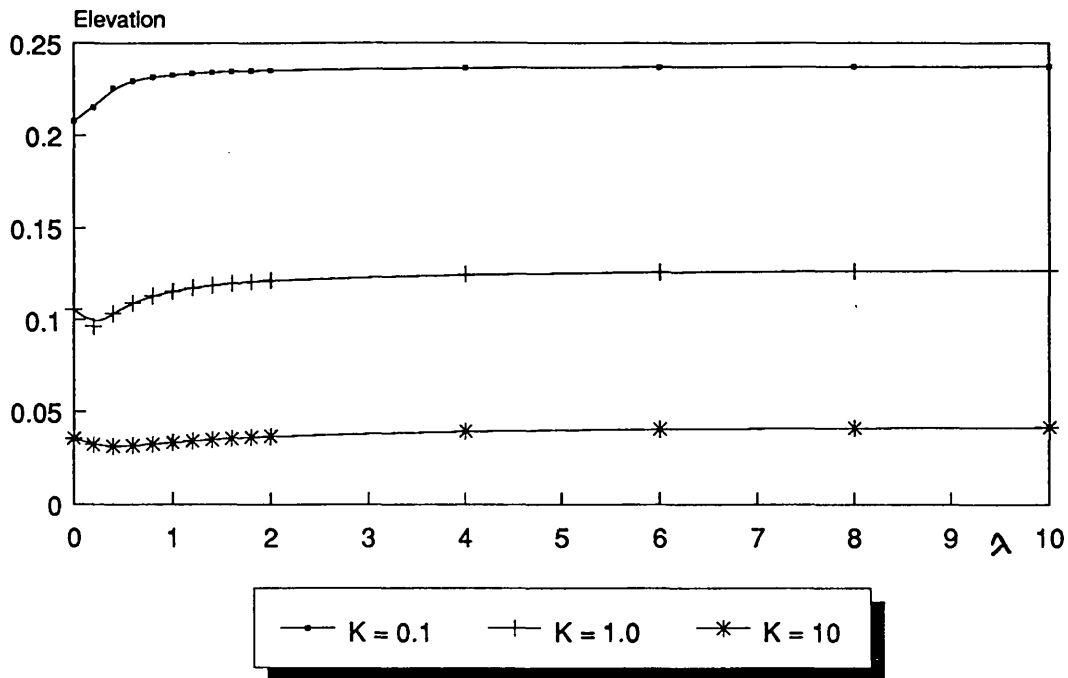


Figure 5.15. Elevation as a function of λ at large distance from the cylinder; $k' = 1$, small depth (0.1).

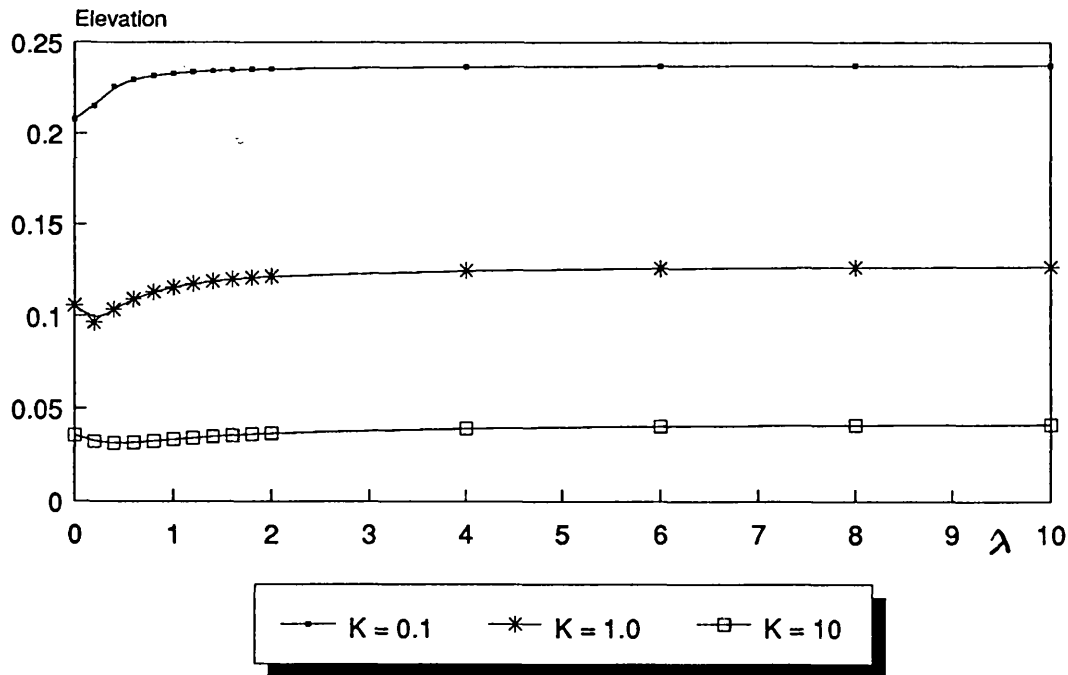


Figure 5.16. Elevation as a function of λ at large distance; $k' = .5$, small depth (.1)

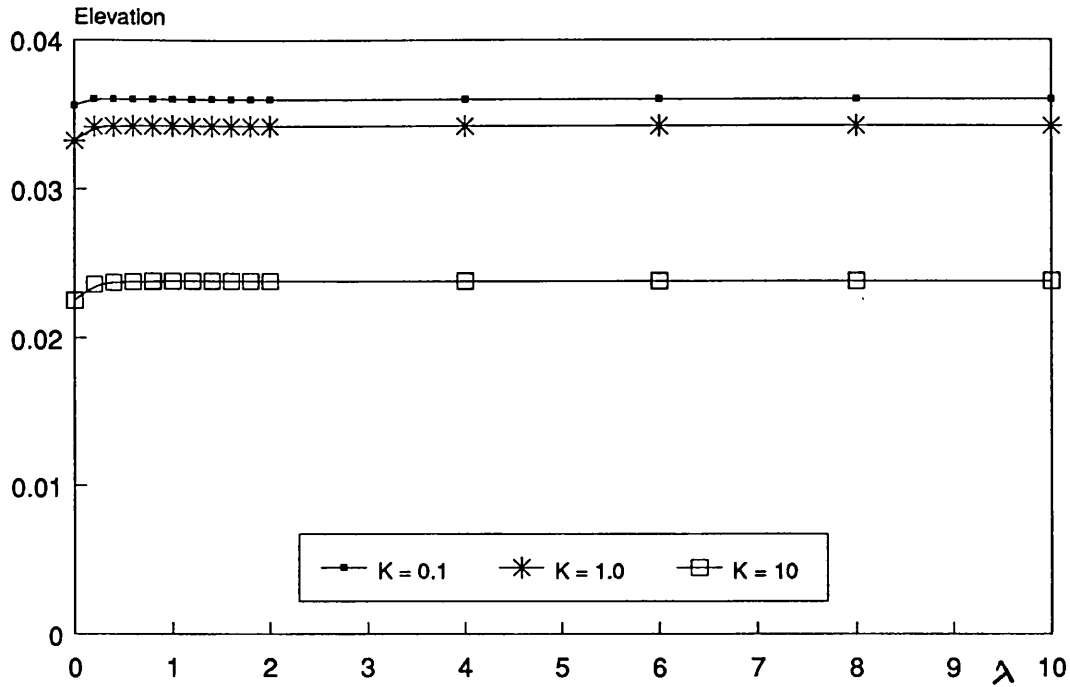


Figure 5.17. Elevation as a function of λ at large distance from the cylinder; $k' = 0.2$, small depth (0.1).

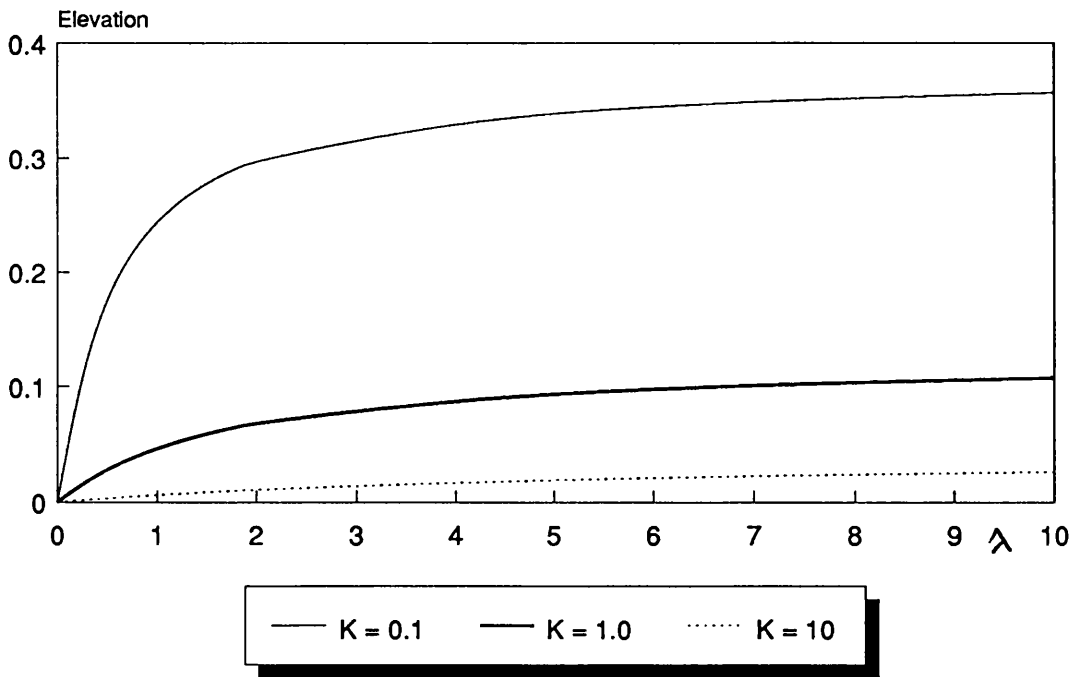


Figure 5.18. Elevation as a function of λ on the cylinder; $k' = 5$, infinite depth.

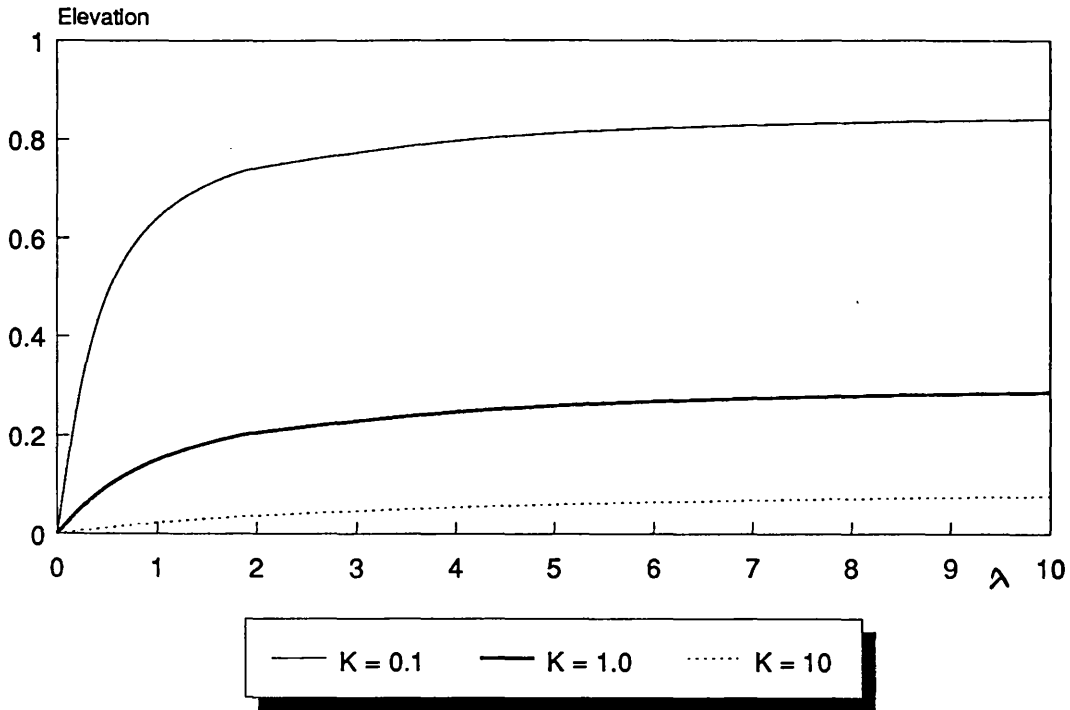


Figure 5.19. Elevation as a function of λ on the cylinder; $k' = 2$, infinite depth.

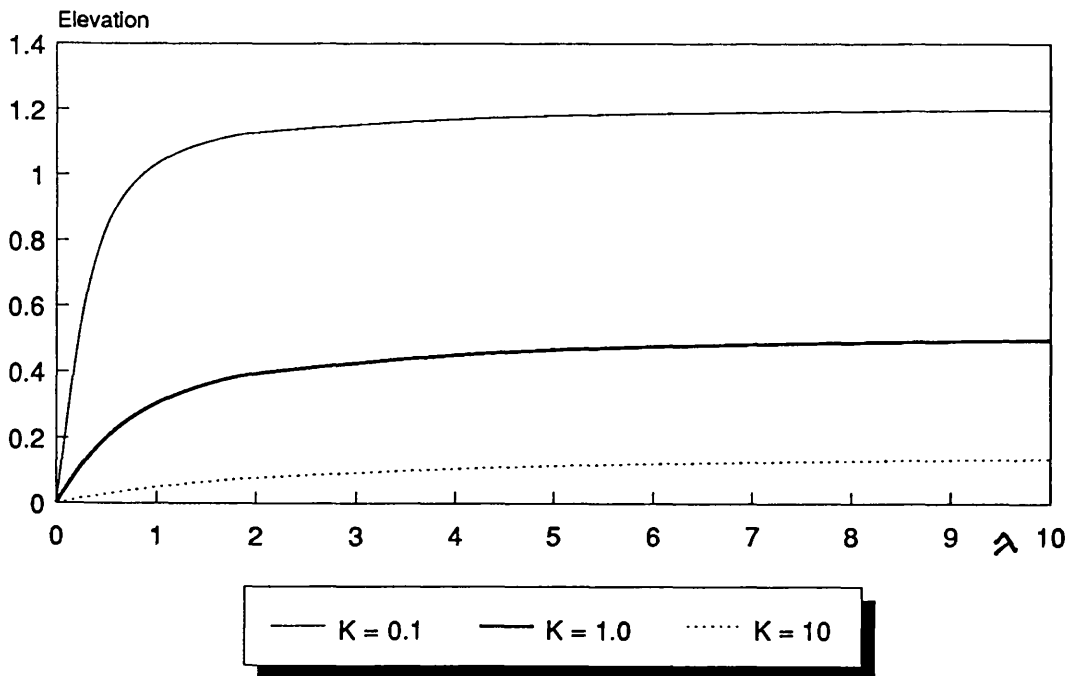


Figure 5.20. Elevation as a function of λ on the cylinder; $k' = 1$, infinite depth.

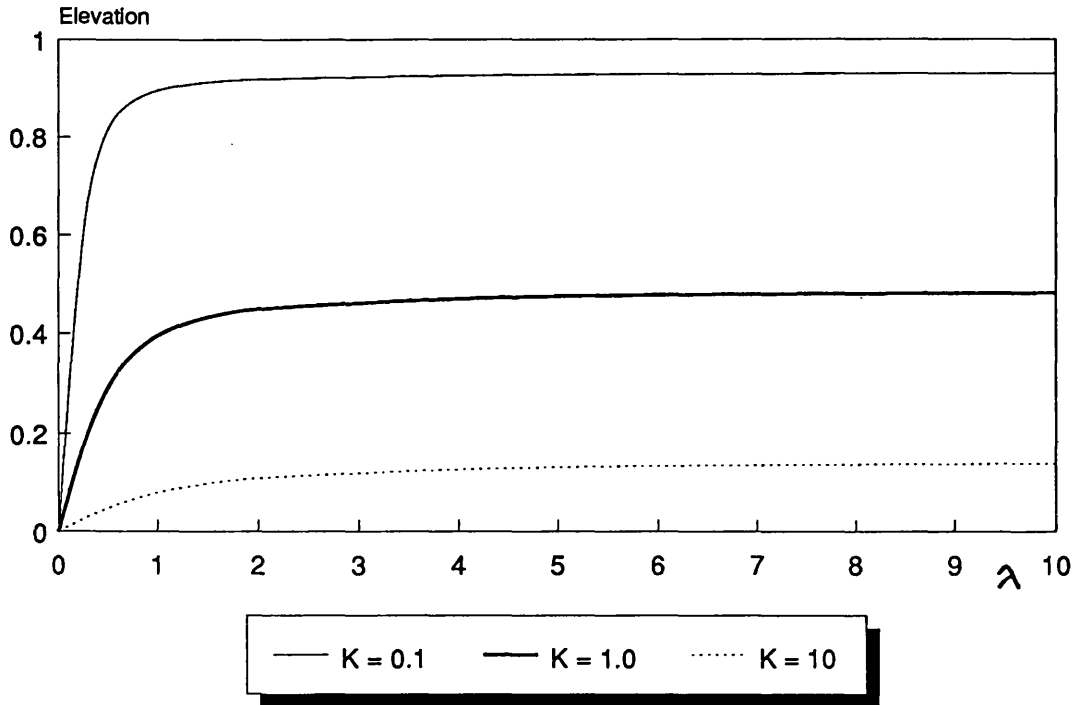


Figure 5.21. Elevation as a function of λ on the cylinder; $k' = 0.5$, infinite depth

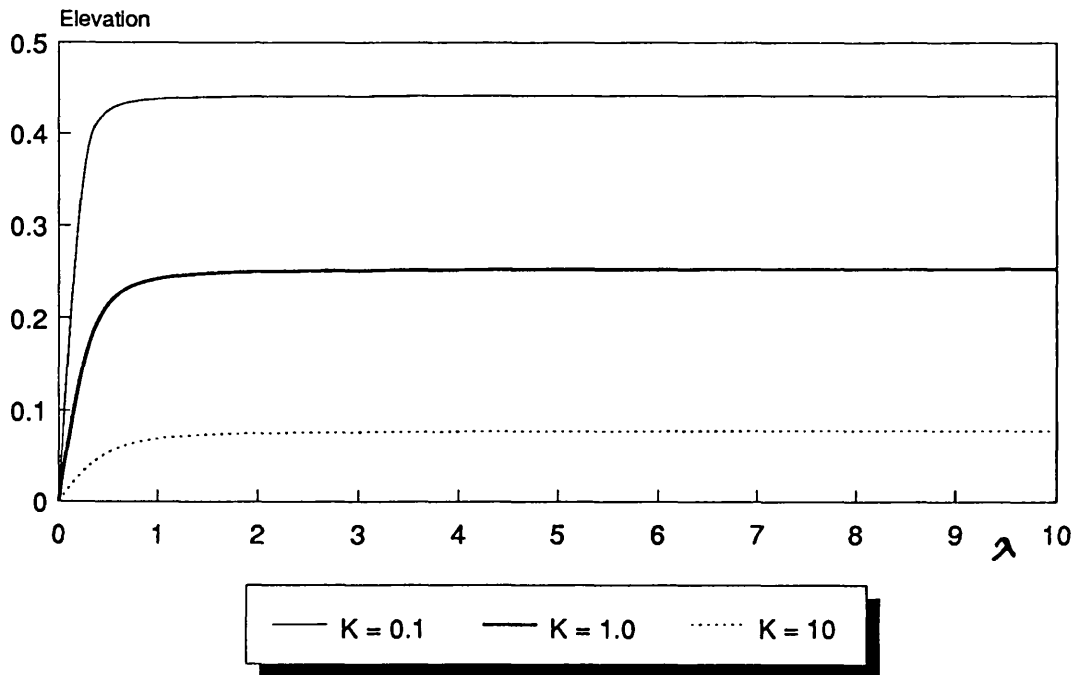


Figure 5.22. Elevation as a function of λ on the cylinder; $k' = 0.2$, infinite depth

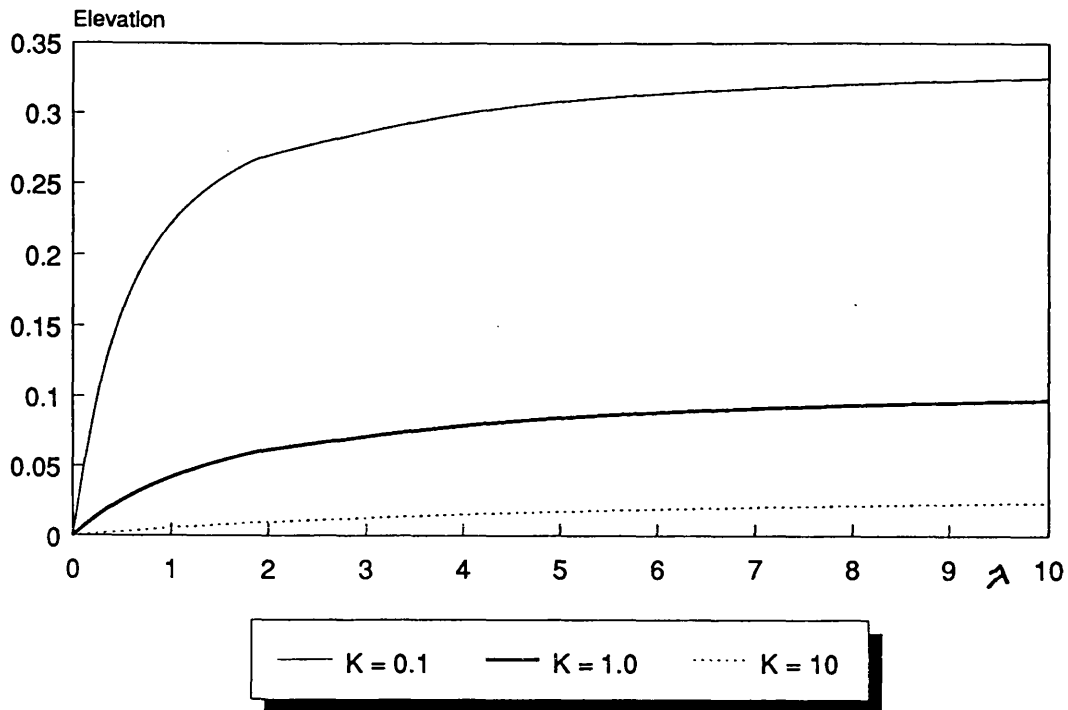


Figure 5.23. Elevation as a function of λ on the cylinder; $k' = 5$, height = 1.

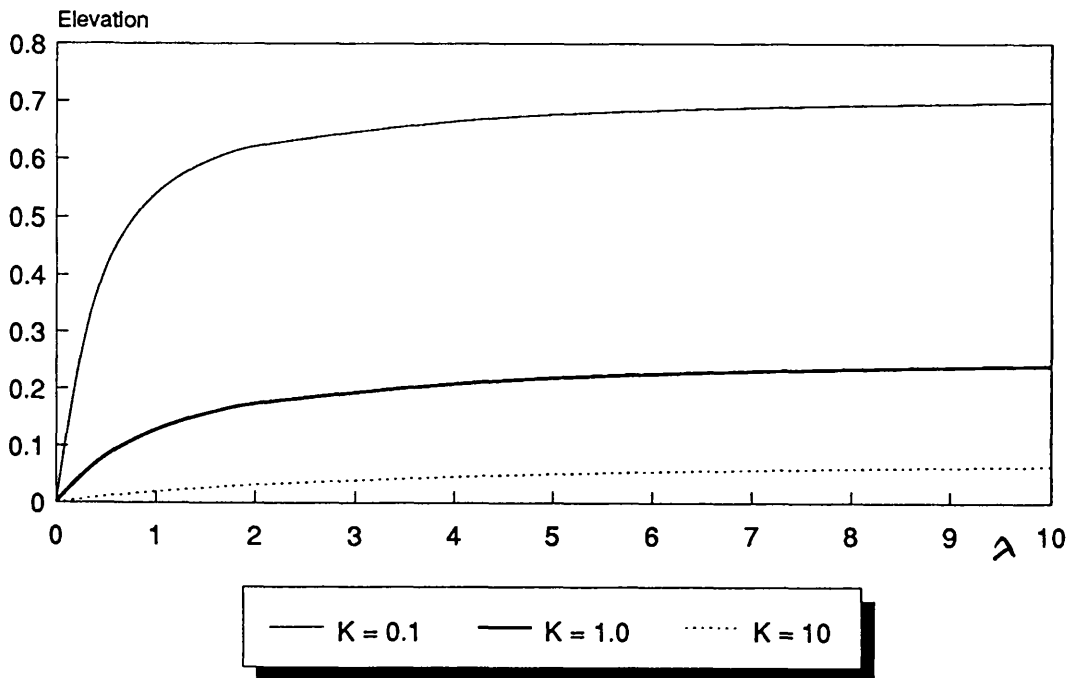


Figure 5.24. Elevation as a function of λ on the cylinder; $k' = 2$, height = 1.

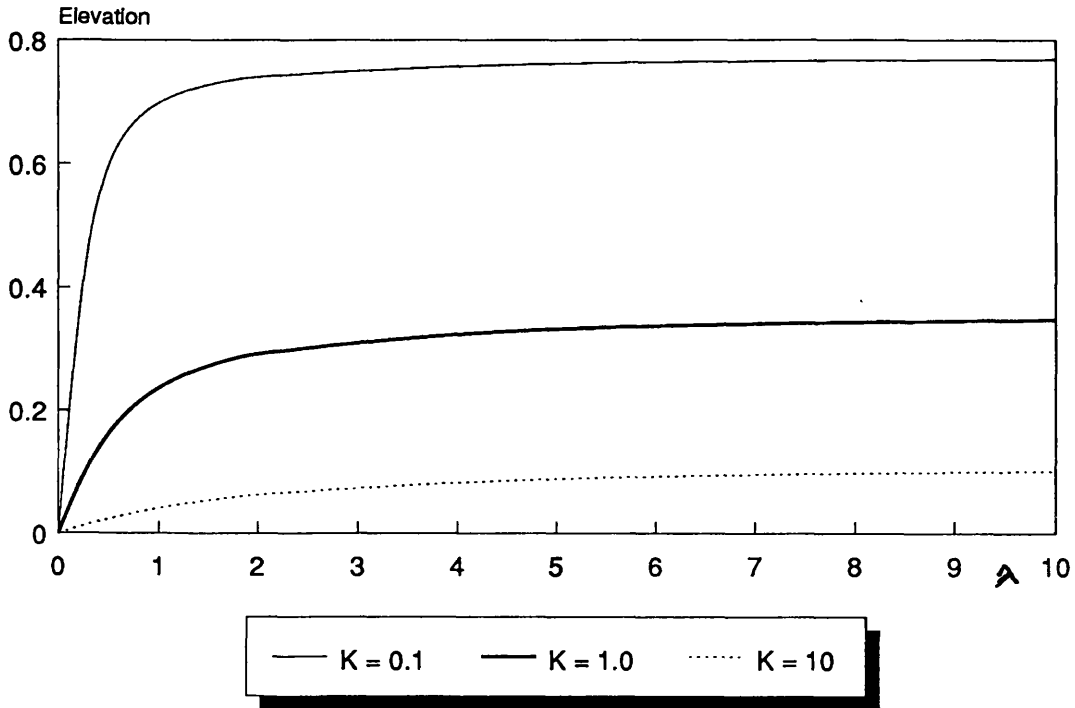


Figure 5.25. Elevation as a function of λ on the cylinder; $k' = 1$, height = 1.

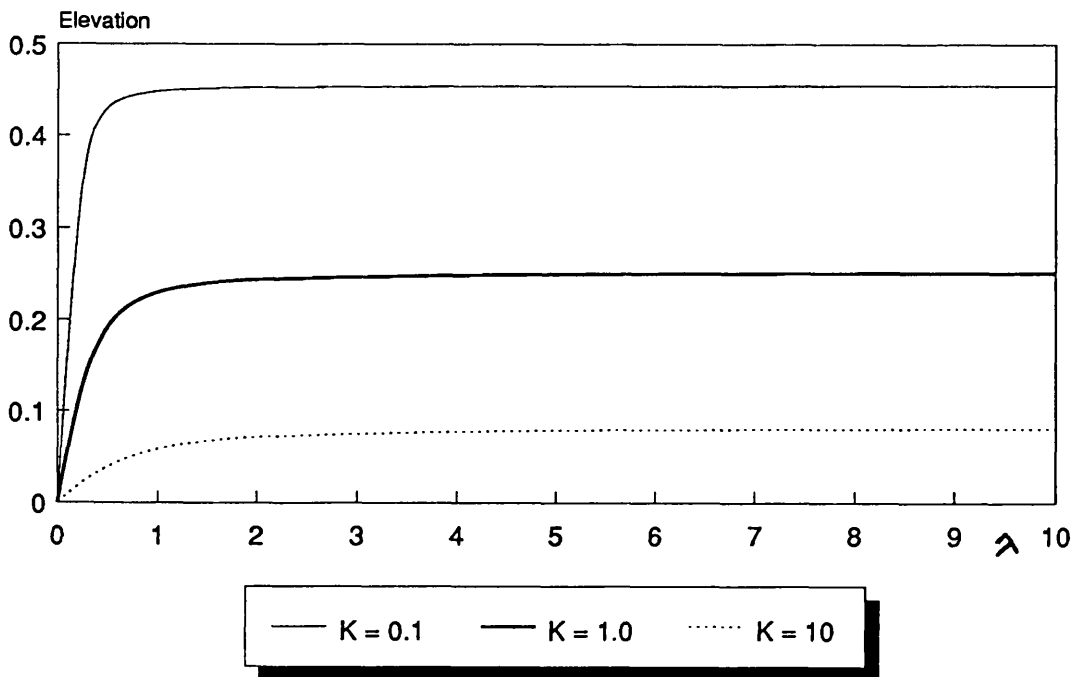


Figure 5.26. Elevation as a function of λ on the cylinder; $k' = 0.5$, height = 1.

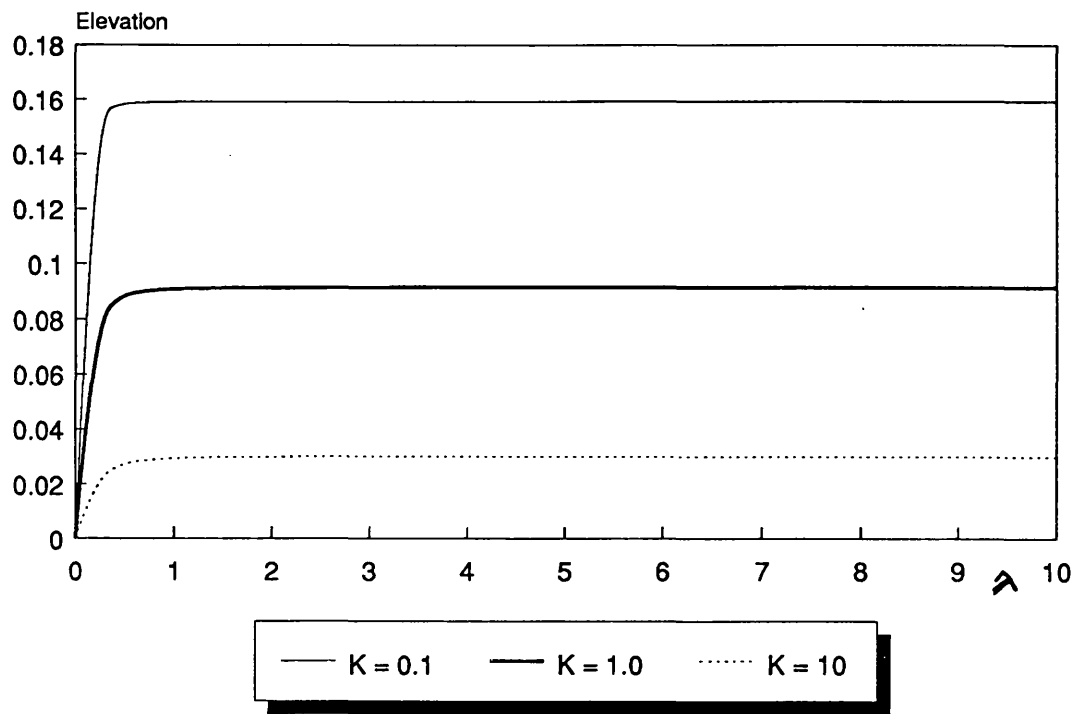


Figure 5.27. Elevation as a function of λ on the cylinder; $k' = 0.2$, height = 1.

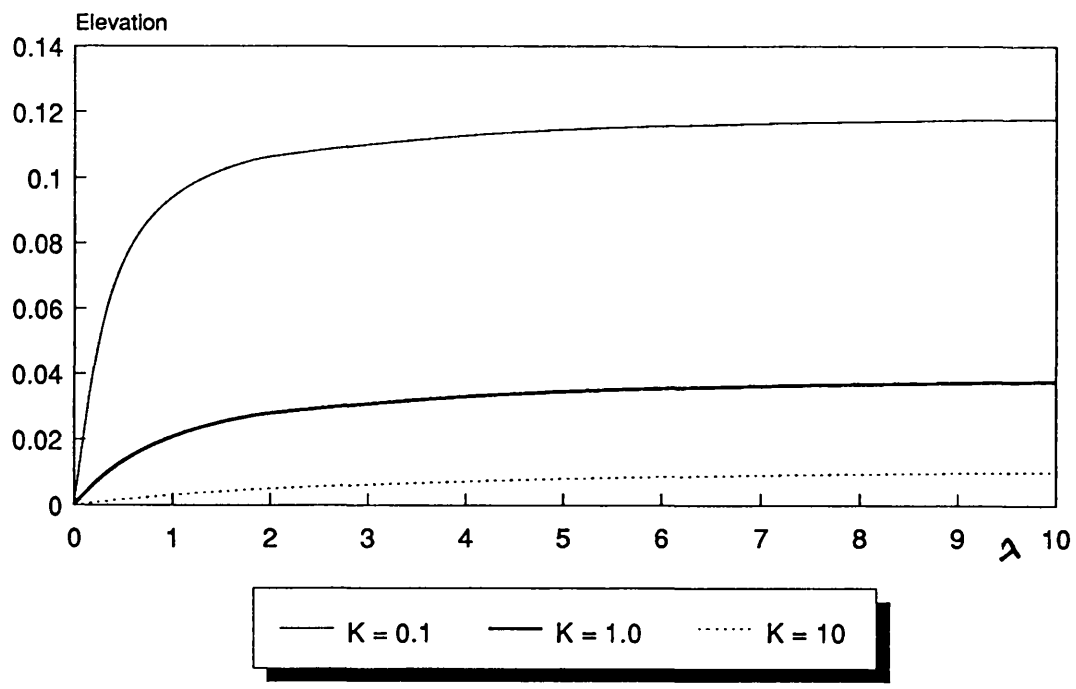


Figure 5.28. Elevation as a function of λ on the cylinder; $k'=5$, small depth (0.1)

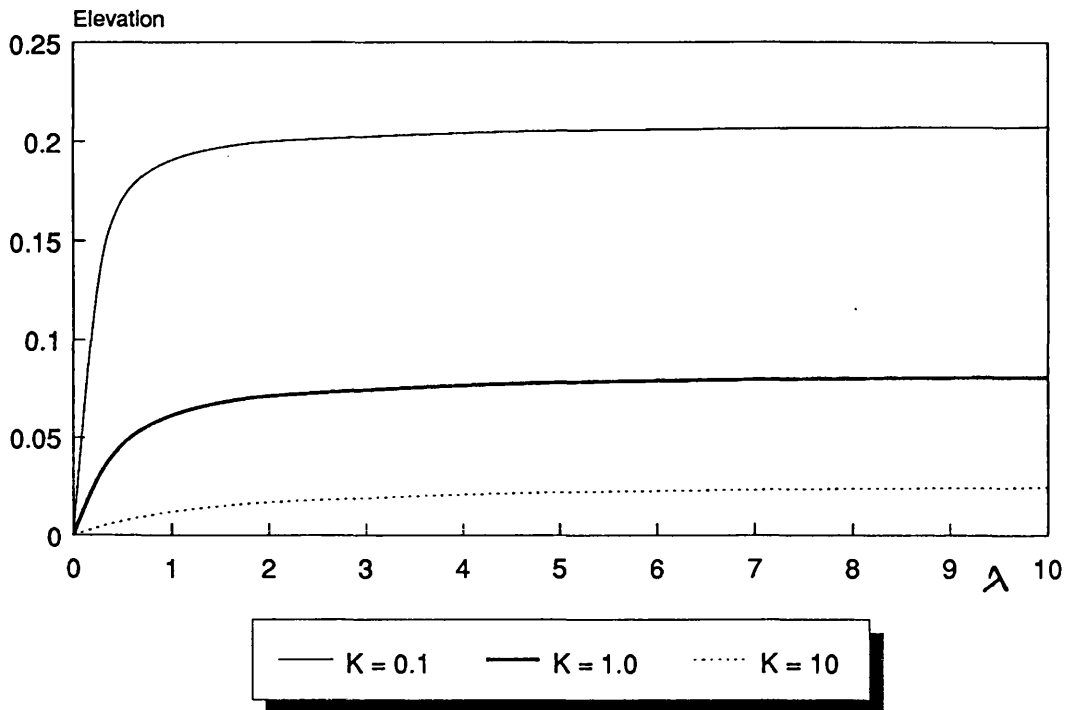


Figure 5.29. Elevation as a function of λ on the cylinder; $k'=2$, small depth (0.1)

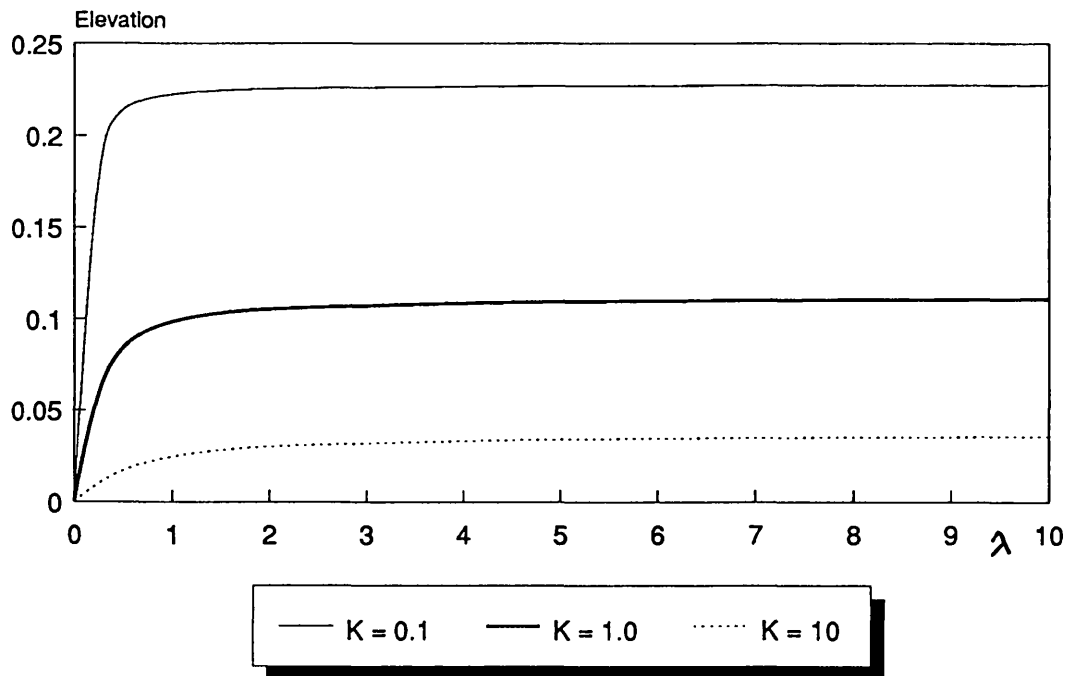


Figure 5.30. Elevation as a function of λ on the cylinder; $k'=1$, small depth (0.1)

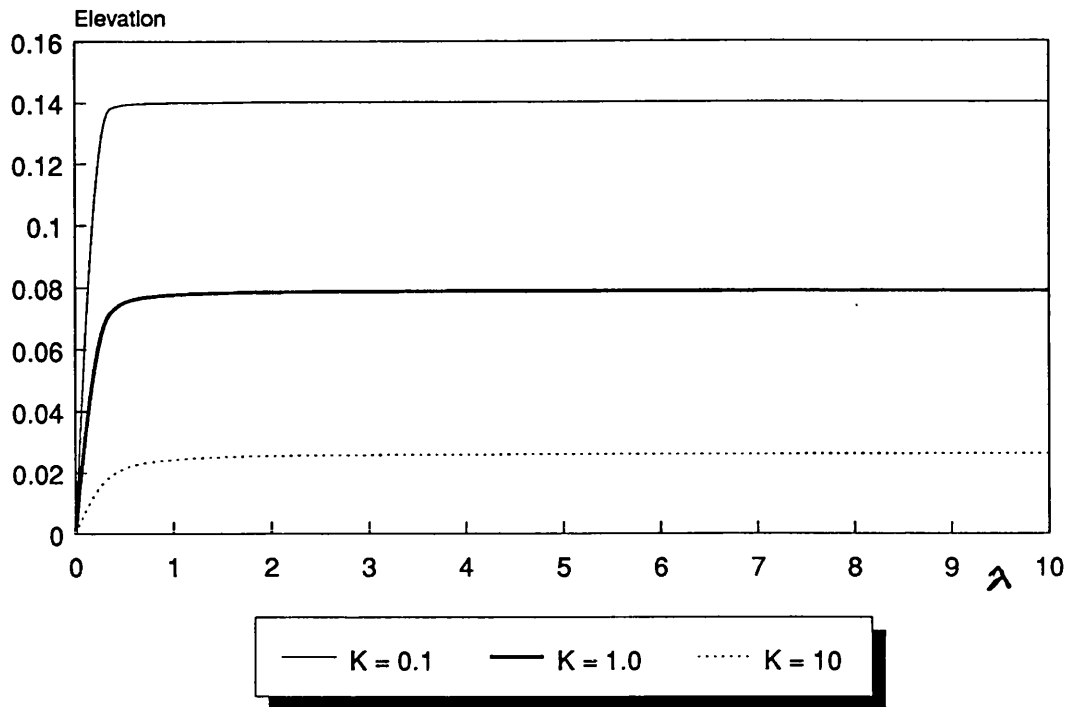


Figure 5.31. Elevation as a function of λ on the cylinder; $k'=0.5$, small depth(0.1)

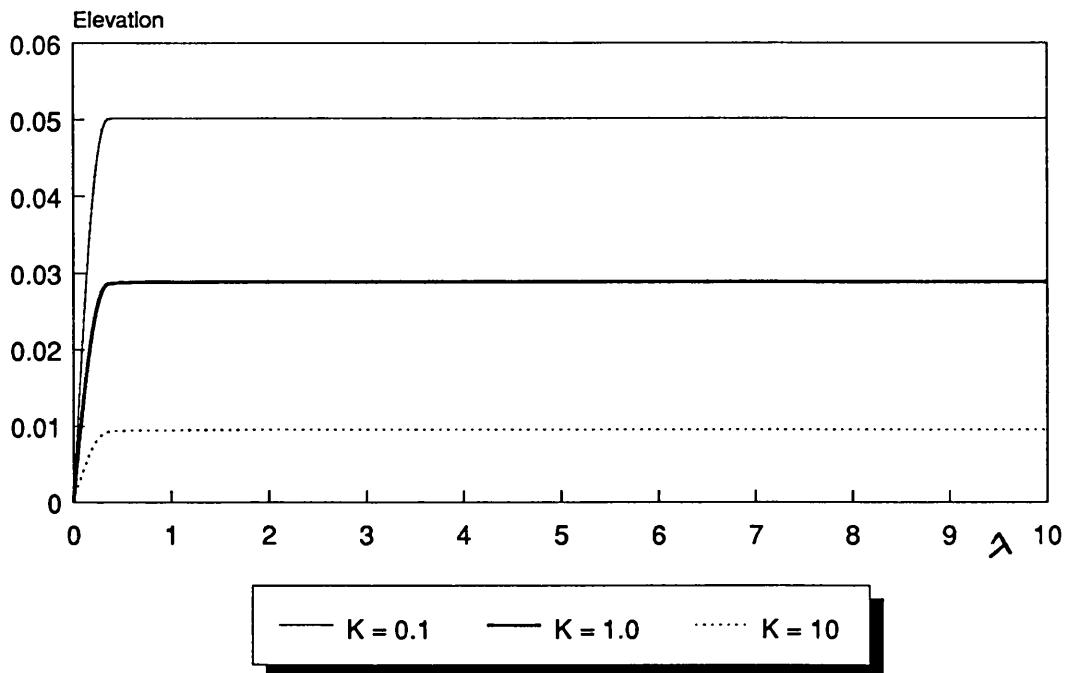


Figure 5.32. Elevation as a function of λ on the cylinder; $k'=0.2$, small depth(0.1)

SCATTERING OF WAVES BY A VERTICAL CYLINDER

6.1 - Introduction

The scattering of a capillary-gravity wave by a surface-piercing obstacle depends on the condition applied at the contact line between the fluid and the obstacle. A model for this condition that incorporates the effect of dynamic contact-angle variation is used to determine the wave-field close to the obstacle and at large distances from it. The solutions depend on the ratio between the wavelength of the incident wave and the radius of the obstacle, which is taken to be a circular cylinder, and on the relative size of the capillary and gravitational restoring forces. A third parameter is a constant of proportionality in the edge condition. Extreme values of this parameter relate to the special cases of orthogonal contact and of a fixed contact line. The strength of the scattered wave and the angular variation of its amplitude at large distances are calculated for a range of values of the parameters. The amplitude of the surface elevation on the boundary of the cylinder is also determined.

The diffraction of a plane gravity wave on the surface of fluid by a surface-piercing cylinder is mathematically equivalent to the diffraction of a plane sound wave by a 'hard' cylinder whose axis is parallel to the wave front and to the shadow of a cylinder illuminated by a distant source of light. The important parameter is the ratio of the wavelength to the radius of the circular cylinder. In the typical acoustic problem this parameter is large, in the optical case it is small, but all values of the parameter are relevant to the surface-wave problem. Phenomena associated with the scattering of waves by an

obstacle were studied in the 19th century and Sommerfeld (1896) presented the solution of the scattering of a surface wave by a semi-infinite plate with a vertical edge. The first solution to be written down for the scattering of a surface wave by a cylindrical obstacle appears to be that of McCamy and Fuchs (1954), which is most readily accessible in the discussion of their solution by Mei(1983). There has been a growing interest in this problem in recent years, mainly in its extension to the scattering of waves by multiple obstacles, an interest which stems from the need to understand the wave forces on the supporting legs of ocean platforms (for example, Kagemoto and Yue(1986)).

An important feature of the solution is that the structure of the scattered wave is quite different near to and far from the obstacle. The change in the intensity of the scattered wave as a function of the angular position of the sampling point is also highly irregular. The acoustic problem is discussed at length by Morse (1948), who also gives some examples of the intensity of the scattered wave for short wavelengths.

In the ocean, the size of the obstacles and their relative spacing are both significant length scales, but in all reasonable cases the effect of capillarity can be neglected. In experiments on a laboratory scale, however, or with a reduced gravitational field, as at the interface between two fluids of nearly equal densities, it is possible that the restoring force of surface tension complements or even dominates that of gravity. It seems reasonable, therefore, to examine the classical scattering problem for surface waves by a cylinder with the inclusion of capillarity. It is, of course, well-known that in unbounded regions capillary-gravity waves behave in much the same way as pure gravity waves, but with a different wave velocity. The change in the dispersion relation is of great significance in problems of interference and if nonlinear interactions of waves are considered, but these

matters do not affect the classical scattering problem. There is, however, an important difference between unbounded waves and waves in the presence of boundaries when capillarity is included. The surface elevation must satisfy the dynamical boundary condition and, when surface tension is not negligible, a term proportional to the curvature of the free surface must be included. This increases the order of the boundary condition and it is necessary to introduce a further condition that specifies the slope of the free surface at its intersection with any surface-piercing obstacle. This in turn implies that some consideration must be given to the correct conditions applicable at a moving contact line. Before describing a suitable edge condition, it is worth noting in anticipation that the scattered wave will contain contributions of all wavelengths, so that even if the incident wave is long compared with the capillary length scale, capillarity cannot be neglected in the scattered wave.

An edge condition that incorporates contact-angle hysteresis and the dynamic variation of the contact angle has been used by Young and Davis (1987) and Hocking for a vertically oscillating plate (1987c), and for the radiation of two-dimensional waves from a heaving body (1988a) and the normal (1987b) and oblique (1988b) reflection of a plane capillary-gravity wave by a plane barrier. The problem considered in *this chapter* is that of the scattering of an incident plane wave by a fixed cylindrical obstacle, placed in the fluid with its axis vertical and piercing the free surface. In contrast to the previous problems, the free-surface elevation is fully *three*-dimensional. The objective is to determine the angular variation of the mean elevation of the free surface, both on the cylinder and at large distances from it. The key parameters measure the ratio of the two restoring forces, capillarity and gravity, and the ratio of the wavelength of the incident wave to the radius of the obstacle. The justification of the form of the edge

condition used here is fully explained in chapter 1.

The quantities of interest are the elevation of the free surface, both on the obstacle and at large distances. Because the amplitude of the scattered wave may vary rapidly with the angular position of the sampling point, an averaged value of the amplitude over all possible directions is more meaningful. These quantities are found for representative values of the surface tension, wavelength, and the constant of proportionality in the edge condition. It should also be mentioned that some of the material given in this chapter is presented in the paper by Mahdmina and Hocking (1990).

6.2 - Formulation

Small-amplitude waves on the surface of water of infinite depth are considered. A plane incident wave of amplitude ϵa , with ϵ small, is scattered by a rigid cylinder of radius a , which is placed with its axis vertical and which extends above the fluid surface. The uniform density of the fluid is denoted by ρ , the surface tension by γ and the gravitational acceleration by g . The non-dimensionalization explained in chapter 2 is used here. The fluid occupies $r \geq 1$, $z \leq 0$. The incident wave has a non-dimensional frequency equal to σ , so a factor $\exp(i\sigma t)$ is removed from all the dependent variables, u , v , w , p and η . The linearized Euler equation then show that

$$(u, v, w) = \frac{i}{\sigma} \text{grad } p, \quad \nabla^2 p = 0. \quad (6.1)$$

The boundary conditions are that p is zero at infinite depth and that there is no flow across the boundary of the cylinder, so that

$$p = 0 \quad \text{as } z \rightarrow -\infty, \quad \frac{\partial p}{\partial r} = 0 \quad \text{at } r = 1. \quad (6.2)$$

The kinematic condition at the free surface is

$$i\sigma\eta = w = \frac{i}{\sigma} \frac{\partial p}{\partial z} \quad \text{at } z = 0. \quad (6.3)$$

At the free surface, the disturbance to the dynamic and hydrostatic parts of the pressure must be balanced by the capillary pressure, which is proportional to the local curvature of the surface. Hence at $z = 0$,

$$K \left[\frac{\partial^2 \eta}{\partial r^2} + \frac{\partial \eta}{r \partial r} + \frac{1}{r^2} \frac{\partial^2 \eta}{\partial \vartheta^2} \right] - \eta = -p; \quad (6.4)$$

where the parameter K , an inverse Bond number, is defined by

$$K = \frac{\gamma}{\rho g a^2}, \quad (6.5)$$

and measures the relative importance of the two restoring forces, capillarity and gravity. The final condition which is needed is the edge condition. The form chosen for this condition is

$$i\sigma\eta = \lambda \frac{\partial \eta}{\partial r} \quad \text{at } r = 1, \quad (6.6)$$

which includes the effect of contact-angle variation as discussed above. If $\lambda = 0$ the contact line does not move and if $\lambda = \infty$ the free surface meets the cylinder orthogonally.

There is a plane incident wave of wavenumber k' moving parallel to the direction $\vartheta = 0$, with surface elevation and pressure given by

$$\eta_1 = \exp(ik'r \cos\vartheta), \quad p_1 = \frac{\sigma^2}{k'} \exp(ik'r \cos\vartheta + k'z), \quad (6.7)$$

and the dynamic surface condition (equation 6.4) then shows that

$$\sigma^2 = k'(1 + Kk'^2). \quad (6.8)$$

This determines the wavenumber for a given frequency, but k' and K shall be regarded as the independent parameters, along with λ , so that equation 6.8 determines the frequency of the incident wave. The triplet (k', K, λ) of parameter values shall be denoted by \mathcal{P} . If the surface elevation and the pressure are written as the sum of incident and scattered components. so that

$$\eta = \eta_i + \eta_s, \quad p = p_i + p_s. \quad (6.9)$$

The two components of the surface elevation, η_i and η_s , must be determined so that the conditions on the cylinder and at the edge are satisfied and that they represent an outward-moving wave.

There are four quantities we wish to calculate. The first is the amplitude of the surface elevation on the cylinder which we denote by H , where

$$H(\vartheta, \mathcal{P}) = |\eta_i + \eta_s| \quad \text{on } r = 1. \quad (6.10)$$

The second is the mean-squared value of this elevation, denoted by

$$E(\mathcal{P}) = \frac{1}{2\pi} \int_{-\pi}^{\pi} H(\vartheta, \mathcal{P})^2 d\vartheta. \quad (6.11)$$

The third is the amplitude of the elevation in the scattered wave at large distance R from the cylinder, which is given by

$$S(\vartheta, \mathcal{P}) = R^{1/2} |\eta_s| \quad \text{as } R \rightarrow \infty. \quad (6.12)$$

The fourth measures the intensity of the wave at large distances, averaged over all directions, and is given by

$$I(\mathcal{P}) = \frac{R}{2\pi} \int_{-\pi}^{\pi} |\eta_s|^2 d\vartheta \quad \text{as } R \rightarrow \infty. \quad (6.13)$$

For pure gravity waves ($K = 0$), the dynamic boundary condition (equation 6.4) is of lower order and cannot be imposed an edge condition. The other conditions, however, ensure that the free surface meets the cylinder orthogonally, which agrees with the requirement of the edge condition (equation 6.6) when $\lambda = \infty$. It is convenient to consider first the special case of orthogonal contact for capillary-gravity waves, that is, for arbitrary values of K .

6.3 - Orthogonal Contact

Since $\frac{\partial p}{\partial r} = 0$ at $r = 1$ from equation 6.2, it follows from equation 6.3 that, when there is no singularity at the contact line, $\frac{\partial \eta}{\partial r} = 0$ at $r = 1$, which is the edge condition when $\lambda = \infty$. In this case the scattered wave can be written as

$$\eta_s = \sum_{n=0}^{\infty} A_n \cos(n\vartheta) H_n^{(2)}(k'r), \quad p_s = \frac{\sigma^2}{k'} \exp(k'z) \eta_s, \quad (6.14)$$

where $H_n^{(2)}$ is the Hankel function that represents an outward-moving wave. The dynamic surface condition (equation 6.4) is then automatically satisfied, since the frequency σ is given by equation 6.8. If the boundary condition $\frac{\partial(\eta_i + \eta_s)}{\partial r} = 0$ at $r = 1$, is now applied, which also ensures that equation 6.2 is satisfied, and expand η_i as a Fourier series in ϑ , the following will be obtained

$$A_n = -2i^n \delta_n \frac{J_n'(k')}{H_n^{(2)'}(k')}, \quad (6.15)$$

where

$$\delta_n = 1 \quad \text{for } n > 0, \quad \delta_0 = \frac{1}{2}. \quad (6.16)$$

It follows that the elevation of the wave is independent of the surface tension parameter K , which only enters the problem through the dispersion relation. The solution is otherwise identical with that for pure gravity waves, and for the acoustic and optical problems.

When $\lambda = \infty$, the parameter set \mathcal{P} can be replaced by the single parameter k' , and write the four quantities describing the wave, defined by the equations 6.10, 6.11, 6.12 and 6.13, by $H_\infty(\vartheta, k')$, $E_\infty(\vartheta, k')$, $S_\infty(\vartheta, k')$ and $I_\infty(\vartheta, k')$, respectively. Putting $r = 1$ into the definition of η_1 and η_s , it is found that

$$H_\infty(\vartheta, k') = \frac{4}{\pi k'} \left| \sum_{n=0}^{\infty} \delta_n \frac{i^n \cos(n\vartheta)}{H_n^{(2)'}(k')} \right|, \quad (6.17)$$

and

$$E_\infty(k') = \frac{8}{\pi^2 k'^2} \sum_{n=0}^{\infty} \delta_n \left| \frac{1}{H_n^{(2)'}(k')} \right|^2. \quad (6.18)$$

The asymptotic values of the Hankel functions as $r \rightarrow \infty$ are proportional to $\exp\{-i(k'r - \frac{1}{4}\pi - \frac{1}{2}n\pi)\}$, so that

$$S_\infty(\vartheta, k') = 2 \left[\frac{2}{\pi k'} \right]^{1/2} \left| \sum_{n=0}^{\infty} \delta_n \frac{(-1)^n J_n'(k')}{H_n^{(2)'}(k')} \cos(n\vartheta) \right|. \quad (6.19)$$

Finally, the intensity of the scattered wave at large distance is given by

$$I_\infty(k') = \frac{4}{\pi k'} \sum_{n=0}^{\infty} \delta_n \left| \frac{J_n'(k')}{H_n^{(2)'}(k')} \right|^2. \quad (6.20)$$

The computed values of these quantities are presented together with those for general values of λ in section 6.5.

6.4 - Finite λ

When λ is finite, the contact between the free surface and the cylinder is no longer orthogonal. The solution does not consist only of components with the single wavenumber k' and contributions from the whole spectrum of wavenumbers must be included. The pressure p can be written in the form $p = p_1 + p_2$, where

$$p_1 = \frac{\sigma^2}{k'} e^{k'z} \left\{ e^{ik'r \cos\vartheta} + \sum_0^{\infty} A_n \cos(n\vartheta) H_n^{(2)}(k'r) \right\}, \quad (6.21)$$

and

$$p_2 = \sum_{n=0}^{\infty} \cos(n\vartheta) \int_0^{\infty} p_n(k) e^{kz} T_n(kr) dk; \quad (6.22)$$

the Bessel functions $T_n(kr)$ are defined by

$$T_n(kr) = J_n(kr) Y_n'(k) - Y_n(kr) J_n'(k). \quad (6.23)$$

The coefficients A_n are given, as before, by equation 6.14, so that the condition $\frac{\partial p}{\partial r} = 0$ at $r = 1$ is satisfied by this form for p . The value of η_1 corresponding to p_1 is given by equations 6.7 and 6.14 and, from equation 6.3, it can be concluded that

$$\eta_2 = \frac{1}{\sigma^2} \sum_{n=0}^{\infty} \cos(n\vartheta) \int_0^{\infty} k P_n(k) T_n(kr) dk. \quad (6.24)$$

The dynamic surface condition (equation 6.4) for η_2 can also be solved, which yields a solution of the form

$$\eta_2 = \sum_{n=0}^{\infty} \cos(n\vartheta) \left\{ \int_0^{\infty} p_n(k) \frac{T_n(kr)}{1 + Kk^2} dk + B_n \frac{K^{1/2}}{K_n'(K^{-1/2})} K_n(K^{-1/2}r) \right\} \quad (6.25)$$

where K_n is the modified Bessel function that is bounded at infinity. Applying Fourier-Bessel Integral Theorem which is explained by Sneddon (1951), the second term in this sum can be expressed as an integral with the same kernel as the first. Standard properties of Bessel functions can be used to evaluate the inversion integral, and therefore the equation 6.25 can be replaced by the equivalent form

$$\eta_2 = \sum_{n=0}^{\infty} \cos(n\vartheta) \int_0^{\infty} \frac{T_n(kr)}{1 + Kk^2} \left\{ P_n(k) - B_n \frac{2K}{\pi M_n(k)} \right\} dk, \quad (6.26)$$

where

$$M_n(k) = J_n'^2(k) + Y_n'^2(k). \quad (6.27)$$

Equating the two expressions in equations 6.24 and 6.26 for η_2 , P_n can be written as

$$P_n = \frac{2K\sigma^2}{\pi M_n(k) \{\sigma^2 - k(1 + Kk^2)\}} B_n + \delta(k - k') C_n, \quad (6.28)$$

where δ is the Dirac delta function and the coefficients B_n and C_n are to be determined. On the boundary of the cylinder,

$$\eta = \sum_{n=0}^{\infty} \left\{ - \frac{4\delta_n i^{n+1}}{\pi k' H_n^{(2)'}(k')} + B_n \int_0^{\infty} \frac{4K}{\pi^2 M_n(k) \{\sigma^2 - k(1 + Kk^2)\}} dk + C_n \frac{2}{\pi\sigma^2} \right\} \cos(n\vartheta), \quad (6.29)$$

where the integral takes its principal value. The slope of the free surface at the edge $r = 1$ is given by

$$\frac{\partial \eta}{\partial r} = \frac{\partial \eta_1}{\partial r} + \frac{\partial \eta_2}{\partial r} = \sum_{n=0}^{\infty} B_n \cos(n\vartheta), \quad (6.30)$$

since η_1 has been chosen to have zero slope there and η_2 is given by the equation 6.25. The edge condition (equation 6.6), for each value of n , reduces to the equation

$$\frac{4\sigma\delta_n i^n}{\pi k' H_n^{(2)'}(k')} + i\sigma B_n F_n(k', K) + C_n \frac{2i}{\pi\sigma} = \lambda B_n, \quad (6.31)$$

where

$$F_n(k', K) = \int_0^{\infty} \frac{4K}{\pi^2 M_n(k) \{\sigma^2 - k(1 + Kk^2)\}} dk \quad (6.32)$$

The part of the solution represented by η_1 is the sum of the incident wave and an outward-moving wave. The coefficients B_n and C_n must be chosen so that, at large values of r , η_2 represents an outward-moving wave for each value of n . The asymptotic value of $T_n(kr)$ for large r is given by

$$T_n(kr) \cong \frac{i}{(2\pi kr)^{1/2}} \left\{ H_n^{(2)'}(k) \exp\left\{i\left(kr - \frac{1}{4}\pi - \frac{1}{2}n\pi\right)\right\} - H_n^{(1)'}(k) \exp\left\{-i\left(kr - \frac{1}{4}\pi - \frac{1}{2}n\pi\right)\right\} \right\}. \quad (6.33)$$

The leading term in the asymptotic value of η_2 comes from using this value for $T_n(kr)$ in equation 6.25, with P_n given by the equation 6.28. The major contributions come from the evaluation of the principle-value integral near the singularity at $k = k'$ and from the delta-function part. Since there must be no inward-moving wave at infinity, therefore

$$\frac{2K\sigma^2}{(1 + 3Kk'^2) M_n(k')} B_n - C_n = 0. \quad (6.34)$$

Using this result, the outward-moving part of η_2 can be calculated and, when this is combined with the outward-moving part of η_1 , the total scattered wave at large distance is found to be

$$\eta_s \cong - \left[\frac{2}{\pi k' r} \right]^{1/2} \exp\{-i(k'r - \frac{1}{4}\pi)\} .$$

$$\sum_{n=0}^{\infty} \cos(n\vartheta) \left\{ \frac{2\delta_n (-1)^n J_n'(k')}{H_n^{(2)'}(k')} + \frac{i^{n+1} H_n^{(1)'}(k')}{1 + Kk'^2} C_n \right\}. \quad (6.35)$$

The coefficients C_n can be found (by substituting equation 6.34 into the equation 6.31) and therefore at large distance R from the body,

$$\begin{aligned} \eta_s R^{1/2} \exp\{i(k'r - \frac{1}{4}\pi)\} = \\ - 2 \left\{ \frac{2}{\pi k'} \right\}^{1/2} \sum_{n=0}^{\infty} \frac{\delta_n (-1)^n \cos(n\vartheta)}{J_n'(k') - iY_n'(k')} \left\{ J_n'(k') - G_n(\mathcal{P}) \right\}, \end{aligned} \quad (6.36)$$

where

$$\begin{aligned} G_n(\mathcal{P}) = \frac{4K\sigma}{\pi(1 + 3Kk'^2)[J_n'(k') - iY_n'(k')]} \\ \lambda - i\sigma F_n(k', k) + \frac{4K\sigma}{(1 + 3Kk'^2)M(k')} \end{aligned} \quad (6.37)$$

The function $S(\vartheta, \mathcal{P})$ (which is defined by the equation

6.12) is determined by taking the modulus of the right-hand side of the equation 6.36. The averaged intensity of the scattered wave (as defined by equation 6.13), is given by

$$I(\mathcal{P}) = \frac{4}{\pi k'} \sum_{n=0}^{\infty} \delta_n \frac{|J_n'(k') - G_n(\mathcal{P})|^2}{M_n(k')}. \quad (6.38)$$

The amplitude of the surface elevation on the cylinder can be found from equation 6.20. When the values of the coefficients B_n and C_n are inserted, then

$$H(\vartheta, \mathcal{P}) = \frac{4}{\pi k'} \left| \sum_{n=0}^{\infty} \frac{\delta_n i^n \cos(n\vartheta)}{H_n^{(2)'}(k')} \right. \\ \left. \frac{\lambda}{\lambda - i\sigma F_n(k', k) + \frac{4K\sigma}{(1 + 3Kk'^2)M_n(k')}} \right|, \quad (6.39)$$

and the mean squared value of the elevation $E(\mathcal{P})$ is defined in the equation 6.11.

When $\lambda = 0$, $H(\vartheta, \mathcal{P}) = 0$ since the contact line is then immobile. When $\lambda = \infty$, these expressions for $H(\vartheta, \mathcal{P})$, $E(\mathcal{P})$, $S(\vartheta, \mathcal{P})$ and $I(\mathcal{P})$ are the same as those derived for orthogonal contact in section 6.3 since $G_n(\mathcal{P})$ is then zero. The relevant properties of the surface elevation can now be calculated by evaluating the above formulae for typical values of the parameter set \mathcal{P} .

At large distance from the cylinder and when k' is large (that is, for short waves relative to the radius of the cylinder), the surface elevation $S(\vartheta, \mathcal{P})$ shows a considerable and rapid dependence on the direction ϑ . Figures 6.1 and 6.2 show the results for $\lambda = 1$ and $\lambda = \infty$, respectively, for $k' = 10$ and $K = 1$. When $\lambda = \infty$, the

results are same as for the acoustic scattering problem, and Figure 6.2 is similar to one given in Morse (1948). In both Figures 6.1 and 6.2 there is a long tail behind the cylinder, indicating that the maximum amplitude of the scattered wave occurs downstream of the cylinder. Figure 6.3 gives the results for the scattered wave with $\lambda = 1$, $k' = 1$ and $K = 1$. For this comparatively long wave the variation of the surface elevation with angular position is much smoother, which is not unexpected since there is only a small phase difference in the incident wave between the front and rear of the cylinder. The averaged intensity of the scattered wave over all directions and at large distance from the cylinder is measured by $I(\mathcal{P})$, and this quantity is shown as a function of λ and for different values of k' in Figures 6.4 (for $K = 0.1$) and 6.5 (for $K = 1$). For values of λ greater than unity $I(\mathcal{P})$ is an increasing function of k' , but for smaller values it is not monotonic. To illustrate this feature of the results, $I(\mathcal{P})$ is shown in Figure 6.6 as a function of k' with $\lambda = 0$ and for three values of K . It has a series of maxima and minima at intervals approximately equal to $\frac{1}{2}\pi$. The curves for different values of K are only slightly different, and they tend to the same limit as k' tends to infinity. It follows from equation 6.20 that $I(\mathcal{P})$ should be independent of K as $k' \rightarrow \infty$, but values of λ greater than 10 would be needed to demonstrate this behaviour in Figures 6.4 and 6.5.

The minima in the values of the mean-squared elevations at large distances from the cylinder as shown in Figures 6.4 and 6.5 exist because there is energy dissipation when λ is neither zero nor infinity. At large distances the elevation increases with K , but approaches a limiting value independent of K as $\lambda \rightarrow \infty$. On the cylinder, however, the elevation decreases as K increases for finite values of λ . Although it does not seem possible to simplify the complicated expressions for the required quantities in general, order-of-magnitude estimates can be found for the limiting case $K \rightarrow 0$. The major contribution

to the integral in equation 6.32 comes from values of k of order $K^{-1/2}$, and $F_n(k', K) = -K^{1/2} + O(K)$. The corresponding value of $G_n(\mathcal{P})$ can be found from equation 6.37 and (using equation 6.38), therefore $I(\mathcal{P}) - I_\infty(k')$ is of order K/λ when $\lambda > K^{1/2}$ and of order $K^{1/2}$ when $\lambda < K^{1/2}$. The edge effect disappears in the limit as $K \rightarrow 0$, as expected. Since $I(\mathcal{P})$ has a minimum as a function of λ it approaches its limit I_∞ from below. But if it is ensured that $\lambda < K^{1/2}$ as $K \rightarrow 0$, particularly if $\lambda = 0$, then the results shown in Figures 6.4 and 6.5 indicate that the limit is approached from above. In the same way it can be shown that the mean-squared elevation on the cylinder has the limiting form

$$E(\mathcal{P}) = \frac{\lambda^2}{\lambda^2 + k'K} E_\infty(k') \quad \text{as } K \rightarrow 0. \quad (6.40)$$

A comparison of Figures 6.9 and 6.10 confirms this trend.

It is also possible to ascertain the effect of the edge condition on the force experienced by the cylinder in the limit as $K \rightarrow 0$. This force can be calculated by integrating the pressure over the surface of the cylinder and the pressure is given as the sum of two parts, p_1 and p_2 , given in equations 6.21 and 6.22. The pressure p_1 provides the force when the edge condition is of orthogonal contact, as in the absence of capillarity. The contribution of p_2 to the force is proportional to P_1 (from equation 6.28), is proportional to KB_1 when K is small. It follows from equations 6.31 and 6.34 that this part of the force is of order K/λ when $\lambda > K^{1/2}$ and of order $K^{1/2}$ when $\lambda < K^{1/2}$. Thus, for a given small value of K , the effect of the edge condition is largest when $\lambda = 0$, that is, when the edge is fixed, and the force is then changed by an amount proportional to $K^{1/2}$.

Results for the total surface elevation on the boundary of the cylinder are shown in Figures 6.7 to 6.10. The values of $H(\vartheta, \mathcal{P})$ are shown in Figure 6.7 for short

waves, $k' = 10$, and in Figure 6.8 for long waves, $k' = 1$; in both figures $K = 1$ and $\lambda = 1$. The angular variation when $k' = 10$ is rapid, but not to so great an extent as for the scattered wave at large distance. For $k' = 1$ the angular variation is not as smooth as it was at large distances. The maximum amplitude now occurs on the upstream side of the cylinder. The average squared value of the elevation, as measured by $E(\mathcal{P})$, is shown in Figures 6.9 and 6.10 as a function of λ for $K = 0.1$ and for $K = 1$, respectively. These figures show that $E(\mathcal{P})$ is a monotonic decreasing function of k' for all values of λ . Comparing Figures 6.9 and 6.10, it can be noticed that the limiting values of $E(\mathcal{P})$ as $\lambda \rightarrow \infty$ are independent of K , as expected from equation 6.18.

6.5 - Numerical Approach

The four functions chosen to describe the scattered wave at large distance and the total elevation on the cylinder are $S(\vartheta, \mathcal{P})$, $I(\mathcal{P})$, $H(\vartheta, \mathcal{P})$ and $E(\mathcal{P})$. To calculate these quantities, first a number of Bessel functions should be calculated. The functions Y_n and their derivatives can be calculated by using recurrence relations, with Y_0 and Y_1 given by a NAG routine. The forward recurrence relation for the J_n functions, however, can only be used when the argument x is greater than n . When $x < n$ the recurrence relation is unstable as n increases, but it can be used backwards, that is, for decreasing n , to compute $J_n(x)$.

The Bessel functions tend to zero very rapidly as n increases, once n is greater than x . Sufficient accuracy was obtained in the summation of the infinite series in the desired expressions when they were truncated at $n = 20$. The chief difficulty in the calculation is the accurate evaluation of the integral $F_n(k', K)$, defined by the equation 6.32. First, it is separated into two parts and write it in the form

$$F_n(k', K) = \frac{4K}{\pi^2 M_n(k')} \int_0^{\infty} \frac{1}{k(Kk^2 + 1) - k'(Kk'^2 + 1)} dk$$

$$- \frac{4K}{\pi^2} \int_0^{\infty} \frac{M_n(k) - M_n(k')}{k - k'} \frac{1}{M_n(k) M_n(k')} \frac{1}{(1 + Kk^2 + Kkk' + Kk'^2)} dk.$$

(6.41)

The first integral in equation 6.41 can be evaluated analytically and it is given by

$$\int_0^{\infty} \frac{1 + 3Kk'^2}{k(Kk^2 + 1) - k'(Kk'^2 + 1)} dk = \frac{1}{2} \ln \left[\frac{1 + Kk'^2}{Kk'^2} \right]$$

$$- 3 \left[\frac{Kk'^2}{4 + 3kk'^2} \right]^{1/2} \tan^{-1} \left[\frac{4 + 3Kk'^2}{Kk'^2} \right]^{1/2}.$$

(6.42)

To calculate the second integral in equation 6.41, the trapezium rule can be used for the bulk of the calculation, but special care is needed when k is small, when k is close to k' , and when k is large. A step length of 0.1 was found to give acceptable accuracy. When $k \rightarrow 0$, $M_n(k) \rightarrow \infty$, but the integrand is finite and has the limiting value $-[k'(1 + Kk'^2)M_n(k')]^{-1}$. When k is equal to k' , the integrand is determinate and therefore l'Hopital's rule can be applied to determine its limiting value, which is

$$\frac{M_n'(k')}{(1 + 3Kk'^2)M_n^2(k')}.$$

(6.43)

As $k \rightarrow \infty$, the integrand has the asymptotic value $-(\pi/2K)k^{-2}$, so the application of the trapezium rule is truncated at some large value of k , say $k = X$, large enough to ensure that this asymptotic value is sufficiently accurate. The evaluation of the integral is

completed by adding the contribution from the asymptotic form, which is $-(\pi/2K)X^{-1}$. When the values of $F_n(k',K)$ have been calculated for particular values of k' and K , it is an easy matter to evaluate the sums of the various series for any value of λ and at any angular position ϑ . Some results found in this manner are shown in Figures 6.1 to 6.10.

$$\lambda = 1, K = 1, k' = 10$$

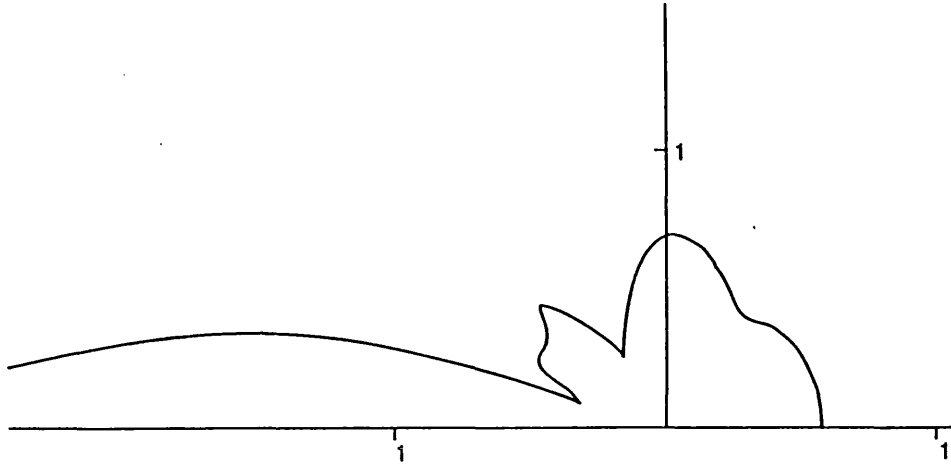


Figure 6.1. Polar diagram of $S(\theta, P)$
the mean surface elevation of the
scattered wave at large distance.

$$\lambda = \infty, K = 1, k' = 10$$

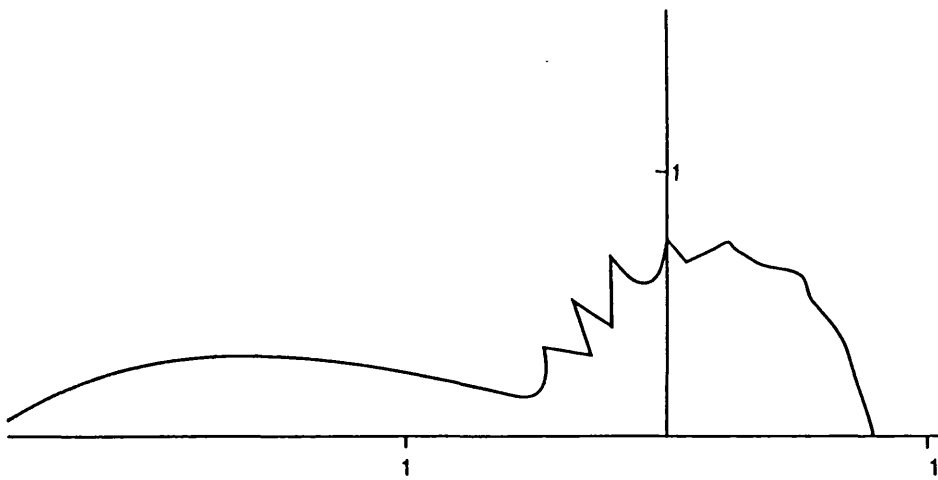


Figure 6.2. Polar diagram of $S(\theta, P)$,
the mean elevation at large distance.

$$\lambda = 1, K = 1, k' = 1$$

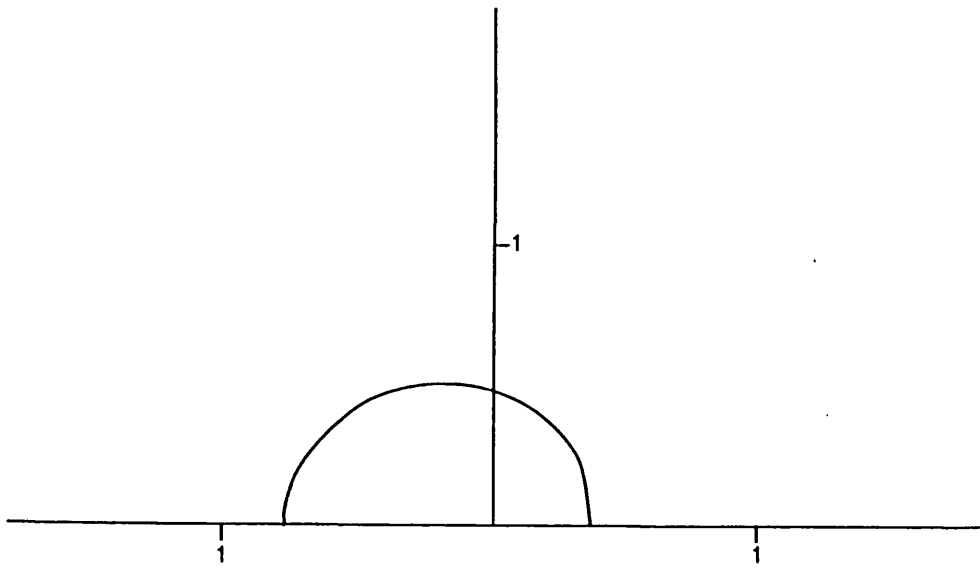


Figure 6.3. Polar diagram of $S(\theta, P)$, the mean elevation at large distance.

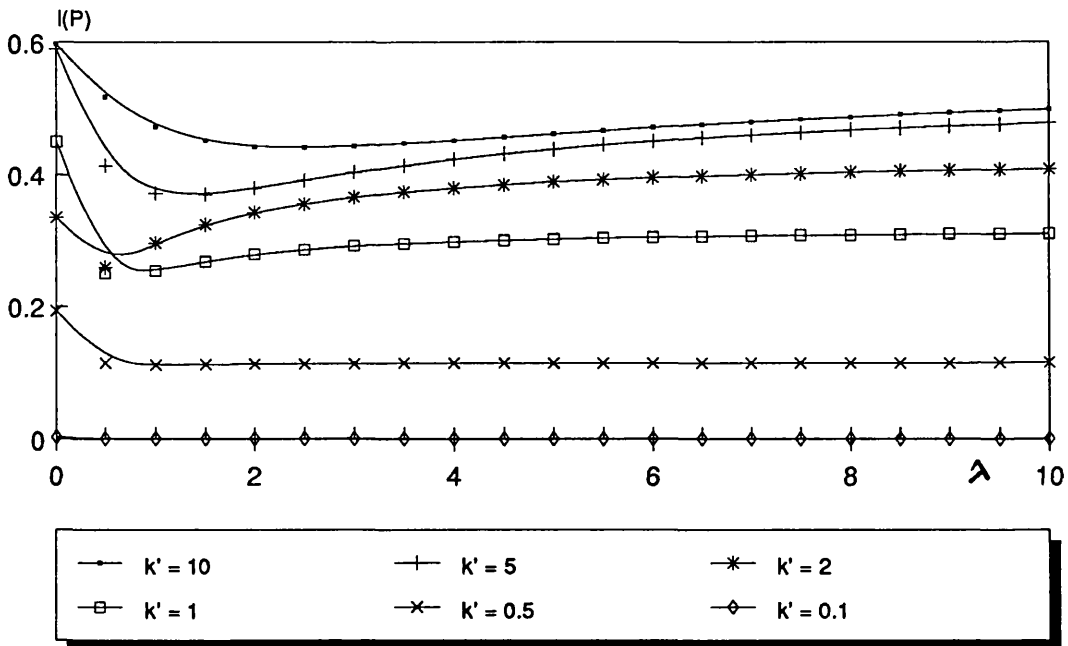


Figure 6.4. The averaged intensity of $I(P)$ as a function of λ ; $K = 0.1$.

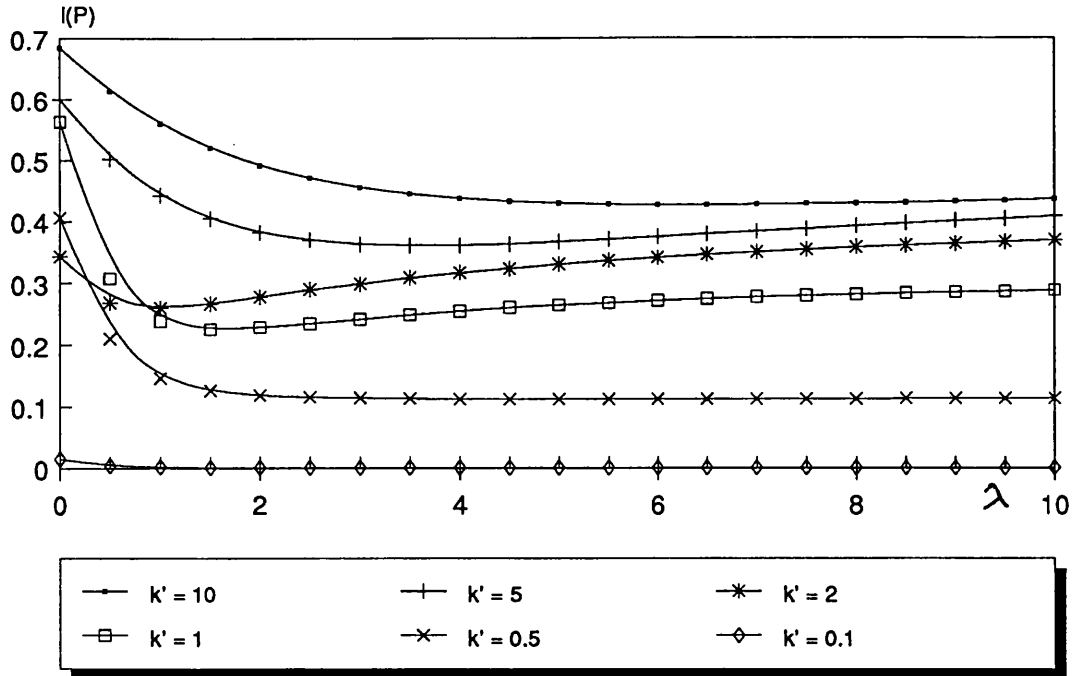


Figure 6.5. The averaged intensity of $I(P)$ as a function λ ; $K = 1$.

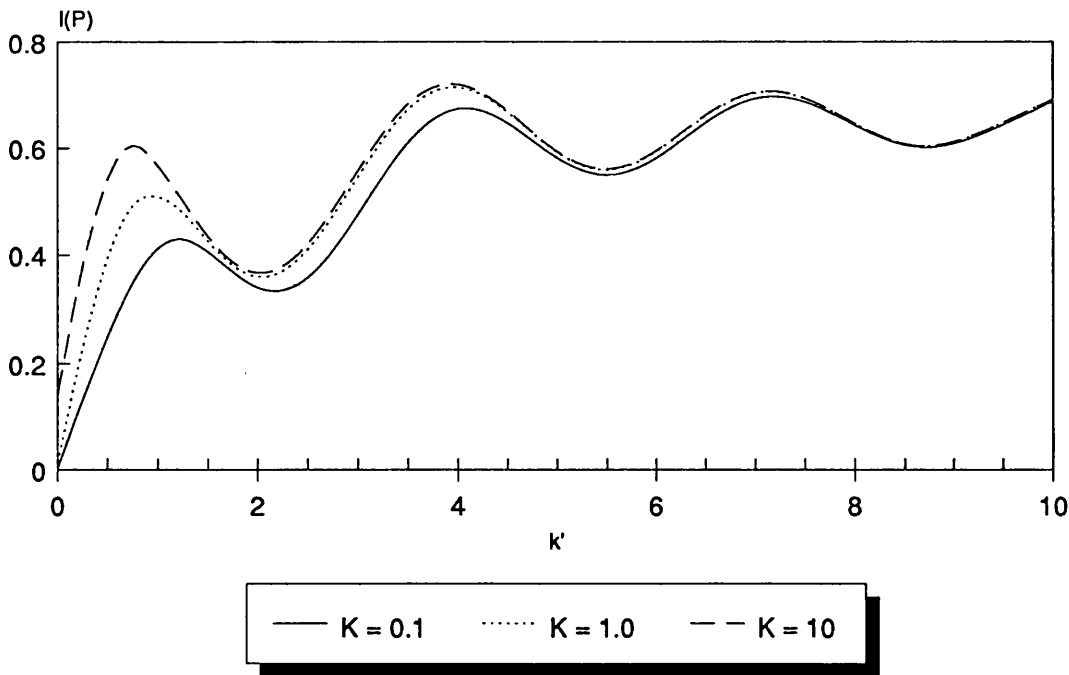


Figure 6.6. The intensity of the wave as a function of k' ; $\lambda = 0$.

$$\lambda = 1, K = 1, k' = 10$$

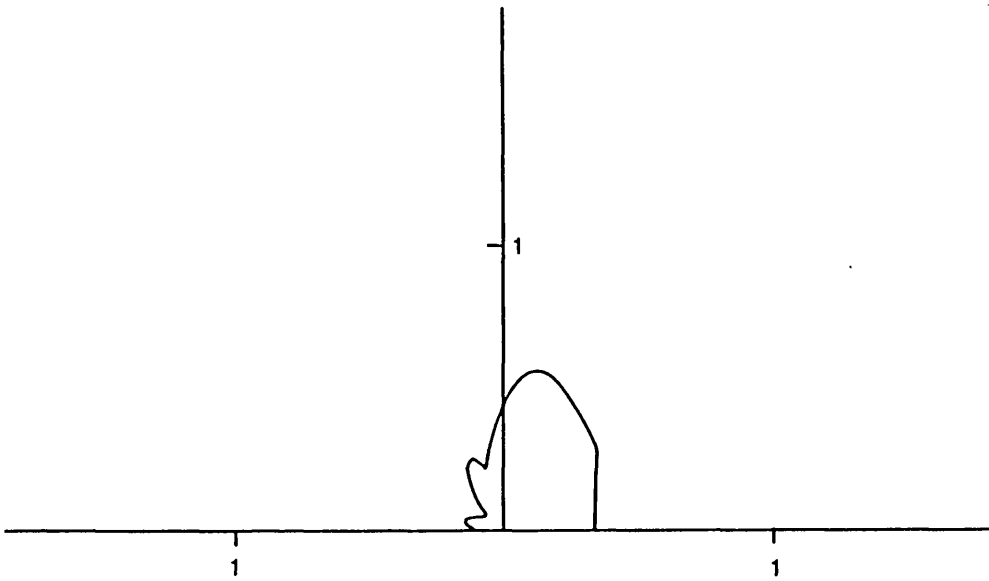


Figure 6.7. Polar diagram of $H(\theta, P)$, the mean elevation on the cylinder.

$$\lambda = 1, K = 1, k' = 1$$

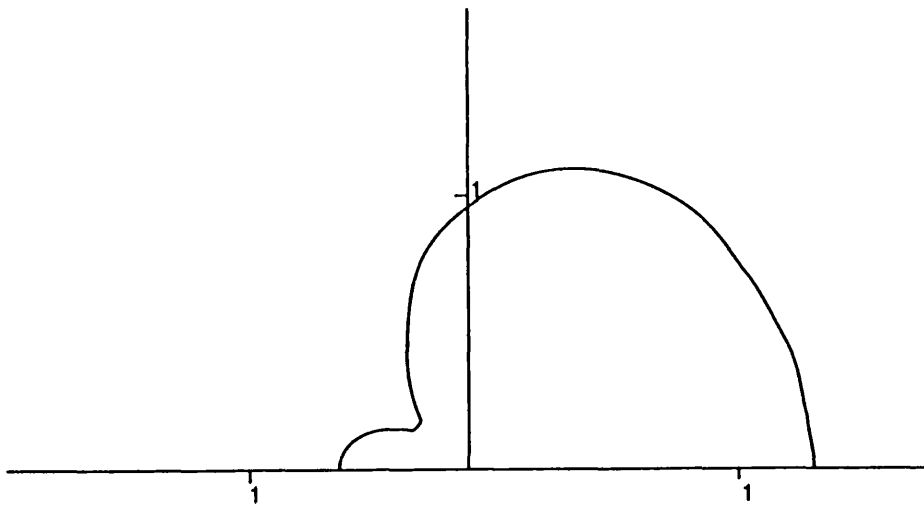


Figure 6.8. Polar diagram of $H(\theta, P)$, the mean elevation on the cylinder.

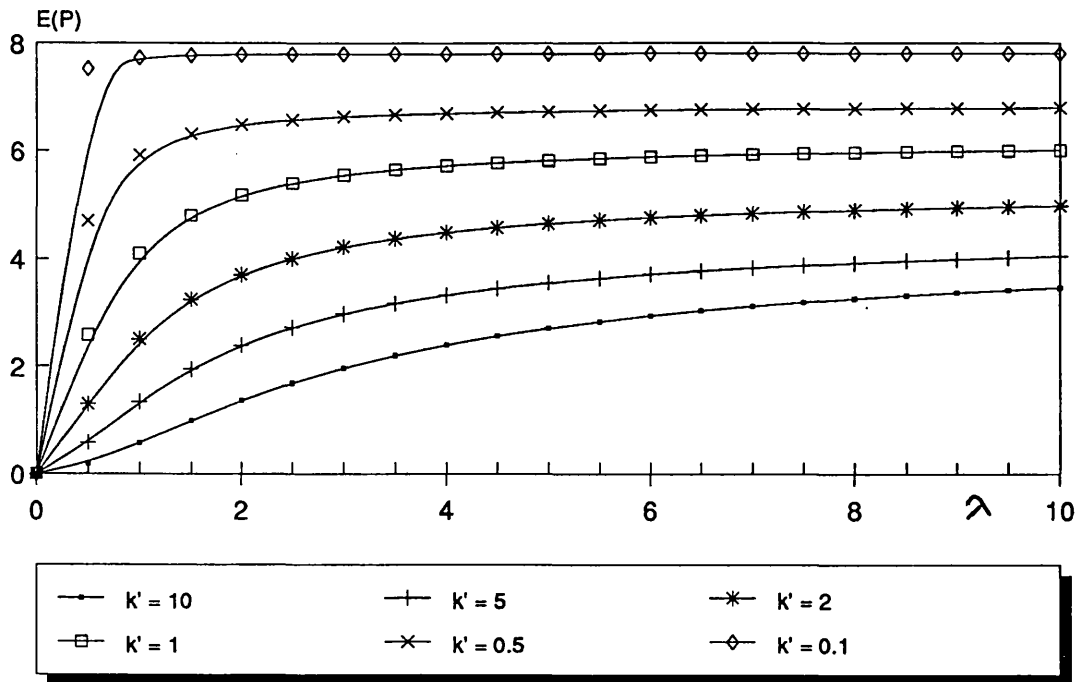


Figure 6.9. The averaged intensity of the elevation on the cylinder; $K = 0.1$.

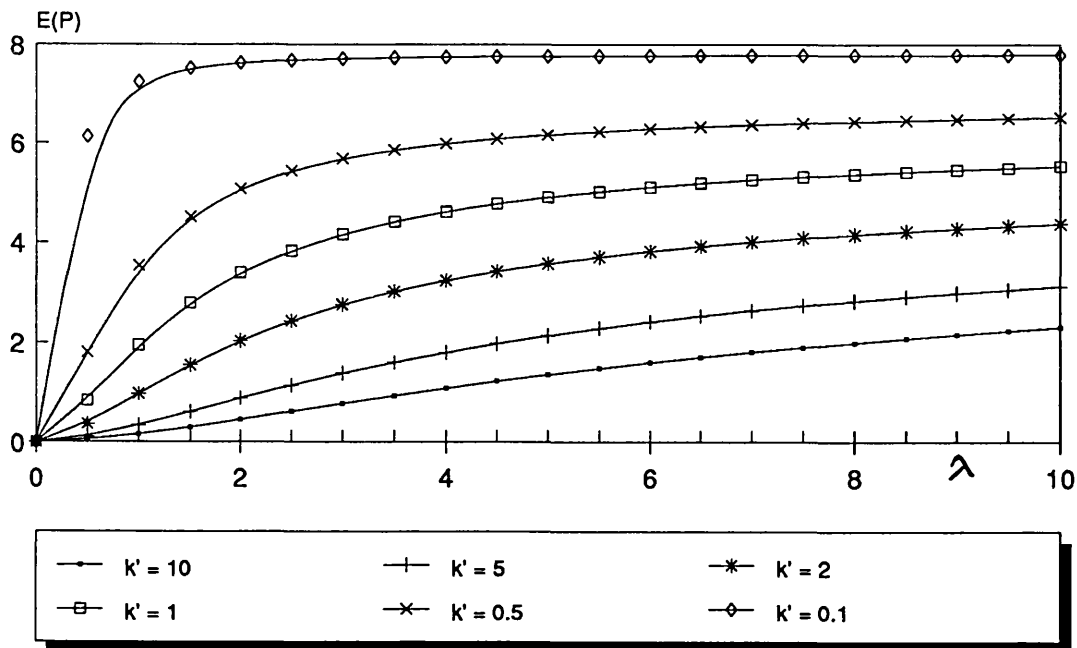


Figure 6.10. The averaged intensity of the elevation on the cylinder; $K = 1$.

CYLINDERS IN SHALLOW WATER

7.1 - Introduction

At a large distance away from a vertical cylinder, the surface elevation of the surface waves can be determined using the shallow water theory, when the depth of the channel or the fluid is small in comparison with the waves' wavelength (as a simpler approach, discussed by Crapper (1984)), where the presence of the surface tension is significant. This is analyzed below, when the cylinder is under a vertical or horizontal oscillation or an incident plane wave is scattered when the cylinder is fixed.

The non-dimensional variables are based on the horizontal and vertical lengths, a and h respectively. Furthermore, the vertical coordinate z and the velocity w in that direction are written as

$$z = h \zeta \quad \& \quad w = h W \quad (7.1)$$

according to the shallow water theory (that is when $h \ll 1$). The time dependence $\exp(-i\sigma t)$ is omitted from the right-hand sides of the equations since they are all multiplied by this factor.

The components of the velocity, using the equations of motion are

$$u = \frac{1}{i\sigma} \frac{\partial p}{\partial r} \cos\vartheta, \quad (7.2)$$

$$v = - \frac{1}{i\sigma} \frac{p}{r} \sin\vartheta, \quad (7.3)$$

$$w = \frac{1}{i\sigma} \frac{\partial p}{\partial z} \cos\vartheta, \quad (7.4)$$

here is $P(r,z) \cos \theta$

where p and σ are the pressure and the frequency respectively. The pressure p is found to be independent of ζ (using equations 7.1 and 7.4 and existence of small depth).

7.2 - Horizontal Oscillation

Here a cylinder of radius a is forced to oscillate horizontally with frequency σ . The boundary condition is

$$w = 0 \quad \text{when } z = -h. \quad (7.5)$$

The continuity equation is found to be (using equations 7.2 & 7.3)

$$\frac{\cos \theta}{i\sigma} \left[\frac{\partial^2 p}{\partial r^2} + \frac{1}{r} \frac{\partial p}{\partial r} - \frac{p}{r^2} \right] = - \frac{\partial w}{\partial z}, \quad (7.6)$$

then noting that the pressure is independent of ζ and equation 7.5, the z -component of the velocity becomes

$$w = \frac{-h \cos \theta}{i\sigma} \left(\frac{\partial^2 p}{\partial r^2} + \frac{1}{r} \frac{\partial p}{\partial r} - \frac{p}{r^2} \right) (\zeta + 1). \quad (7.7)$$

On the free surface of the fluid

$$\frac{\partial \eta}{\partial t} = w \quad \text{at } z = 0. \quad (7.8)$$

Therefore, surface elevation η , is (using equations 7.8 & 7.7)

$$\eta = \frac{-h \cos \theta}{\sigma^2} \left[\frac{\partial^2 p}{\partial r^2} + \frac{1}{r} \frac{\partial p}{\partial r} - \frac{p}{r^2} \right]. \quad (7.9)$$

The dynamic surface condition

$$\eta - K \left[\frac{\partial^2 \eta}{\partial r^2} + \frac{1}{r} \frac{\partial \eta}{\partial r} + \frac{1}{r^2} \frac{\partial^2 \eta}{\partial \theta^2} \right] = p \omega_0 a, \quad (7.10)$$

gives the relationship between the frequency of the surface waves σ , the wavenumber k' , and the depth h , (as

discussed in chapter 2) which is

$$\sigma^2 = k'^2 h(1 + Kk'^2). \quad (7.11)$$

It can be deduced from equation 7.9 that

$$\frac{\partial^2 \eta}{\partial \vartheta^2} = -\eta. \quad (7.12)$$

The following two equations for the surface elevation, therefore, can be obtained (using equations 7.9-7.12)

$$K \left[\frac{\partial^2 \eta}{\partial r^2} + \frac{1}{r} \frac{\partial \eta}{\partial r} - \frac{1}{r^2} \eta \right] - (1 + Kk'^2) \eta = 0 \quad \& \quad (7.13)$$

$$\left[\frac{\partial^2 \eta}{\partial r^2} + \frac{1}{r} \frac{\partial \eta}{\partial r} - \frac{1}{r^2} \eta \right] + k'^2 \eta = 0, \quad (7.14)$$

(since $[(KM - (1 + Kk'^2)) (M + k'^2)] \eta = 0$ with $M \equiv \frac{\partial^2}{\partial r^2} + \frac{1}{r} \frac{\partial}{\partial r} - \frac{1}{r^2}$),

with solutions $K_1 \left[\left((1 + Kk'^2) / K \right)^{1/2} r \right]$ and $H_1^{(1)}(k'r)$

respectively (since only outgoing waves are required and therefore $I_1 \left[\left((1 + Kk'^2) / K \right)^{1/2} r \right]$ cannot be considered for the first equation, and also because of the time dependence which is $\exp(-i\sigma t)$, the Hankel function $H_1^{(2)}(k'r)$ has to be excluded for the second equation).

Therefore

$$\eta = A H_1^{(1)}(k'r) + B K_1 \left[\left((1 + Kk'^2) / K \right)^{1/2} r \right], \quad (7.15)$$

where the coefficients A and B (both functions of K, k' and λ) are determined using the following edge conditions

$$u = e^{-i\sigma t} \cos \vartheta \quad \text{on} \quad r = 1, \quad (7.16)$$

and

$$\frac{\partial \eta}{\partial t} = \lambda \frac{\partial \eta}{\partial r} \quad \text{on} \quad r = 1. \quad (7.17)$$

Hence,

$$B = \frac{-i\sigma e^{-i\sigma t} [\lambda k' H_1^{(1)'}(k') + i\sigma H_1^{(1)}(k')]}{C(K, k')} \quad (7.18)$$

and

$$A = \frac{-B [\lambda \alpha K_1(\alpha) + \lambda \alpha K_1'(\alpha)]}{\lambda k' H_1^{(1)'}(k') + i\sigma H_1^{(1)}(k')}, \quad (7.19)$$

where

$$C(K, k') = -\lambda \alpha k' K K_1'(\alpha) H_1^{(1)'}(k') [\alpha^2 + k'^2] + \\ i\sigma [\alpha(1 - K\alpha^2) K_1'(\alpha) H_1^{(1)}(k') - \\ k'(1 + Kk'^2) K_1(\alpha) H_1^{(1)'}(k')], \quad (7.20)$$

and

$$\alpha = \left((1 + Kk'^2) / K \right)^{1/2}. \quad (7.21)$$

Therefore the surface elevation at a large distance away from the cylinder η_ω , is (noting that $r \rightarrow \infty$, $K_1(\alpha r) \rightarrow 0$)

$$|\eta_\omega| = |A| |H_1^{(1)}(k'r)|. \quad (7.22)$$

The quantity $|A|$ is the amplitude of the radiated wave.

7.3 - Limiting Cases Of The Horizontal Oscillation

In this section the limiting value of the surface elevation at large distances away from the cylinder in shallow water is obtained when

- a) k' is small;

- b) k' is large;
- c) K is small.

The following notation is introduced (to be used in this section)

$$k_1 = \frac{8k'i}{\pi^2}, \quad f_1(k, k', K) = Kk'^4 - Kk^4 - k^2,$$

$$\hat{J}_1(k) = Y_1'^2(k) + J_1'^2(k).$$

When k' is small

$$\alpha \approx K^{-1/2}, \quad \sigma^2 \approx k'^2 h \text{ (using equation 7.11),}$$

$$H_1^{(1)}(k') \approx -\frac{2i}{\pi k'} \approx -\frac{1}{k'} H_1^{(1)'}(k') \gg 1,$$

therefore (using equation 7.19)

$$|A|^2 \approx \frac{\pi^2 k'^2}{4} \frac{k'^4 h^2 K_1^2(\alpha) + \lambda^2 k'^2 h \alpha^2 K_1'^2(\alpha)}{k'^2 h K_1^2(\alpha) + \lambda^2 \alpha^2 K_1'^2(\alpha)} \quad (7.23)$$

The upper and the lower limits of λ , ∞ and 0 respectively, correspond to the free-end and pinned-end edge conditions, where at these limits A is expressed as

$$|A|^2 \approx \frac{\pi^2 k'^4 h}{4}, \quad (7.24)$$

and the surface elevation (using equation 7.22) is

$$|\eta_\omega|^2 = |A|^2 \left| \left(\frac{2}{\pi k' r} \right)^{1/2} e^{i(k'r - \frac{3}{4}\pi)} \right|^2, \quad (7.25)$$

hence in the transformed coordinate,

$$|\bar{\eta}|^2 = |\eta_\omega|^2 r = \frac{\pi}{2} h k'^3, \quad (7.26)$$

which is the limit of $|\bar{\eta}|^2$ when the depth is arbitrary as

discussed below . In chapter 5, the surface elevation at large distance away from the cylinder is obtained in equation 5.21, and when k' and h are very small, then L in the limit is (using equation 5.22)

$$L \approx \frac{(\hbar\pi k'^4 / 2) - \left[(4k'^2 \hbar i / \pi^2) N_1 \right]}{(\kappa k'^5 \pi \hbar^{1/2} / 2) - \left[(4k' \hbar^{1/2} i / \pi^2) N_2 \right]}, \quad (7.27)$$

where according to the numerical values

$$\kappa k'^2 L \ll k' \hbar^{1/2} \quad (7.28)$$

and hence

$$\kappa k'^2 L - k' \hbar^{1/2} \approx - k' \hbar^{1/2}, \quad (7.29)$$

therefore, $|\bar{\eta}|^2$ is expressed as

$$|\bar{\eta}|^2 \approx \pi k'^3 \hbar / 2 \quad (7.30)$$

which confirms the above result (equation 7.26).

Next, since for large values of k' ($k' \gg 1$)

$$\sigma^2 \approx \kappa k'^4 \hbar, \quad \alpha \approx k',$$

$$K_1(\alpha) \approx -K_1'(\alpha) \approx \left(\frac{\pi}{2k'} \right)^{1/2} e^{-k'},$$

$$H_1^{(1)}(k') \approx -i H_1^{(1)'}(k') \approx \left(\frac{2}{\pi k'} \right)^{1/2} e^{i(k' - \frac{3}{4}\pi)},$$

$$H_1^{(2)}(k') \approx -i H_1^{(2)'}(k') \approx \left(\frac{2}{\pi k'} \right)^{1/2} e^{-i(k' - \frac{3}{4}\pi)}.$$

then (using equation 7.22) $|\bar{\eta}|^2$ is expressed as

$$|\bar{\eta}|^2 \approx \frac{1}{k'^2} \frac{K^2 k'^2 h^2 + hK\lambda^2}{2hK^3 k'^2 + 4K^2 \lambda^2 + 4\lambda K^2 h^{1/2} K^{1/2} k'}, \quad (7.31)$$

and hence

$$|\bar{\eta}|^2 \approx \begin{cases} \frac{h}{4Kk'^2} & \text{as } \lambda \rightarrow \infty, \\ \frac{h}{2Kk'^2} & \text{at } \lambda = 0. \end{cases} \quad (7.32)$$

Similarly at pinned-end and free-end edge conditions,

$$L \approx \begin{cases} \sigma & \text{when } \lambda \rightarrow \infty, \\ (hK)^{1/2} F(K, k') & \text{when } \lambda = 0, \end{cases} \quad (7.33)$$

such that

$$F(K, k') = \frac{1 - k_1 \int_0^\infty \frac{1 + Kk^2}{k J_1(k) f_1(k, k', K)} dk}{1 - Kk_1 \int_0^\infty \frac{k}{J_1(k) f_1(k, k', K)} dk}, \quad (7.34)$$

Therefore, $|\bar{\eta}|^2$ is expressed as (using partial approach

$$|\bar{\eta}|^2 \approx \begin{cases} \frac{h}{4Kk'^2} & \text{when } \lambda \rightarrow \infty, \\ \frac{h}{2Kk'^2} & \text{when } \lambda = 0, \end{cases} \quad (7.35)$$

which again confirms the above result (according to equation 7.32).

Finally, since for small capillarity coefficient K ,

$$\alpha \approx K^{-1/2} \gg 1, \quad \sigma^2 \approx k'^2 h,$$

$$K_1(\alpha) \approx -K_1'(\alpha) \approx \left(\frac{\pi}{2\alpha}\right)^{1/2} e^{-\alpha},$$

then, $|\bar{\eta}|^2$ is (using equation 7.22)

$$|\bar{\eta}|^2 \approx \frac{2h}{\pi k'} \frac{1}{\hat{J}_1(k')}, \quad (7.36)$$

at both extreme values of λ . This result will be confirmed later (in equation 7.41). When capillarity coefficient and depth are both small, the equation for surface elevation at large distances away from the cylinder will be of the following form

$$|\bar{\eta}|^2 \approx \frac{2}{\pi k'} \frac{|KLk'^2 - \sigma - \sigma Kk'^2|^2}{k'^2 \hat{J}_1(k')}, \quad (7.37)$$

where

$$L \approx \begin{cases} -h^{1/2} \pi & \text{when } \lambda = 0, \\ 2Kk' i \hat{J}_1(k') \int_0^{\infty} \frac{k}{\hat{J}_1(k) f_1(k, k', K)} dk & \\ \sigma & \text{when } \lambda \rightarrow \infty. \end{cases} \quad (7.38)$$

Hence,

$$|\bar{\eta}|^2 \approx \begin{cases} \frac{2h}{\pi k' \hat{J}_1(k')} & \text{when } \lambda = 0, \\ \frac{2h}{\pi k' \hat{J}_1(k')} & \text{when } \lambda \rightarrow \infty. \end{cases} \quad (7.39)$$

As it can be seen according to equations 7.26, 7.32 and 7.36, the approach of finding the surface elevation in shallow water, using shallow water theory is less complicated than the approach used for determining the same thing by determining the elevation of the free surface when the fluid is of arbitrary depth and hence let

the depth tend to zero.

7.4 - Vertical Oscillation

There have been many investigations on the interaction between surface waves and partially immersed bodies, which may be fixed or floating or may be forced to move. In most of the studies on this topic, surface tension has safely been ignored. In chapter 4, the problem of infinite depth vertical cylinder oscillating vertically was studied. In this section, however, corresponding problem to the one solved in that chapter for small depth fluid using shallow water theory is considered.

The motion is independent of the radial angle ϕ , since the movement of surface waves produced by vertical oscillation of an upright cylinder in water is axisymmetric. The forced oscillation has frequency σ . The velocity components in non-dimensionalization form are (as discussed in chapter 2)

$$u = \frac{1}{i\sigma} \frac{\partial p}{\partial r} \cos \phi, \quad (7.40)$$

$$w = \frac{1}{i\sigma} \frac{\partial p}{\partial z} \cos \phi, \quad (7.41)$$

and the continuity equation is (using equations 7.40 and 7.41)

$$\frac{1}{i\sigma} \left[\frac{\partial^2 p}{\partial r^2} + \frac{1}{r} \frac{\partial p}{\partial r} \right] = - \frac{\partial w}{\partial z}, \quad (7.42)$$

resulting the relationship between w and ζ as (noting that p is independent of ζ and the boundary condition 7.5)

$$w = - \frac{h}{i\sigma} \left[\frac{\partial^2 p}{\partial r^2} + \frac{1}{r} \frac{\partial p}{\partial r} \right] (\zeta + 1). \quad (7.43)$$

The surface elevation at a large distance away from the cylinder (using the free surface condition 7.8 and the equation 7.43) is

$$\eta = - \frac{h}{\sigma^2} \left[\frac{\partial^2 p}{\partial r^2} + \frac{1}{r} \frac{\partial p}{\partial r} \right], \quad (7.44)$$

where by simultaneous solution with the dynamic surface condition, equation 7.10, and using equation 7.11 to replace σ , the solutions of η are determined as $J_0(k'r)$, $Y_0(k'r)$, $K_0 \left[\left((1 + Kk'^2) / K \right)^{1/2} r \right]$ & $I_0 \left[\left((1 + Kk'^2) / K \right)^{1/2} r \right]$. However, the third term should be omitted to satisfy the radiation condition. Then the linear combination of the Bessel functions $H_0^{(1)}(k'r)$ & $H_0^{(2)}(k'r)$ is acceptable, and since the time dependence is $\exp(-i\sigma t)$, therefore η is

$$\eta = A H_0^{(1)}(k'r) + B K_0 \left[\left((1 + Kk'^2) / K \right)^{1/2} r \right], \quad (7.45)$$

where through the following boundary conditions

$$u = 0 \quad \text{on } r = 1, \quad (7.46)$$

and

$$\frac{\partial \eta}{\partial t} - \exp(-i\sigma t) = \lambda \frac{\partial \eta}{\partial r} \quad \text{on } r = 1, \quad (7.47)$$

the coefficients A and B are determined as

$$A = \frac{-k' K_0'(\alpha)}{C(k', K, \lambda, h)} \quad \& \quad B = \frac{-\alpha H_0^{(1)'}(k')}{C(k', K, \lambda, h)}, \quad (7.48)$$

such that

$$C(k', K, \lambda, h) = \left\{ H_0^{(1)'}(k') K_0'(\alpha) \left[\alpha^2 + k'^2 \right] \right\} + i\sigma \left[\alpha K_0(\alpha) H_0^{(1)'}(k') + k' H_0^{(1)}(k') K_0'(\alpha) \right]. \quad (7.49)$$

Hence the surface elevation at large distances away from the cylinder η_∞ , can be obtained as

$$|\eta_\infty| \approx |A|^2 \frac{2}{\pi k'}. \quad (7.50)$$

7.5 - Limiting Cases Of The Vertical Oscillation

When k' is small ($k' \ll 1$),

$$\alpha \approx K^{-1/2}, \quad \sigma^2 \approx k'^2 h, \quad K_0(\alpha) \approx K_0(K^{-1/2}),$$

$$H_0^{(1)}(k') \approx -\frac{2i}{\pi} \log(k'),$$

$$H_0^{(1)'}(k') \approx \frac{2i}{\pi k'} \gg 1,$$

and hence (using equation 7.50)

Next, when k' is large,

$$\sigma^2 \approx K k'^4 h, \quad \alpha \approx k',$$

$$K_0(\alpha) \approx -K_0'(\alpha) \approx \left(\frac{\pi}{2k'}\right)^{1/2} e^{-k'},$$

$$H_0^{(1)}(k') \approx -i H_0^{(1)'}(k') \approx \left(\frac{2}{\pi k'}\right) e^{i(k' - \frac{1}{4}\pi)},$$

and therefore (using equation 7.50)

$$|\eta_\infty|^2 r \approx \begin{cases} \frac{1}{2K k'^4 h} & \text{at } \lambda = 0, \\ \frac{1}{8\lambda^2} & \text{as } \lambda \rightarrow \infty. \end{cases} \quad (7.52)$$

Finally, when K is small,

$$\alpha \approx K^{-1/2} \gg 1, \quad \sigma^2 \approx k'^2 h,$$

$$K_0(\alpha) \approx -K_0'(\alpha) \approx \left(\frac{\pi}{2\alpha}\right)^{1/2} e^{-\alpha},$$

and hence

$$|\eta_\infty|^2 r \approx \begin{cases} \frac{2K}{\pi k' h [J_0'^2(k') + Y_0'^2(k')]} & \text{when } \lambda = 0, \\ \frac{2k' K^2}{\pi \lambda^2 [J_0'^2(k') + Y_0'^2(k')]} & \text{when } \lambda \rightarrow \infty. \end{cases} \quad (7.53)$$

In this section, the limiting value of the surface elevation at extreme values of k' and K cannot be compared with the arbitrary depth's results, as in chapter 4 only fluid and cylinder of infinite depth are considered.

7.6 - Scattering Of Waves In Shallow Water

The scattering of a capillary-gravity wave by a surface-piercing obstacle depends on the condition applied at the contact line between the fluid and the obstacle. There has been a growing interest in this problem in recent years, mainly in its extension to the scattering of waves by multiple obstacles, an interest that stems from the need to understand the wave forces on the supporting legs of ocean platforms. Hocking (1987b) studied reflection of capillary-gravity waves by a vertical plate. Same problem has been investigated by Mahdmina & Hocking (1990) for a vertical cylinder of infinite height. However, the problem of scattering of a capillary-gravity wave by a vertical cylinder is studied in shallow water, here.

A plane incident small amplitude wave of amplitude ϵa (with $\epsilon \ll 1$), is scattered by a rigid cylinder of radius a which is placed in the water (with uniform density of ρ , surface tension of γ , gravitational acceleration of g and small height of h) along its vertical axis which extends above the surface. A plane incident wave of wavenumber k' moves in the direction of $\vartheta = 0$. The surface elevation η , can be written as

$$\eta = \eta_i + \eta_s \quad (7.54)$$

$$\eta_i = \exp(ik'r \cos\vartheta), \quad (7.55)$$

where subscripts i and s indicate incident and scattered components respectively. These components should be determined such that the conditions on the cylinder and at the edge are satisfied and present an outward-moving wave.

The scattered components of the velocity are (in the non-dimensionalization form as discussed in chapter 2)

$$u = \frac{1}{i\sigma} \frac{\partial p}{\partial r} \cos(n\vartheta), \quad (7.56)$$

$$v = -\frac{1}{i\sigma} \frac{np}{r} \sin(n\vartheta), \quad (7.57)$$

$$w = \frac{1}{i\sigma} \frac{\partial p}{\partial z}. \quad (7.58)$$

Then, the z-component of velocity is (noting that p is independent of ζ in shallow water theory and substituting equations 7.56-7.58 into equations of motion)

$$w = -\frac{h}{i\sigma} \cos(n\vartheta) \left(\frac{\partial^2 p}{\partial r^2} + \frac{1}{r} \frac{\partial p}{\partial r} - \frac{n^2}{r^2} p \right) (\zeta + 1), \quad (7.59)$$

and the surface elevation η , is (using the free surface condition 7.8 and the equation 7.11)

$$\eta = -\frac{\cos(n\vartheta)}{k'^2(1 + Kk'^2)} \left[\frac{\partial^2 p}{\partial r^2} + \frac{1}{r} \frac{\partial p}{\partial r} - \frac{n^2}{r^2} p \right]. \quad (7.60)$$

However, in conjunction with the dynamic surface condition

$$\eta - K \left[\frac{\partial^2 \eta}{\partial r^2} + \frac{1}{r} \frac{\partial \eta}{\partial r} - \frac{n^2}{r^2} \eta \right] = p, \quad (7.61)$$

and consequently the scattered component of the surface elevation η_s , is

$$\eta_s = A_n H_n^{(1)}(k'r) + B_n K_n \left[\left((1 + Kk'^2)/K \right)^{1/2} r \right], \quad (7.62)$$

hence (from equation 7.64)

$$\eta = e^{(ik'r \cos\vartheta)} + \sum_{n=0}^{\infty} \left\{ A_n H_n^{(1)}(k'r) + B_n K_n \left[\left((1 + Kk'^2)/K \right)^{1/2} r \right] \right\} \cos(n\vartheta), \quad (7.63)$$

with the edge conditions of

$$u = 0 \quad \text{on } r = 1, \quad (7.64)$$

and the condition given in equation 7.17.

The first term of the right-hand side of equation 7.63 can be written (as discussed in chapter 6) as

$$\exp(ik'r \cos\vartheta) = \sum_{n=0}^{\infty} 2i^n J_n(k'r) \cos(n\vartheta). \quad (7.65)$$

Therefore A_n and B_n can be obtained as (using equations 7.63, 7.17 & 7.64)

$$A_n = -2i^n \frac{E_n(K, k', \lambda)}{F_n(K, k', \lambda)}, \quad (7.66)$$

where,

$$E_n(K, k', \lambda) = \lambda J_n'(k') K_n'(\alpha) [k'^2 - \alpha^2] + i\sigma \left[k' J_n(k') K_n'(\alpha) - \alpha K_n(\alpha) J_n'(k') \right], \quad (7.67)$$

$$F_n(K, k', \lambda) = \lambda H_n^{(1)'}(k') K_n'(\alpha) [k'^2 - \alpha^2] + i\sigma \left[k' K_n'(\alpha) H_n^{(1)}(k') - \alpha H_n^{(1)'}(k') K_n(\alpha) \right], \quad (7.68)$$

and

$$B_n = \frac{k' (1 + Kk') \left[2i^n J_n'(k') + A_n H_n^{(1)'}(k') \right]}{(K\alpha^2 - 1) \alpha K_n'(\alpha)}. \quad (7.69)$$

7.7 - Limiting Cases Of The Scattering Problem

In this section as in the section 7.5, the limiting cases cannot be compared with their results obtained through arbitrary depth, since the corresponding problem (in chapter 6) is studied only for infinite depth.

However, when k' is small ($k' \ll 1$),
 $\alpha \approx K^{-1/2}$, $\sigma^2 \approx k'^2 h$, $K_n(\alpha) \approx K_n \left(K^{-1/2} \right)$,

$$H_n^{(1)}(k') \approx -\frac{i}{\pi} \left(\frac{2}{k'} \right)^n \Gamma(n),$$

$$H_n^{(1)'}(k') \approx \frac{ni}{2\pi} \left(\frac{2}{k'} \right)^{n+1} \Gamma(n),$$

$$J_n(k') \approx \left(\frac{k'}{2} \right)^n / \Gamma(n+1),$$

$$J_n'(k') \approx \left(\frac{k'}{2} \right)^{n-1} \frac{n}{2 \Gamma(n+1)},$$

and hence (using equation 7.66)

$$|A_n|^2 \approx 4(-1)^n \frac{k'^{4n} \pi^2}{2^{4n} n^2 \Gamma^2(n)}. \quad (7.70)$$

Next, when k' is large ($k' \gg 1$),

$$\sigma^2 \approx Kk'^4 h, \quad \alpha \approx k',$$

$$K_n(\alpha) \approx -K_n'(\alpha) \approx \left(\frac{\pi}{2k'} \right)^{1/2} e^{-k'},$$

$$H_n^{(1)}(k') \approx -i H_n^{(1)'}(k') \approx$$

$$\left(\frac{2}{\pi k'}\right)^{1/2} e^{i(k' - \pi/4 - n\pi/2)},$$

$$J_n(k') \approx \left(\frac{2}{\pi k'}\right)^{1/2} \cos\left(k' - \frac{n\pi}{2} - \frac{\pi}{4}\right),$$

$$J'_n(k') \approx -\left(\frac{2}{\pi k'}\right)^{1/2} \sin\left(k' - \frac{n\pi}{2} - \frac{\pi}{4}\right),$$

and therefore (using equation 7.66)

$$|A_n|^2 \approx (-1)^{n+1} \left[-1 - e^{-4i(k' - \pi/4 - n\pi/2)}\right]. \quad (7.71)$$

Finally, when K is small ($K \ll 1$)

$$\alpha \approx K^{-1/2} \gg 1, \quad \sigma^2 \approx k'^2 h,$$

$$K_n(\alpha) \approx \left(-\frac{\pi}{2\alpha}\right) e^{-\alpha},$$

and hence,

$$|A_n|^2 \approx 4(-1)^n \frac{J_n'^2(k')}{H_n^{(1)'}{}^2(k')}. \quad (7.72)$$

HORIZONTAL OSCILLATION OF PLATES

Here, the horizontal oscillation of a vertical plate in the presence of surface tension is studied, such that two different cases are considered. The first has the plate and the fluid of finite and infinite depths respectively. In the second case, surface waves are produced by horizontal oscillation of the plane wavemaker at one end of a channel. In latter, the waves generated by a plane wavemaker in fluid of infinite depth and in fluid of a depth equal to that of the wavemaker are determined. The second problem is summarized in the recent paper by Hocking & Mahdmina (1991).

8.1 - Finite Length Plate And Infinite Depth Fluid

Waves are produced on the free surface of the fluid by the heaving motion of a plate which is partially immersed in the fluid. These waves will carry energy away from the plate which will result in the decay of a free motion of the plate or requiring an input of energy to sustain a forced motion. This has been the topic of many studies, but for gravity waves only. Ursell (1949) has studied the case of a horizontal circular cylinder with its axis in the free surface. The heaving motion of a vertical cylinder has been solved by Yeung (1981). In many applications the modifying effects of capillarity have been ignored, since the main application has been to ship motions and capillarity is not important in such cases. However, the effect of surface tension cannot be neglected on the scale of laboratory experiments. It may be of some interest to determine the radiation of energy from a heaving body by capillary-gravity waves. Hocking (1988a)

has studied the vertical oscillation of a partially immersed horizontal circular cylinder and a simple source-and-plate model which produces surface waves. He has calculated the amplitude of these waves and the amount of energy dissipated, when the surface tension is included.

Here, the horizontal oscillation of a plate which is partially immersed in the fluid is studied. The surface elevation of capillary-gravity waves produced by this motion of the free surface at large distance away from the plate is calculated. Since, only two-dimensional motions are considered, the radiated waves are plane. In order to ensure a flat interface in equilibrium, it is assumed that the plate's surface is vertical where it intersects the free surface and that the static contact angle is 90° . The solution is linear, since the amplitude of the motion is assumed to be sufficiently small. It is also necessary to restrict the static range of contact angles to be small, since hysteresis effects have been included with small-amplitude waves present. Viscosity is ignored throughout the study. The edge condition which is used in this chapter, is the one justified in chapter 1, which was incorporated by Hocking (1987a).

A plate of length $2h$ which is partially immersed in a fluid of infinite depth, is forced to oscillate horizontally, along the x -axis. The depth of the submerged plate is h . This oscillation can be thought of as infinitely many sources and sinks which produce waves on the free surface of the fluid. The propagation of these waves at large distance away from the plate is to be determined. The x -axis is horizontal and the y -axis is along the upward vertical from an origin in the free surface. As explained in chapter 2, all lengths are scaled by $1/\hat{k}$, with $2\pi/\hat{k}$ is the wavelength of surface waves of angular frequency σ , such that

$$\hat{\sigma}^2 = g\hat{k} + \frac{\gamma\hat{k}^3}{\rho}, \quad (8.1)$$

g is the acceleration due to gravity, γ surface tension and ρ the density of the fluid. The non-dimensional fluid velocity, the dynamic pressure, the time and the velocity potential are $\mathbf{u} = (u, v)$, p , t and ϕ respectively. The time dependence is $\exp(i\sigma t)$ which appears in all the terms and therefore it is omitted. The equations for the linearized fluid motion can then be written as

$$\frac{\partial \mathbf{u}}{\partial t} = -\text{grad } p, \quad \nabla^2 \phi = 0. \quad (8.2)$$

The velocity potential has two components of ϕ_1 and ϕ_2 . The boundary conditions on ϕ_1 and ϕ_2 are;

$$\text{On } x = 0, \quad \frac{\partial \phi_1}{\partial x} = \begin{cases} 1 & \text{when } -h < y < 0, \\ -1 & \text{when } 0 < y < h. \end{cases} \quad (8.3)$$

$$\text{On } x = 0, \quad \frac{\partial \phi_2}{\partial x} = 0, \quad (8.4)$$

$$\frac{\partial \phi_2}{\partial y} \rightarrow 0 \quad \text{as } y \rightarrow -\infty. \quad (8.5)$$

Since the plate oscillates horizontally, there is a distribution of sources between $y = -h$ and 0 . The corresponding sinks are distributed between $y = 0$ and h . The components of the velocity potential will be

$$\phi_1 = \frac{1}{2\pi} \int_{-h}^0 \left\{ \log \left[x^2 + (y + y_1)^2 \right] - \log \left[x^2 + (y - y_1)^2 \right] \right\} dy_1 \quad (8.6)$$

and

$$\phi_2 = \int_0^{\infty} P(k) \cos(kx) e^{ky} dk. \quad (8.7)$$

The pressure (using equation 8.2) is

$$p = \frac{-i\sigma}{2\pi} \int_{-h}^0 \left\{ \log \left[x^2 + (y + y_1)^2 \right] - \log \left[x^2 + (y - y_1)^2 \right] \right\} dy_1 - i\sigma \int_0^{\infty} P(k) \cos(kx) e^{ky} dk. \quad (8.8)$$

Noting that the condition on the free surface is

$$\frac{\partial \eta}{\partial t} = \frac{i}{\sigma} \frac{\partial p}{\partial y} \quad \text{on } y = 0, \quad (8.9)$$

the equation of surface elevation can be found as

$$\eta = \frac{i}{\pi\sigma} \log \left(1 + \frac{h^2}{x^2} \right) - \frac{i}{\sigma} \int_0^{\infty} P(k) \cos(kx) k dk. \quad (8.10)$$

The surface elevation can be obtained also from the dynamic surface condition on the free surface, as

$$\eta - K \frac{\partial^2 \eta}{\partial x^2} = p. \quad (8.11)$$

If the surface elevation η , is assumed to be

$\eta = \int_0^{\infty} A(k) \cos(kx) dk$, then by substituting into equation 8.11, the solution satisfying the dynamic surface condition can be shown to be

$$\eta = -i\sigma \int_0^{\infty} \frac{1}{1 + Kk^2} P(k) \cos(kx) dk. \quad (8.12)$$

The complementary solution to the dynamic surface condition, however, is either $C \exp(K^{-1/2}x)$ or $C \exp(-K^{-1/2}x)$. Since the radiation condition must be satisfied, only the second solution can be permitted, hence the solution to equation 8.11 when $C = B K^{1/2}$ is

$$\eta = -i\sigma \int_0^{\infty} \frac{1}{1 + Kk^2} P(k) \cos(kx) dk + B K^{1/2} \exp(-K^{-1/2}x) \quad (8.13)$$

In order to equate equations 8.10 and 8.13, the first and second term of equations 8.10 and 8.13 should be written in Fourier cosine integral form (using the tables of integral transforms). By using

$$\log\left(1 + \frac{h^2}{x^2}\right) = \frac{2}{\pi} \int_0^{\infty} \frac{1 - e^{-hk}}{k} \cos(kx) dk \quad (8.14)$$

and

$$K^{1/2} e^{(-K^{-1/2})x} = \frac{2}{\pi} \int_0^{\infty} \frac{K}{1 + Kk^2} \cos(kx) dk, \quad (8.15)$$

and the relationship between the non-dimensional angular frequency and the capillarity coefficient K (as determined in chapter 2) is

$$\sigma^2 = 1 + K, \quad (8.16)$$

then the two equations for η can be equated and hence $P(k)$ can be determined

$$P(k) = \frac{2 i \left[BKk\sigma - i(1 + Kk^2) \cdot (1 - e^{-hk}) \right]}{\pi k \left[k(1 + Kk^2) - \sigma^2 \right]} + C \delta(k-1) \quad (8.17)$$

Now substituting $P(k)$ into equation 8.10 with $x \rightarrow \infty$, the surface elevation at a large distance away from the plate can be found as

$$\eta_{\infty} = -\frac{i}{\sigma} \int_0^{\infty} \frac{2i}{\pi} \frac{\{BKk\mathcal{G} - i(1 + Kk^2)(1 - e^{-hk})\}}{[k(1 + Kk^2) - \sigma^2]} \cos(kx) dk$$

$$- \frac{i}{\sigma} \int_0^{\infty} C \delta(k-1) k \cos(kx) dk. \quad (8.18)$$

In the above equation, if k approaches unity and satisfies the radiation condition with the knowledge that the time dependence is $\exp(i\sigma t)$, the parameter C in terms of B can be found as

$$C = \frac{2 \{BK\mathcal{G} - i(1 + K)(1 - e^{-h})\}}{1 + 3K}. \quad (8.19)$$

and hence η_{∞} becomes

$$\eta_{\infty} = \frac{-2i e^{-ix}}{\mathcal{G}(1 + 3K)} \{BK\mathcal{G} - i(1 + K)(1 - e^{-h})\}. \quad (8.20)$$

For the edge condition of

$$\frac{\partial \eta}{\partial t} = \lambda \frac{\partial \eta}{\partial x} \quad \text{at } x = 0, \quad (8.21)$$

to be satisfied, the parameter B must be

$$B = \frac{2\sigma^2 i (1 - e^{-h}) - \sigma^2 J_2}{(\lambda + i\sigma K^{1/2})(1 + 3K) + \sigma^2 J_1 + 2\sigma K}, \quad (8.22)$$

where

$$J_1 = \int_0^{\infty} \frac{2\sigma i K(1 + 3K)}{(1 + Kk^2)\pi [k(1 + Kk^2) - \sigma^2]} dk, \quad (8.23)$$

and

$$J_2 = \int_0^{\infty} \frac{2(1 - e^{-hk})(1 + 3K)}{\pi k [k(1 + Kk^2) - \sigma^2]} dk. \quad (8.24)$$

The principal value integrals of J_1 and J_2 shall be evaluated in section 8.2.

The surface elevation at a large distance away from the plate has been calculated for a range of values of the parameters h , K and λ . These represent half of the length of the plate, the capillarity coefficient and the ratio of contact line speed to the variation in the contact angle, respectively. The parameter h is taken to be 10, 5, 2, 1 and 0.1. The capillarity coefficient is given the values 0.01, 0.1, 0.2, 0.3 and 0.4. The capillarity increases as the value of the surface tension increases and hence the amplitude of the waves decreases. The range of the parameter λ is between 0 and 10.

From Figures 8.1-8.5, it can be deduced that for $h \leq 2$, the value of $|\eta_\infty|^2 r$ increases monotonically as K increases, as is expected. However, for large K (e.g. 0.4), when $h = 10$ or 5, this rule does not quite hold. For this reason, in Figures 8.6-8.10, the behaviour of these curves for values of $0 < \lambda < 1$, where the odd behaviour happens, has been concentrated on. Figures 8.1-8.4 show that the smaller the height of the plate, the more distinguishable the curves will be. Since $|\eta_\infty|^2 r$ has a minimum as a function of λ , when $h \geq 1$, it approaches its limit at $\lambda = 10$ from below. When $h < 1$, Figure 8.5 indicates that the limit is approached from above. Figures 8.6-8.10 show the variation of the surface elevation for $0 < \lambda < 1$.

8.2 - Numerical Approach

The principal value integral J_2 (in equation 8.24), can be written as

$$J_2 = \frac{2(1+3K)}{\pi} \int_0^\infty \frac{1 - e^{-hk}}{k(k-1)(1+Kk^2+Kk+K)} dk$$

$$= \frac{2(1+3K)}{\pi} \left\{ \int_0^{\infty} \frac{1-e^{-h}}{(k-1)(1+Kk^2+Kk+K)} dk - \int_0^{\infty} \frac{k - k e^{-h} - 1 + e^{-hk}}{k(k-1)(1+Kk^2+Kk+K)} dk \right\}, \quad (8.25)$$

where the first integral on the right-hand side can be evaluated analytically as

$$\int_0^{\infty} \frac{1-e^{-h}}{(k-1)(1+Kk^2+Kk+K)} dk = \frac{1-e^{-h}}{1+3K} \left\{ \ln \left[\frac{(1+K)}{K} \right]^{1/2} - \left[\frac{3}{\{(3K+4)/K\}^{1/2}} \right] \tan^{-1} \left[\frac{3K+4}{K} \right]^{1/2} \right\}. \quad (8.26)$$

To calculate the second integral in equation 8.25, the trapezium rule can be used for the bulk of the calculation, but special care is needed when k is small, when k is close to 1, and when k is large. When k is 0 or 1, the integrand is indeterminate and l'Hopital's rule can be applied to determine its limiting value. A step length of 0.1 gives acceptable accuracy. The second integrand tends to $-\frac{1-e^{-h}-h}{1+K}$ and $\frac{1-e^{-h}(1+h)}{1+3K}$, when k approaches zero and unity respectively. The application of the trapezium rule at some large value of k (e.g. $k = X$), is truncated (large enough to ensure that the asymptotic value is sufficiently accurate, and $X = 200$ was found to give good accuracy). The evaluation of the integral is completed by adding the contribution from the asymptotic form, which is $(1-e^{-h})/(2KX^2)$. The value of the integrand between 0 and X is evaluated numerically. Therefore

$$J_2 = \frac{2(1+3K)}{\pi} \left\{ \frac{1-e^{-h}}{1+3K} \cdot \left[\ln \left[\frac{(1+K)}{K} \right]^{1/2} - \right. \right. \\ \left. \left. \left[\frac{3}{\{(3K+4)/K\}^{1/2}} \right] \cdot \tan^{-1} \left[\frac{3K+4}{K} \right]^{1/2} \right] - \right. \\ \left. \int_0^X \frac{k - k e^{-h} - 1 + e^{-hk}}{k(k-1)(1+Kk^2 + Kk + K)} dk - \frac{1 - e^{-h}}{2KX^2} \right\}. \quad (8.27)$$

Now the principal value integral J_1 is considered. First it is separated into two parts and is written in the form

$$J_1 = \int_0^{\infty} \frac{2\sigma i K (1+3K)}{(1+Kk^2)\pi \cdot [k(1+Kk^2) - \sigma^2]} dk = \frac{2\sigma i K (1+3K)}{(1+K)\pi} \cdot \\ \left\{ \int_0^{\infty} \frac{k}{k(1+Kk^2) - \sigma^2} dk - \int_0^{\infty} \frac{1}{1+Kk^2} dk \right\} \quad (8.28)$$

Hence,

$$J_1 = \frac{2\sigma i K}{\pi} \left[\frac{1}{1+K} \log \left\{ \frac{(1+K)}{K} \right\}^{1/2} + \right. \\ \left. \left[\frac{\{(3K+2)/\{K(3K+4)\}^{1/2}}{1+K} \right] \tan^{-1} \left(\frac{3K+4}{K} \right)^{1/2} - \frac{\pi(1+3K)}{2\sqrt{K}(1+K)} \right]. \quad (8.29)$$

Therefore the surface elevation of the surface waves at a large distance from the wavemaker is evaluated, by using equation 8.20 into which the value of the parameter B , given in equation 8.22 must be substituted, using equations 8.23 and 8.24 in which the quantities J_1 and J_2 are given.

8.3 - Waves Produced By A Wavemaker In A channel

Waves on the free surface of a fluid in a gravitational field can be produced by the normal motion of a rigid plate immersed in the fluid. The displacement of the fluid by the plate leads to a deformation of the free surface, which propagates away from the plate. The wavemaker problem is that of determining the characteristics of this propagating wave train, given the motion of the wavemaker. If the wavemaker oscillates with a given amplitude and frequency, the steady state at a large distance from the plate shall consist of a plane wave with the given frequency, and the amplitude and phase of this wave are the quantities to be determined; this calculation was first performed by Havelock. If the fluid is in a channel of finite depth and the wavemaker is at one end of the channel, several different motions of the vertical boundary can be considered. For example, the whole of the plane wall can be made to oscillate rigidly, either remaining vertical or being hinged at the bottom, or only the top section of the boundary could be moved, the lower section being held at rest. The response of the fluid to motions with an arbitrary time-dependence, including the transient motion at the initiation of a harmonic oscillation, can be solved by means of a Laplace transformation. The solutions for a range of wavemaker velocities differing in their dependence on depth and time have been obtained by Faltas(1988). However, a difficulty exists in determining the transient motion after an impulsive start, because an initial singularity in the slope of the free surface at the wavemaker is predicted. This phenomenon was described in an unpublished note by Peregrine (1972), and is treated at length by Roberts (1987). He considered the transient motion for power-law motions of the wavemaker and concluded that the singularity could only be removed by starting the motion sufficiently smoothly.

The solutions so far described have ignored the presence of surface tension, which also acts to provide a restoring force on the free surface. The dispersion relation for waves controlled by the combination of gravity and surface tension is well known and suffices to determine the properties of such capillary-gravity waves in the absence of vertical boundaries. The wavemaker problem inclusive of surface tension was discussed by Rhodes-Robinson (1971) assuming that the slope of the free surface at the edge could be prescribed and varied in phase with the horizontal motion of the wavemaker. The transient waves produced by the initial motion of the wavemaker are the subject of a recent paper by Joo et al (1990). These authors concentrated on the motion induced by a plane wavemaker of the same depth as the fluid, and on an impulsive acceleration (ramp) and impulsive velocity (step). They specifically include dynamic-contact-angle effects in their analysis, but assume that the varying slope of the free surface at the contact line is a known function of the time. Most of their results, however, are for a fixed contact angle. For the ramp motion of the wavemaker they encounter no singularity in the free-surface elevation, which they determine for small values of both time and distance from the wavemaker. For the step motion they find that an initial singularity is still present, even though surface tension has been included. They conclude that the correct formulation for small time and distance requires the full non-linear free-surface conditions.

This work, in common with other attempts at describing the transient motion for capillary-gravity waves generated by a wavemaker, is unsatisfactory because it assumes that it is possible to prescribe the slope of the free-surface, where in general, there is no mechanism to control this slope. The exception is when the contact angle remains fixed, which is a dynamically possible situation, valid in the limit in which there is no dynamic variation of the contact angle, or when this variation is

so small that it can safely be neglected. Since it is known that the contact angle at a moving contact line between a fluid and a solid varies with the speed of the contact line, this variation can be prescribed and so the free surface can respond to the motion of the contact line relative to the wavemaker. A condition of this kind has been used to determine the amplitudes of capillary-gravity waves generated by the vertical motion of a plate (Hocking (1987c)) and the reflection of an incident wave by a fixed plate (Hocking (1987b)) and by a circular cylinder (Mahdmina & Hocking(1990)). It is supposed, for simplicity, that the contact angle can vary around a value of 90° , the variation being proportional to the velocity of the contact line relative to the boundary. Extreme cases of this condition include the possibility of orthogonal contact, as is present in the absence of surface tension, and of a fixed contact line with a necessarily varying contact angle.

The wavemaker problems for capillary-gravity waves that are studied here make use of this edge condition. The particular case of a plane vertical wavemaker is considered, which is impulsively brought into a harmonic oscillation of small amplitude. Two special cases are important; fluid of finite depth with the wavemaker extending from top to bottom of the fluid, and fluid of infinite depth with only the top portion of the vertical boundary of the fluid brought into motion. The amplitude of the steady-state wave train is obtained, generalizing the results of Havelock (1929). More importantly, the examination of the small-time solution shows that, when the postulated edge condition is employed, there is no singularity in the free-surface elevation or the slope at the wavemaker, even when it is started impulsively. It is not necessary to include non-linear terms in the free-surface condition to arrive at an acceptable solution.

When the depth of the fluid is small compared with

the wavelength, the shallow-water approximation can be used to simplify the analysis considerably. The waves produced by a vertical motion of the wavemaker and the reflection of an incident wave by a stationary plate, which were found previously for arbitrary depth by Hocking, can also be found for shallow water by a similar analysis, and these results are included here for completeness.

Consider an inviscid fluid in a channel of depth d' , with a wavemaker of immersed depth h' at one end of the channel. The wavemaker is assumed to oscillate with a frequency σ' and with a small amplitude ε' about its mean position. The end portion of the end of the channel below the wavemaker is fixed. The surface waves of frequency σ' in the fluid of depth d' have a wave length $2\pi/k'$, given by

$$\sigma'^2 = (gk' + \frac{\gamma}{\rho}k'^3) \tanh(k'd'), \quad (8.30)$$

where g is the gravitational acceleration and γ the surface tension. The length scale for non-dimensionalization (as discussed in chapter 2) is chosen to be $1/k'$. The horizontal x -coordinate is measured from the end of the channel and the vertical z -coordinate from the equilibrium free surface. The equations for small-amplitude waves with no variation across the width of the channel are satisfied by a potential ϕ that satisfies Laplace's equation, with the horizontal and vertical velocity components and the pressure, p , being given by

$$u = \frac{\partial \phi}{\partial x}, \quad w = \frac{\partial \phi}{\partial z}, \quad p = -\frac{\partial \phi}{\partial t}. \quad (8.31)$$

The bottom condition on ϕ is

$$\begin{aligned} \frac{\partial \phi}{\partial z} &= 0 \quad \text{on} \quad z = -d \quad (d \text{ finite}), \\ \frac{\partial \phi}{\partial z} &\rightarrow 0 \quad \text{as} \quad z \rightarrow -\infty \quad (d \text{ infinite}), \end{aligned} \quad (8.32)$$

where $d = k'd'$. The motion is forced by the wavemaker, and the condition on p at the end of the channel for $t > 0$, is

$$\begin{aligned}\frac{\partial \phi}{\partial x} &= \sigma \exp(-i\sigma t) & \text{for } 0 > z > -h, \\ \frac{\partial \phi}{\partial x} &= 0 & \text{for } -h > z > -d,\end{aligned}\quad (8.33)$$

with $h = k'h'$ and

$$\sigma^2 = (1 + K) \tanh(d). \quad (8.34)$$

Because the amplitude of the lateral displacement of the wavemaker is small, this condition can be applied at the mean position $x = 0$.

The elevation of the free surface is equal to $\varepsilon'\eta(x,t)$ and the conditions at the free surface are

$$\frac{\partial \eta}{\partial t} = w, \quad \eta - K \frac{\partial^2 \eta}{\partial x^2} = + p; \quad (8.35)$$

since waves are assumed to be of small amplitude, these conditions can be applied at $z = 0$. The parameter K measures the relative importance of capillarity and gravity and (as explained in chapter 2) is defined by

$$K = \frac{\gamma k'^2}{\rho g}. \quad (8.36)$$

The edge condition (as discussed in chapter 1) to be applied is

$$\frac{\partial \eta}{\partial t} = \lambda \frac{\partial \eta}{\partial x} \quad \text{at } x = 0. \quad (8.37)$$

The final requirement is that there should be no waves travelling towards the wavemaker from infinity, that is a radiation condition should be applied. For waves of the same frequency as that of the wavemaker this condition can be expressed in the form

$$\frac{\partial \eta}{\partial t} + \sigma \frac{\partial \eta}{\partial x} \rightarrow 0 \quad \text{as } x \rightarrow \infty, \quad (8.38)$$

which completes the formulation of the problem.

The chosen form for the wavemaker velocity can be replaced by more general functions of time; it could also be allowed to vary with the depth below the free surface. A similar analysis to that presented here can be performed to deal with these variations. The oscillation of the wavemaker begins at $t = 0$ and the complex form of its velocity allows for both an initial impulsive velocity and an impulsive acceleration by taking the real or imaginary part of the solution, respectively. Because the analysis takes different forms for finite and infinite fluid depth, the two cases are treated separately.

8.4 - Finite Depth

For fluid of depth $d = h$, the whole end of the channel at $x = 0$ is made to move. A Laplace transform in t is taken, with parameter s , and indicate the transform of ϕ by $\hat{\phi}$, for example. Then $\hat{\phi} = \phi_1 + \phi_2$, where ϕ_1 satisfies the inhomogeneous condition 8.33 and the bottom condition is the equation 8.32. The value of ϕ_1 is given by

$$\phi_1 = \frac{-\sigma}{s + i\sigma} \sum_{n=0}^{\infty} \frac{2(-1)^n}{h k_n^2} \cos\{k_n(z + h)\} \exp(-k_n x), \quad (8.39)$$

where

$$k_n = (n + \frac{1}{2}) \frac{\pi}{h}. \quad (8.40)$$

The value of ϕ_2 that satisfies equation 8.32 and the null conditions on $x = 0$ has the form

$$\phi_2 = \int_0^{\infty} \hat{A}(s, k) \frac{\cosh\{k(z + h)\}}{\cosh(kh)} \cos(kx) dk. \quad (8.41)$$

The pressure associated with ϕ_1 is zero on the surface, and η can be found from the second part of equation 8.35

as

$$\hat{\eta} = -s \int_0^{\infty} \frac{\hat{A}}{1 + Kk^2} \cos(kx) dk - K^{1/2} \hat{B}(s) \exp(-x / K^{1/2}), \quad (8.42)$$

where the condition that $\hat{\eta}$ being bounded at infinity, has been used. The slope of the free surface at the contact line is equal to $B(t)$. The second term can be written as a Fourier integral, so that

$$\hat{\eta} = - \int_0^{\infty} \frac{s\hat{A} + 2BK/\pi}{1 + Kk^2} \cos(kx) dk. \quad (8.43)$$

From the first condition of equation 8.35

$$s\hat{\eta} = \frac{\mathcal{G}}{s + i\sigma} \sum_{n=0}^{\infty} \frac{2}{hk_n} \exp(-k_n x) + \int_0^{\infty} k\hat{A} \tanh(kh) \cos(kx) dk, \quad (8.44)$$

where it can be written as a single Fourier integral as

$$s\hat{\eta} = \int_0^{\infty} \left[k\hat{A} + \frac{\sigma}{s + i\sigma} \frac{2}{\pi k} \right] \tanh(kh) \cos(kx) dk. \quad (8.45)$$

By equating the expressions of equations 8.43 and 8.45 for $\hat{\eta}$, $\hat{A}(s, k)$ can be written in terms of $\hat{B}(s)$ in the form

$$(s^2 + \sigma_k^2) \hat{A} = - \frac{2Ks}{\pi} \hat{B} - \frac{2\sigma}{\pi(s + i\sigma)} \frac{(1 + Kk^2) \tanh(kh)}{k}, \quad (8.46)$$

where

$$\sigma_k^2 = k(1 + Kk^2) \tanh(kh), \quad \sigma_1 = \sigma. \quad (8.47)$$

The edge condition 8.37 provides another equation linking \hat{A} and \hat{B} in the form

$$\int_0^{\infty} \left[k\hat{A} + \frac{\sigma}{s + i\sigma} \frac{2}{\pi k} \right] \tanh(kh) dk = \lambda \hat{B}. \quad (8.48)$$

Hence \hat{B} can be determined from the equation

$$\left[\lambda + \frac{2Ks}{\pi} \int_0^{\infty} \frac{k \tanh(kh)}{s^2 + \sigma_k^2} dk \right] \hat{B} = \frac{2\sigma s^2}{\pi(s + i\sigma)} \int_0^{\infty} \frac{\tanh(kh)}{k(s^2 + \sigma_k^2)} dk. \quad (8.49)$$

Inverting both sides of the equation, $B(t)$ satisfies the following integral equation

$$\lambda B(t) + \frac{2K}{\pi} \int_0^{\infty} k \tanh(kh) \int_0^t \cos(\sigma_k \tau) B(t-\tau) d\tau dk =$$

$$\int_0^{\infty} \frac{2\sigma \tanh kh}{\pi k} \left[\frac{\sigma_k^2 \cos \sigma_k t - \sigma^2 \cos \sigma t - i\sigma(\sigma_k \sin \sigma_k t - \sigma \sin \sigma t)}{\sigma_k^2 - \sigma^2} \right] dk \quad (8.50)$$

The slope of the free surface at the contact line is equal to $B(t)$ and the elevation of the free surface there can be found by inverting $\lambda \hat{B}/s$, so that

$$\eta(0, t) = \lambda \int_0^t B(\tau) d\tau. \quad (8.51)$$

The transient motion introduced by the initial motion of the wavemaker is found by considering equation 8.49 for large values of s , where for finite λ , $\hat{B} = O(s^{-4/3} \ln s)$, so that $B(t) = O(t^{1/3} \ln t)$ as $t \rightarrow 0$. The fixed-contact-angle case is given formally by $\lambda = \infty$ and then $B(t) = 0$. The initial free-surface elevation can be found from equation 8.51 when λ is finite, and $\eta(0, t) = O(\lambda t^{4/3} \ln t)$. For $\lambda = \infty$, $\lambda \hat{B}$ can be found from equation 8.49 and then 8.51 shows that, in this case, $\eta(0, t) = O(t \ln t)$. It follows that, the edge condition used here does not introduce any initial singularity in either the free-surface elevation or slope at the contact line.

The solution for large t is dominated by the

contribution from the pole at $s = -i\sigma$. At this value of s the denominators of the two integrals in equation 8.49 become zero at $k = 1$, and the contour for both integrals with respect to k must be indented to lie below this singularity, since the contour in the s -plane must lie to the right of $-i\sigma$. The value of η for large t and large x can be found from equation 8.42 and the dominant contribution comes from the pole at $k = 1$ in the value of \hat{A} given by equation 8.46. In this way, after the transients have disappeared, the wavemaker produces a wave whose elevation at large distance from the wavemaker has the form $R \exp\{i(x - \sigma t)\}$, where

$$R = \frac{2\sigma^2}{q} \left[\frac{J_2 + \frac{i\lambda\pi}{2\sigma K}}{J_1 + \frac{i\lambda\pi}{2\sigma K} + \frac{i\pi}{q}} \right]. \quad (8.52)$$

The quantity q introduced in this expression is defined as

$$q = 1 + 3K + \frac{2h(1 + K)}{\sinh(2h)}, \quad (8.53)$$

which is proportional to the group velocity of surface waves of frequency σ , and

$$J_1 = \int_0^{\infty} \frac{k \tanh(kh)}{\sigma_k^2 - \sigma^2} dk, \quad (8.54)$$

$$J_2 = \int_0^{\infty} \frac{(k^2 - 1)\tanh(kh)}{k(\sigma_k^2 - \sigma^2)} dk. \quad (8.55)$$

Note that the integral J_1 is a principal integral, but the integrand in J_2 is not singular. The free-surface elevation at the wavemaker in the steady state can be found from equation 8.49 and 8.51 and has the form

$$\eta(0, t) = e^{-i\sigma t} \frac{\lambda\sigma}{K} \left[\frac{J_1 - J_2 + \frac{i\pi}{q}}{J_1 + \frac{i\lambda\pi}{2\sigma K} + \frac{i\pi}{q}} \right]. \quad (8.56)$$

The elevation of $|R|$, the amplitude of the wave generated by the wavemaker, and of $\eta(0,t)$ are straightforward numerical tasks. Some numerical values of these two quantities as functions of λ for $h = 1$ and for three values of K are displayed in Figures 8.11 and 8.12. The wave amplitude decreases monotonically as K increases. Each curve has a shallow minimum as a function of λ and approaches its limiting value as $\lambda \rightarrow \infty$ from below. It should be remembered that, when λ is finite and non-zero, there is some energy dissipation at the wavemaker which may account for the dip in the amplitude of the generated wave. The surface elevation at the wavemaker (Figure 8.12) is a monotonic increasing function of λ and also decreases as K increases.

8.5 - Infinite Depth

When the fluid is of infinite depth, with a boundary at $x = 0$ of which the top portion, of depth h , is the wavemaker, the analysis can proceed similar to that of a finite depth fluid. A suitable form for ϕ_1 that satisfies the forcing condition 8.33 is given by

$$\phi_1 = \frac{2\sigma}{\pi(s + i\sigma)} \int_0^{\infty} \frac{1 - \cos(\kappa h)}{\kappa^2} \sin(\kappa z) \exp(-\kappa x) d\kappa. \quad (8.57)$$

The pressure on the free surface from this part of the solution vanishes, and the vertical velocity \hat{w}_1 is given by $(\sigma \eta \text{ at } z=0)$,

$$\hat{w}_1 = \frac{2\sigma}{\pi(s + i\sigma)} \int_0^{\infty} \frac{1 - \cos(\kappa h)}{\kappa} \exp(-\kappa x) d\kappa, \quad (8.58)$$

which can also be written as a Fourier integral in the form

$$\hat{w}_1 = \frac{2\sigma}{\pi(s + i\sigma)} \int_0^{\infty} \frac{1 - e^{-kh}}{k} \cos(kx) dk. \quad (8.59)$$

The appropriate form for ϕ_2 is

$$\phi_2 = \int_0^{\infty} \hat{A}(s, k) \cos(kx) e^{kz} dk. \quad (8.60)$$

Following the same steps as in the finite-depth case, an equation for \hat{B} can be found which corresponds to equation 8.49, namely

$$\left[\lambda + \frac{2Ks}{\pi} \int_0^{\infty} \frac{k}{s^2 + \sigma_k^2} dk \right] \hat{B} = \frac{2\sigma s^2}{\pi(s + i\sigma)} \int_0^{\infty} \frac{1 - e^{-kh}}{k(s^2 + \sigma_k^2)} dk, \quad (8.61)$$

where

$$\sigma_k^2 = k(1 + Kk^2), \quad \sigma^2 = 1 + K. \quad (8.62)$$

The transient motion near the contact line has the same form as in the case of finite-depth, since the integrals in equation 8.61 for large s are similar to those in 8.49. For large t , the wave generated by the wavemaker in the same way as before can be determined and the complex amplitude of the wave, denoted by R , is now given by

$$R = \frac{2\sigma^2(1 - e^{-h})}{q'} \left[\frac{J_2' + \frac{i\lambda\pi}{2\sigma K}}{J_1' + \frac{i\lambda\pi}{2\sigma K} + \frac{i\pi}{q'}} \right]. \quad (8.63)$$

where $q' = 1 + 3K$. This expression for R is very similar to that in the finite-depth case given by equation 8.52, but the integrals are defined by

$$J_1' = \int_0^{\infty} \frac{k}{\sigma_k^2 - \sigma^2} dk, \quad (8.64)$$

which is a principal-value integral, and by

$$J_2' = \int_0^{\infty} \frac{k^2 - k'^2}{k(\sigma_k^2 - \sigma^2)} dk, \quad (8.65)$$

where

$$k'^2 = \frac{1 - e^{-kh}}{1 - e^{-h}}. \quad (8.66)$$

The free surface elevation at the wavemaker is

$$\eta(0,t) = e^{-i\sigma t} \frac{\lambda\sigma}{K} (1 - e^{-h}) \left[\frac{J_1' - J_2' + \frac{i\pi}{q'}}{J_1' + \frac{i\lambda\pi}{2\sigma K} + \frac{i\pi}{q'}} \right]. \quad (8.67)$$

Numerical values of $|R|$ and of $\eta(0,t)$ as functions of λ for $h = 1$ and for various values of K are displayed in Figures 8.13 and 8.14. The main features are similar to those of the corresponding results for the finite-depth case shown in Figures 8.11 and 8.12. The minima of the wave amplitudes are somewhat more pronounced.

8.6 - Small Depth

If the depth of the channel is small compared with the wavelength, the simplifications of shallow-water theory can be applied and the results arrived at more readily than by the methods used for arbitrary depths. The wavemaker problem of section 8.4 with h small is considered here. The variables are expanded in powers of h , noting that $\sigma^2 = h(1 + K)$ to the leading order. If $z = h\zeta$, the Laplace's equation for ϕ becomes, $\partial^2\phi / \partial\zeta^2 = 0$ to the leading order, so that $\phi = \phi(x,t)$. Then

$$u = \frac{\partial\phi}{\partial x}, \quad w = -h(\zeta + 1) \frac{\partial^2\phi}{\partial x^2}, \quad (8.68)$$

where w has been determined from the equation of continuity and the bottom boundary condition. If all the

dependent variables are assumed to have a factor of $\exp(-i\sigma t)$ due to the time-dependence of the forcing motion of the wavemaker, the pressure and surface elevation are given as (using equations 8.31 and 8.35)

$$p = i\sigma\phi, \quad \eta = -\frac{ih}{\sigma} \frac{\partial^2 \phi}{\partial x^2}, \quad \eta - K \frac{\partial^2 \eta}{\partial x^2} = +i\sigma\phi. \quad (8.69)$$

The boundary conditions at $x = 0$ are;

$$\frac{\partial \phi}{\partial x} = \sigma \exp(-i\sigma t), \quad i\sigma\eta = \lambda \frac{\partial \eta}{\partial x}, \quad (8.70)$$

and it is also required that

$$\eta \approx R \exp\{i(x-\sigma t)\} \quad \text{as } x \rightarrow \infty. \quad (8.71)$$

Eliminating ϕ , the equation for η can be written in the form

$$\left[\frac{\partial^2}{\partial x^2} + 1 \right] \left[K \frac{\partial^2 \eta}{\partial x^2} - (1 + K)\eta \right] = 0, \quad (8.72)$$

and the solution that satisfies the condition at infinity is

$$\eta = R \exp\{i(x-\sigma t)\} + C \exp\left\{-\left[\frac{1+K}{K}\right]^{1/2} x - i\sigma t\right\}. \quad (8.73)$$

The values of R and C are determined by the boundary conditions 8.70 and therefore

$$R = h \frac{1 + \frac{i\lambda}{h^{1/2} K^{1/2}}}{1 + i \left[\frac{K}{1+K} \right]^{1/2} + \frac{i\lambda}{h^{1/2} K^{1/2}} \frac{1+2K}{1+K}}, \quad (8.74)$$

so that R/h depends on the parameters $\lambda / h^{1/2}$ and K . The surface elevation at the wavemaker depends on the value of $R + C$ and is given by

$$\eta(0,t) = e^{-i\sigma t} \frac{i\lambda h^{1/2}}{K^{1/2}}.$$

$$\frac{1 + \frac{i\lambda}{h^{1/2} K^{1/2}}}{1 + i \left[\frac{K}{1+K} \right]^{1/2} + \frac{i\lambda}{h^{1/2} K^{1/2}} \frac{1+2K}{1+K}}. \quad (8.75)$$

The value of \mathcal{R} given by equation 8.74 can also be found by considering the limiting behaviour of the result for general depth from equation 8.52 as h tends to zero. In this limit the integrals J_1 and J_2 can be evaluated analytically. The values of $|\mathcal{R}|$ calculated from equation 8.74 are shown in Figure 8.15 for $h = 0.1$. The values calculated from equation 8.52 are indistinguishable on the resolution of the diagram. The surface elevation calculated from equations 8.56 and 8.75 for $h = 0.1$ are also in close agreement, although there is some discrepancy when $K = 0.1$ and λ is small. This is not unexpected, since the shallow-water limit requires $h \ll K^{1/2}$ which is hardly satisfied when $h = K = 0.1$.

It is possible to find the transient solution of the shallow-water equations by taking a Laplace transform as in section 8.4. However, this does not give the correct result for the short-time behaviour because the limits $h \rightarrow 0$ and $t \rightarrow 0$ do not commute. The impulsive initial motion of the wavemaker creates waves of all wavelengths, including those that are short compared with the fluid depth. But the shallow-water approximation assumes that all variations in the x -direction are small compared with those in the z -direction and this assumption is not valid for t small.

The shallow-water approach can also be used for other types of wave motion. For example, if the wavemaker is given a vertical velocity instead of a horizontal one, the boundary conditions 8.70 must be replaced by

$$\frac{\partial \phi}{\partial x} = 0, \quad -i\sigma\eta - \sigma = \lambda \frac{\partial \eta}{\partial x}, \quad \text{at } x = 0, \quad (8.76)$$

when the wavemaker has a vertical velocity equal to $\sigma \exp(-i\sigma t)$. With η of the same form as in the equation 8.73, these conditions determine R and C, and hence

$$|R|^2 = \frac{\frac{K}{1 + 2K}}{1 + \frac{2\lambda}{h^{1/2} (1 + K)^{1/2}} + \frac{\lambda^2}{hK} \cdot \frac{1 + 2K}{1 + K}}. \quad (8.77)$$

When $\lambda = \infty$ there is no generated wave because then the free surface can slip freely along the wavemaker. When the edge is forced to move with the wavemaker, that is, when $\lambda = 0$, the amplitude of the generated wave is independent of the depth of the fluid and has its maximum value as a function of λ . This maximum value, as a function of K, is always less than $1/\sqrt{2}$ and approaches that value as $K \rightarrow \infty$. The amplitude of the wave produced by a vertically oscillating plate for arbitrary depths was obtained by Hocking, and the result for shallow water can be deduced by taking a suitable limit, but the direct derivation for shallow water by the method used here is much simpler.

Another problem that can be solved in the shallow-water case is the reflection of an incident wave by a rigid plane. If it is supposed that the incident wave has unit amplitude, the appropriate form for η is

$$\begin{aligned} \eta = & \exp[-i(x + \sigma t)] + R \exp\{i(x - \sigma t)\} \\ & + C \exp\left\{-\left[\frac{1 + K}{K}\right]^{1/2} x - i\sigma t\right\}, \end{aligned} \quad (8.78)$$

and the boundary conditions are

$$\frac{\partial \phi}{\partial x} = 0, \quad -i\sigma\eta = \lambda \frac{\partial \eta}{\partial x}, \quad \text{at } x = 0. \quad (8.79)$$

These conditions lead to an expression for R which gives

$$|R| = \frac{1 - \frac{2\lambda}{h^{1/2} (1+K)^{1/2}} + \frac{\lambda^2}{hK} \frac{1+2K}{1+K}}{1 + \frac{2\lambda}{h^{1/2} (1+K)^{1/2}} + \frac{\lambda^2}{hK} \frac{1+2K}{1+K}}. \quad (8.80)$$

For both $\lambda = 0$ and $\lambda = \infty$ the reflected wave has unit amplitude, since in these cases there is no energy loss at the contact line. For other values of λ the amplitude of the reflected wave is reduced. As a function of λ , $|R|$ has a minimum value $|R|_{\min}$ when $\lambda = \lambda_{\min}$, where

$$\lambda_{\min}^2 = \frac{hK(1+K)}{1+2K}, \quad |R|_{\min} = \frac{(1+2K)^{1/2} - K^{1/2}}{(1+K)^{1/2}}. \quad (8.81)$$

The smallest value of $|R|_{\min}$ as a function of K is $\sqrt{2} - 1$ as $K \rightarrow \infty$. The reflection of an incident wave in water of arbitrary depth was obtained by Hocking (1987b).

Two main results have been established in this section (section 8.3). It has been shown that capillary-gravity waves generated by a wavemaker can be predicted from the known motion of the wavemaker, provided an appropriate edge condition is applied, and without assuming a prescribed slope of the free surface at the contact line. The special cases of a fixed contact angle and a contact line fixed on the wavemaker have been included. The solutions have been given for a particular motion of the wavemaker, namely an impulsively started harmonic oscillation, and the velocity of the wavemaker has been uniform over the immersed part of the wavemaker. Extensions to other time variations and to depth-dependent velocities can easily be made.

The second result has been to show that, with capillarity and an appropriate edge condition, the transient motion after an impulsive start does not introduce a singularity in either the position or the

slope of the free surface. It is not necessary to ensure that the initial motion of the wavemaker is sufficiently smooth, nor does one need to include non-linear effects to remove the singularity that occurs when the surface tension is neglected.

The problem in section 8.5 for large t is the same as the problem solved in section 8.1. The quantities $|\eta_\infty|$ and $|R|$ (obtained from equations 8.20 and 8.63 respectively) which both correspond to the amplitude of the waves at large distances away from the wavemaker, can be shown, are identical. They are obtained by two different methods and can be compared in Figures 8.2 and 8.13, in particular for $K = 1$ which shows that they are identical.

Figures 8.11 and 8.12 show the change of amplitude and surface elevation with λ , for different values of the capillarity coefficient, when the depth of the fluid (and length of the plate) is finite. The curves corresponding to the amplitude have minima which is due to loss of energy, whereas at $\lambda = 0$ and as $\lambda \rightarrow \infty$ (the two extreme cases of pinned-end and free-end) the amplitude has larger value. Surface elevation, however, is a monotonic increasing function of λ and monotonic decreasing function of the capillarity coefficient, K .

Figure 8.15 corresponds to the amplitude of the waves when the depth of the fluid is small (shallow water).

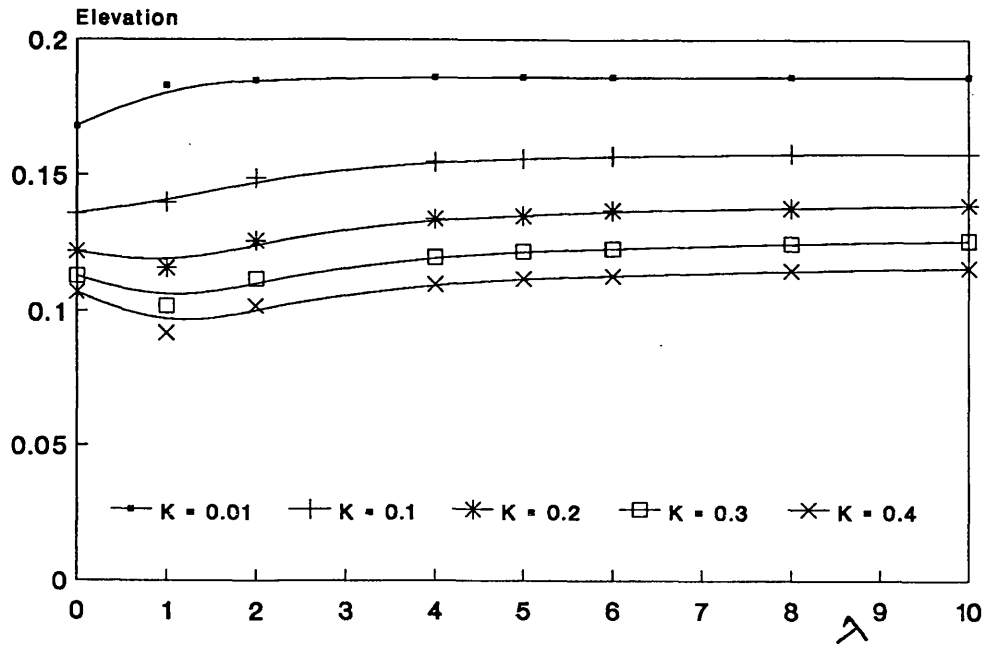


Figure 8.1. Elevation at large distance as a function of λ ; $h = 0.1$.

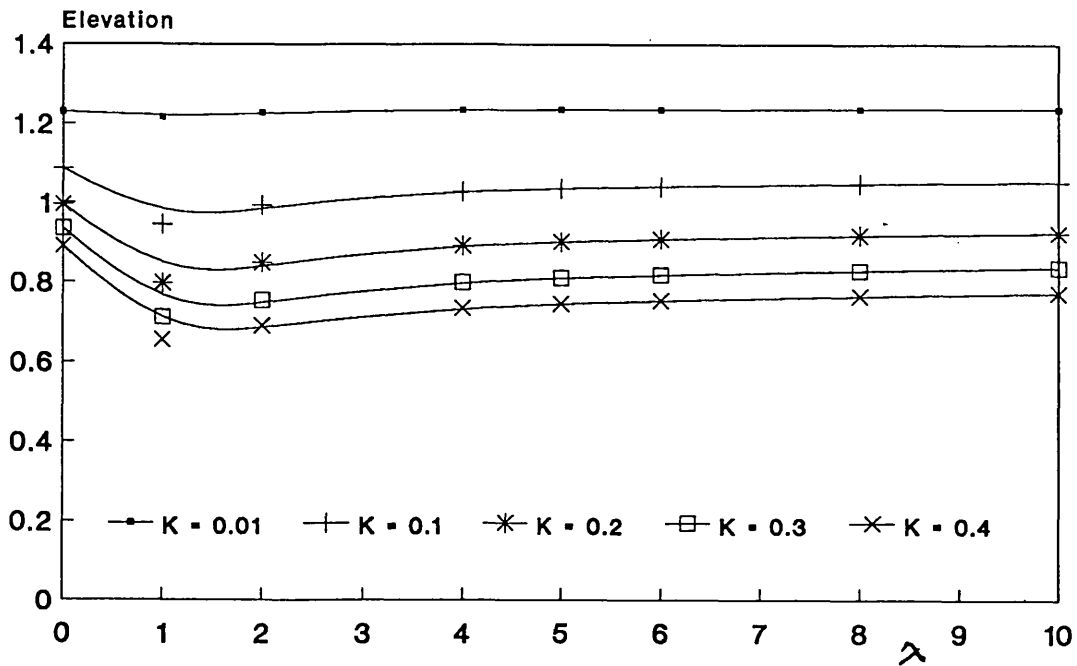


Figure 8.2. Elevation at large distance as a function of λ ; $h = 1$.

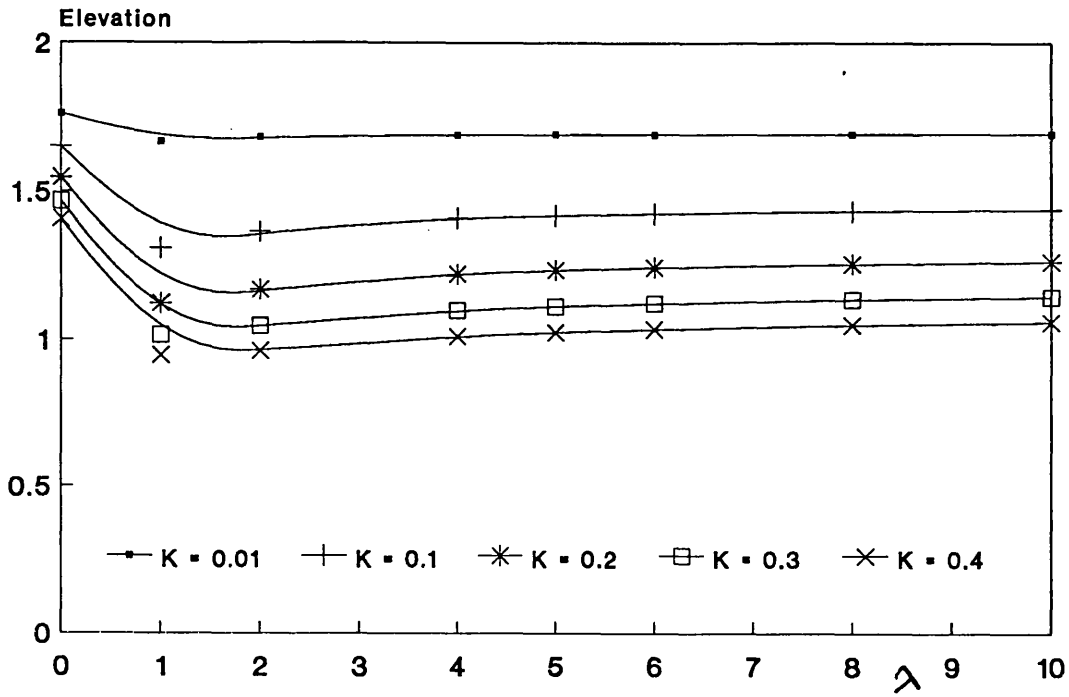


Figure 8.3. Elevation at large distance as a function of λ ; $h = 2$.

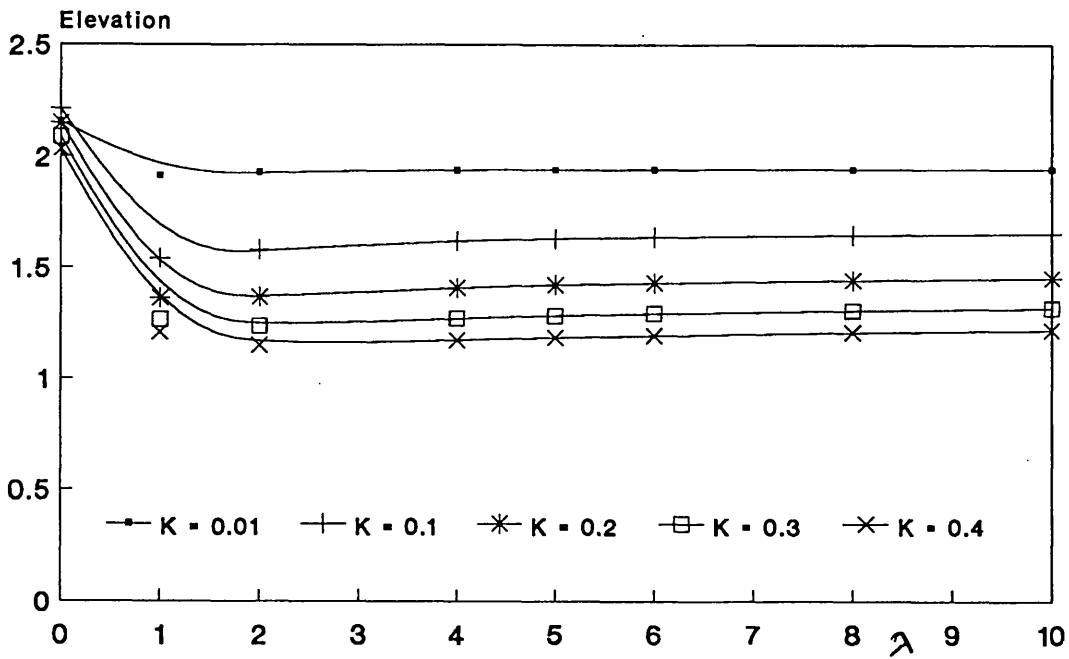


Figure 8.4. Elevation at large distance as a function of λ ; $h = 5$.

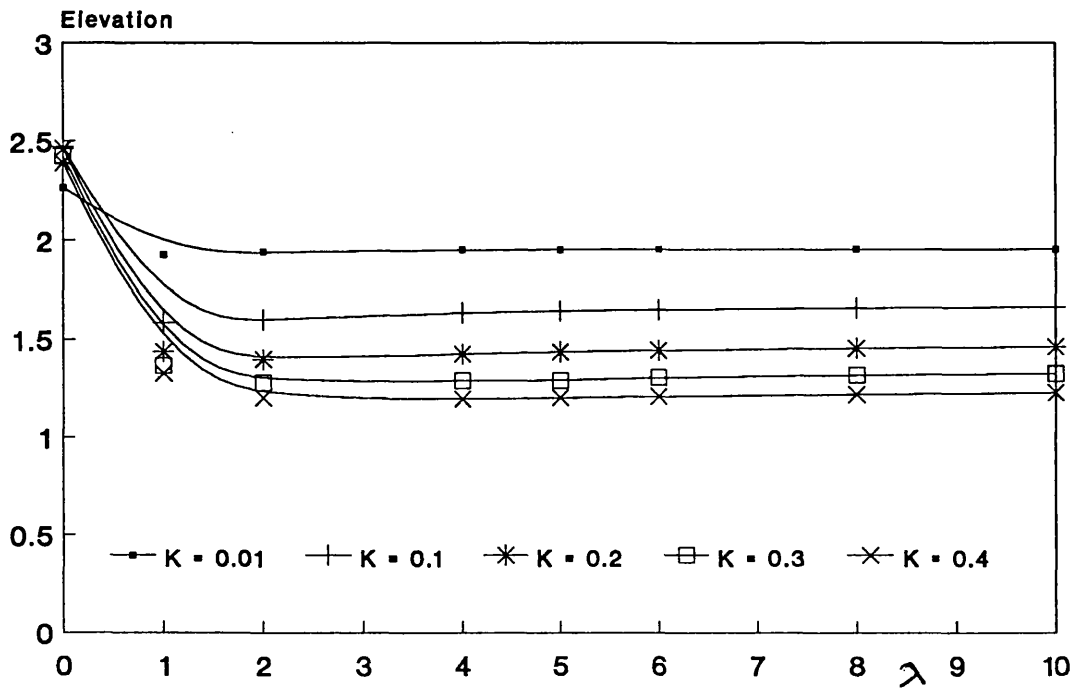


Figure 8.5. Elevation at large distance as a function of λ ; $h = 10$.

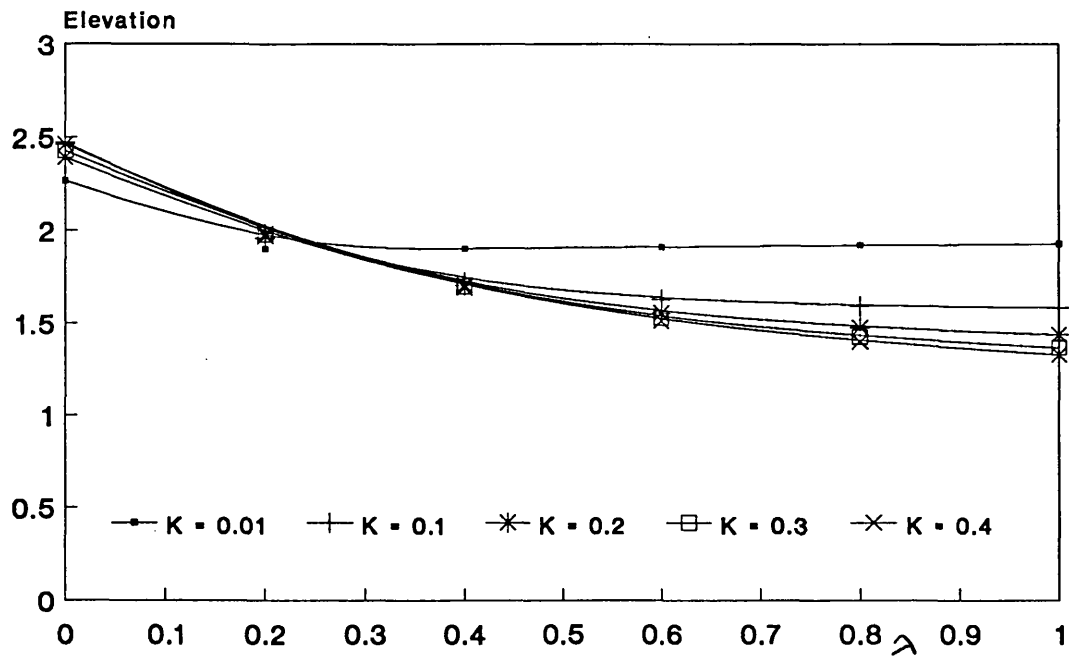


Figure 8.6. Elevation at large distance as a function of λ ; $h = 10$.

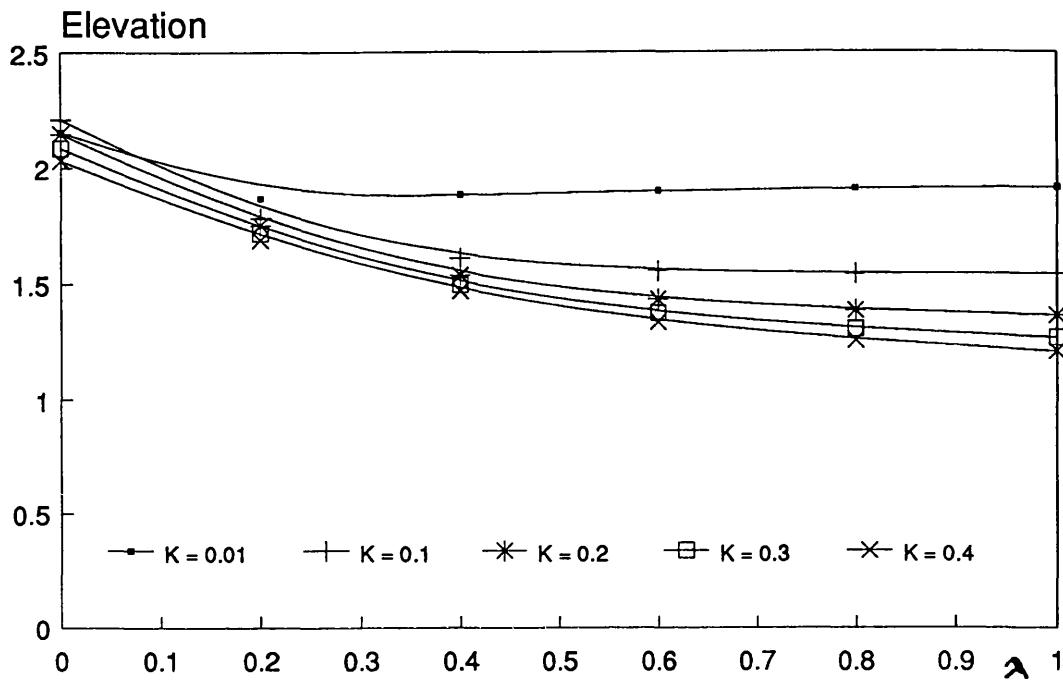


Figure 8.7. Elevation at large distance as a function of λ ; $h = 5$.

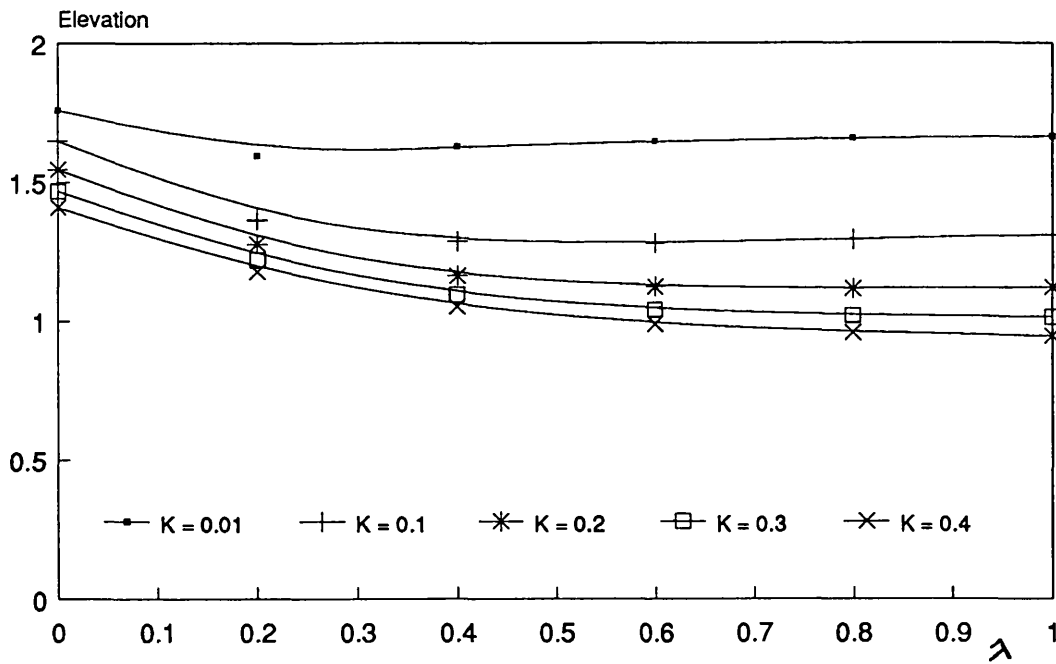


Figure 8.8. Elevation at large distance as a function of λ ; $h = 2$.

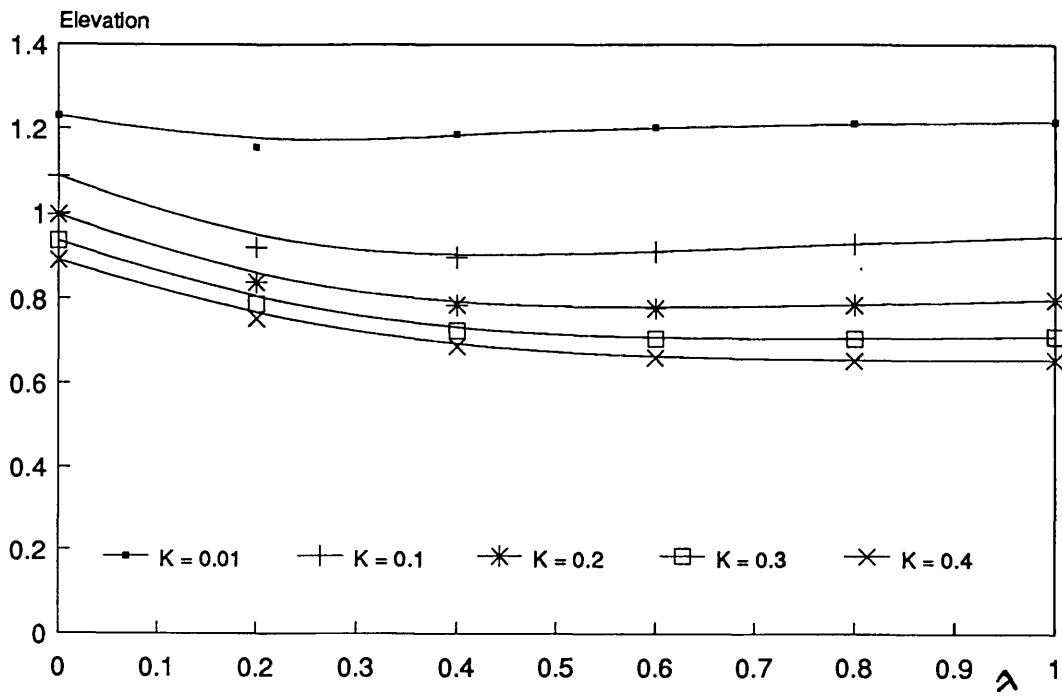


Figure 8.9. Elevation at large distance as a function of λ ; $h = 1$.

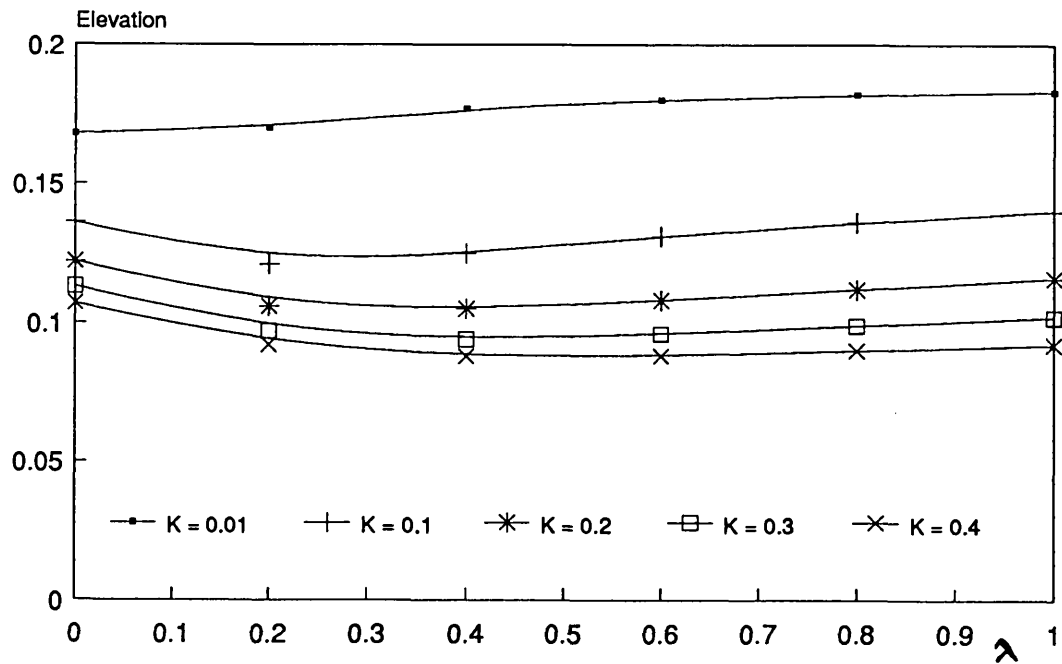


Figure 8.10. Elevation at large distance as a function of λ ; $h = 0.1$.

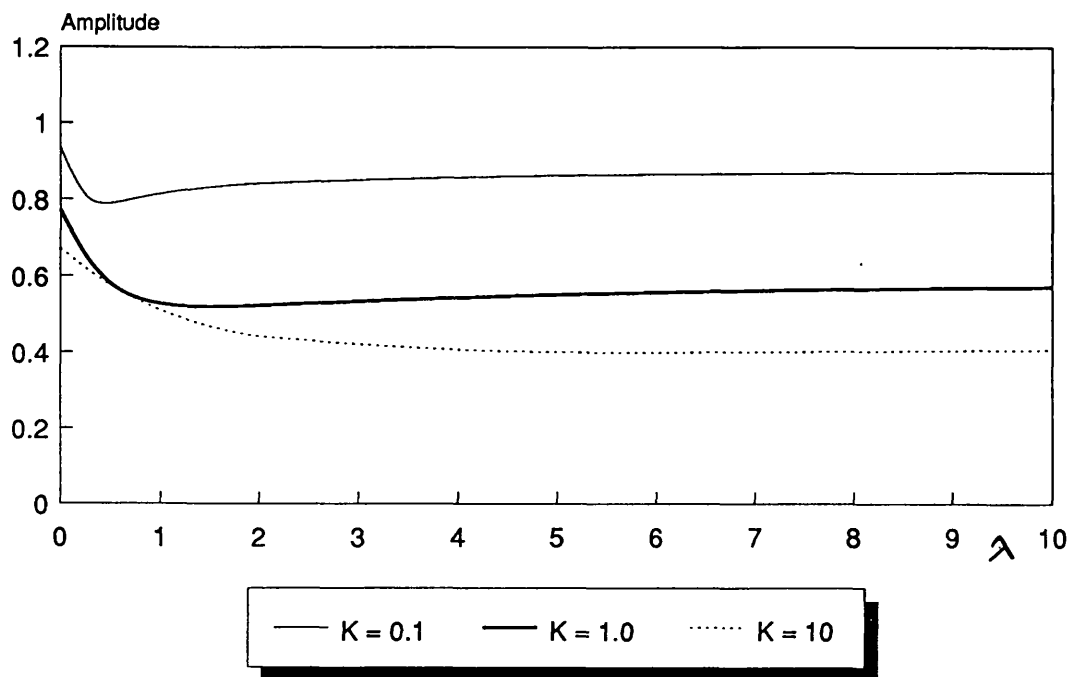


Figure 8.11. Elevation at large distance with $h = 1$ (finite depth).

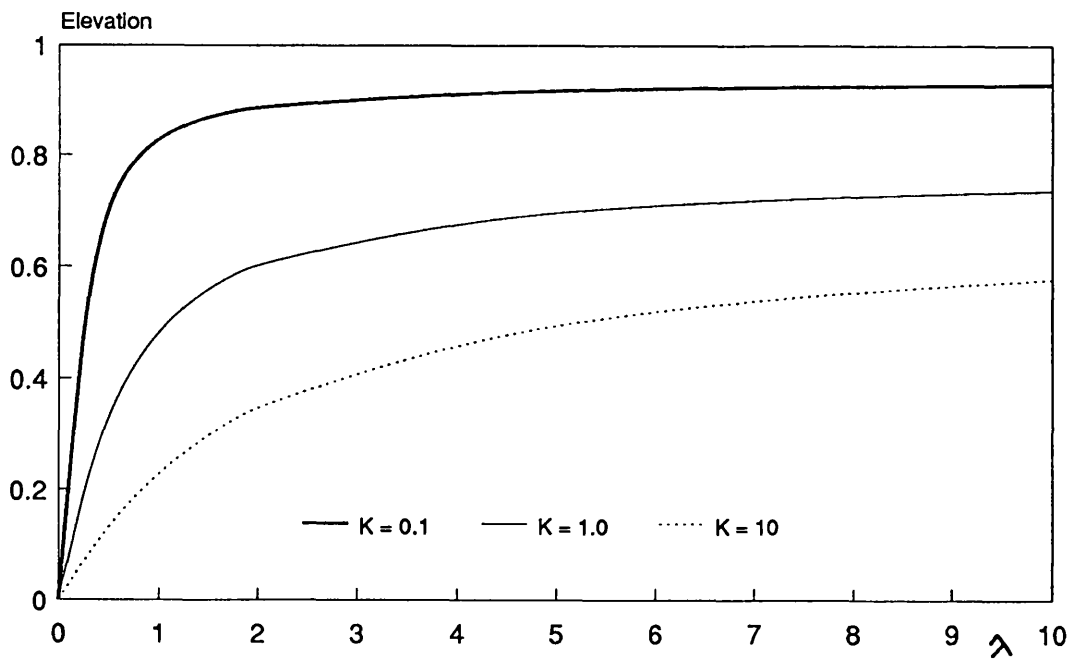


Figure 8.12. Elevation on the wavemaker with $h = 1$ (finite depth).

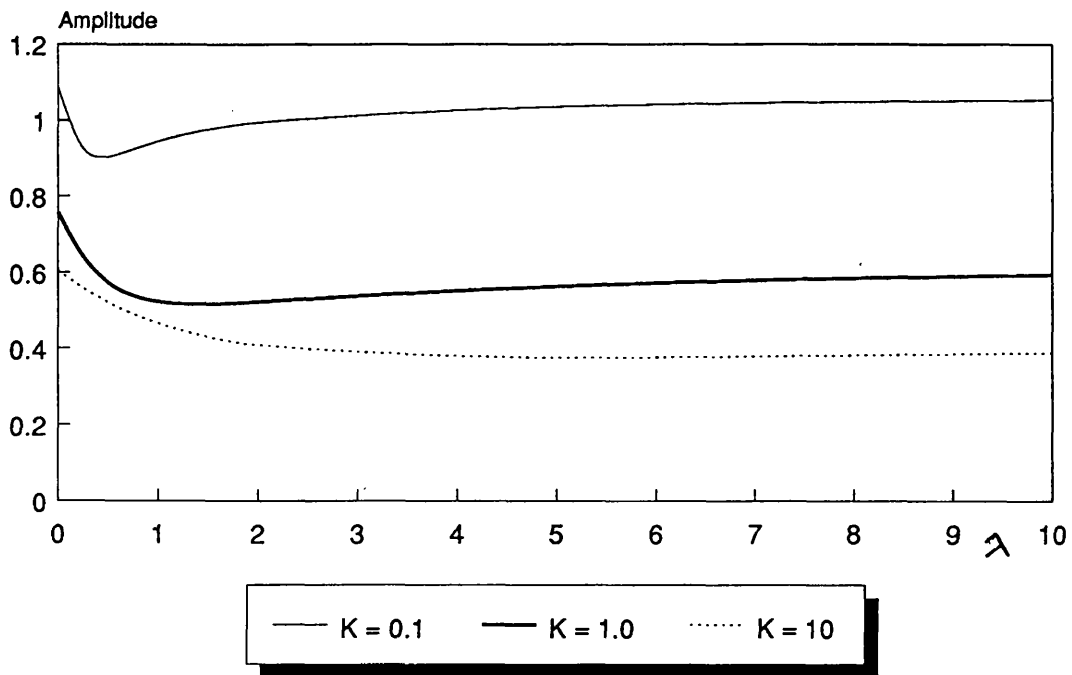


Figure 8.13. Elevation at large distance with $h = 1$ (infinite depth).

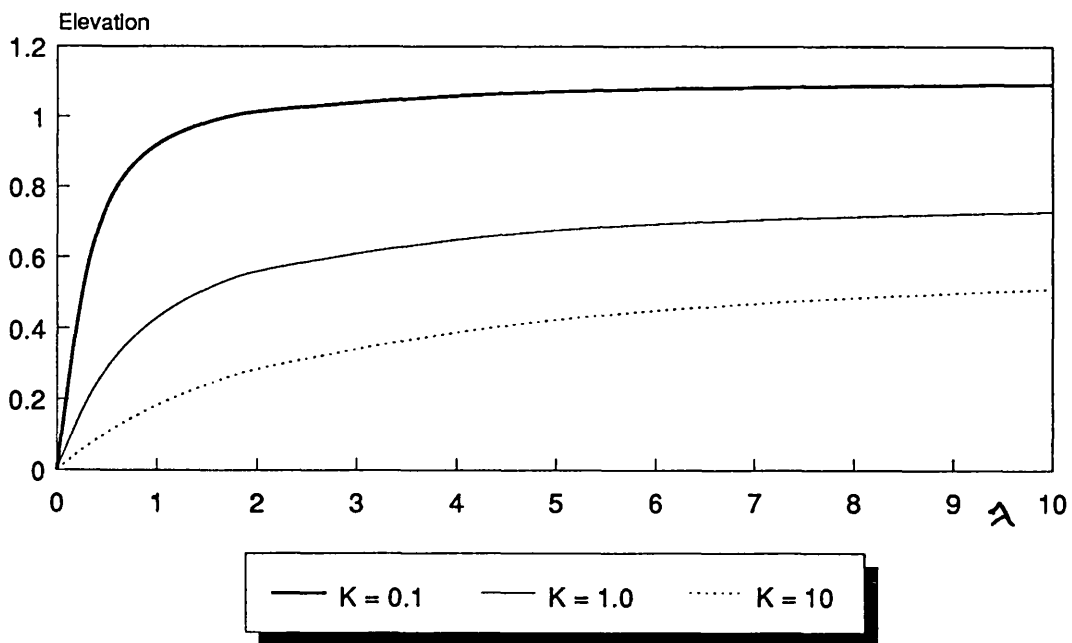


Figure 8.14. Elevation on the wavemaker with $h = 1$ (infinite depth).

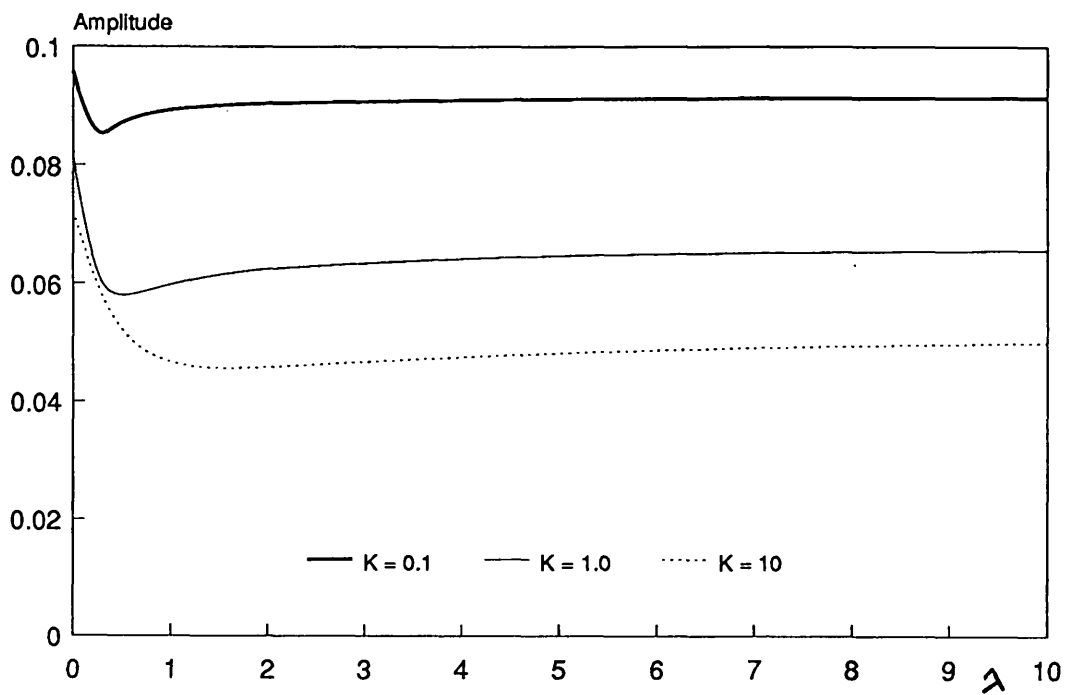


Figure 8.15. Elevation at large distance with $h = 0.1$ (shallow water).

CHAPTER IX

CONCLUSION

In this thesis, the radiation and reflection of capillary-gravity waves and their properties was studied. Some of the previous work on the generation of capillary-gravity waves are based on the unjustified assumption that the slope of the free surface at the contact line can be prescribed. A more acceptable condition is one that relates the slope to the motion of the contact line relative to the wavemaker; in this way the dynamic properties of the contact angle can be incorporated. This edge condition, which was used throughout this thesis, includes both the extreme cases of pinned- and free-end conditions.

The problems which are studied here are, determining the frequency of a contained fluid, radiation of waves from a vertically or horizontally oscillating cylinder and scattering of a plane wave with a fixed cylinder. In each case both the radiated waves elevation at a large distance away from the cylinder and the surface elevation on the cylinder were obtained. All these problems are studied for steady state. The waves generated by a plane wavemaker are also determined in the fluid of infinite depth and in fluid of a depth equal to that of the wavemaker. An important reason for including surface tension is that in its absence the transient motion initiated by an impulsive start is singular; when surface tension is included this singularity is removed. Shallow water theory was also used for small depth fluid to obtain the elevation at a large distance away from the cylinder or the plate which simplifies the analysis considerably.

In chapter 3, a theoretical determination of the damping of surface waves by capillary action was

presented. A free-oscillation problem is studied (in this chapter) and hence the real and the imaginary parts of the frequency σ are determined. The imaginary parts give the damping rate associated with capillarity and the edge condition. As predicted this is zero for the free- and pinned-end cases, but intermediate values of λ give significant damping rates. During the computation, for each mode, λ is chosen to be infinity initially, which corresponds to the free-end case and as λ decreases, the graph goes to its maximum which corresponds to a loss of energy, and then decreases towards the pinned-end case with $\lambda = 0$. The case of $m = 0$ corresponds to the axisymmetric case with the lowest loss of energy. In all three cases, the largest frequency corresponds to the larger mode. For K and m equal to unity (corresponding to the splashing mode), the real and the imaginary parts are of the same order, suggesting a big loss of energy.

In chapter 4, the vertical oscillation of a vertical cylinder in the fluid was studied. For a given capillarity coefficient K , the surface elevation decreases monotonically as λ increases for $k' < 1$. For a given capillarity coefficient K ($= 100, 1$ or 0.1), the value of the surface elevation at large distances away from the cylinder, decreases monotonically as λ increases for k' less than unity, and its variation (i.e. the variation of the surface elevation) tends to be negligible when k' is large (such as 8,4,2,1). The surface elevation (at a large distance away from the cylinder) for small values of k' , behaves as $K^{1/2}$ and is directly proportional to K for values of $\lambda < 0.5$ and $\lambda \geq 0.5$ respectively, and furthermore for a given value of k' , it (the surface elevation) decreases as capillarity coefficient increases and λ approaches infinity. The value of the surface elevation depends on the radius of the cylinder which changes with k' if values of λ and Kk'^2 are zero and constant respectively, the surface elevation decreases when the radius decreases while k' increases. The surface elevation on the cylinder, however, tends to be a constant

approaching zero for large values of k' (typically 4 or larger) and $K \geq 1$.

In chapter 5, the horizontal oscillation of a cylinder in a fluid was studied, for both finite and infinite depth of the fluid, equal to the height of the cylinder. The surface elevation at large distances away from the cylinder $|\eta_{\infty}|$, is a monotonically decreasing function of K and λ . The surface elevation on the cylinder $|\eta|_{r=1}$, is a monotonically increasing function of λ .

In chapter 6, the scattering of waves by a fixed vertical cylinder was studied. At large distances from the cylinder and when k' is large (that is, for short waves relative to the radius of the cylinder), the surface elevation shows a considerable and rapid dependence in the direction of ϑ . When $\lambda = \infty$, the results are same as for the acoustic scattering problem. The averaged intensity of the scattered wave over all directions and at a large distance from the cylinder is an increasing function of k' for values of λ greater than unity, but for smaller values it is not monotonic. This intensity seems to have (from curves) a series of maxima and minima at intervals approximately equal to $\frac{\pi}{2}$, and is independent of K as $k' \rightarrow \infty$. There are minima in the values of the mean-squared elevations at large distances from the cylinder because there is energy dissipation when λ is neither zero nor infinity. At large distances the elevation increases with K , but approaches a limiting value independent of K as $\lambda \rightarrow \infty$. On the cylinder, however, the elevation decreases as K increases for finite values of λ . It is also possible to ascertain the effect of the edge condition on the force experienced by the cylinder in the limit as $K \rightarrow 0$. This force can be calculated by integrating the pressure over the surface of the cylinder and the pressure is given as the sum of p_1 and p_2 . The pressure p_1 provides the force when the edge condition is of orthogonal contact, as in the absence of capillarity. The contribution of p_2 to the force is proportional to p_1 . This part of the force is of

order of K/λ and $K^{1/2}$, when $\lambda > K^{1/2}$ and $\lambda < K^{1/2}$ respectively. Thus, for a given small value of K , the effect of the edge condition is maximum when $\lambda = 0$, that is, when the edge is fixed, and the force is then changed by an amount proportional to $K^{1/2}$. The average squared value of the elevation is a function of λ for K of 0.1 and 1, respectively. The averaged squared elevation is a monotonic decreasing function of k' for all values of λ , and the limiting values of it as $\lambda \rightarrow \infty$ are independent of K .

In chapter 7, the cylinders in shallow water are studied. Three cases with their limiting values have been considered; vertical, horizontal oscillation of the vertical cylinder in the fluid and the scattering of waves with the cylinder which is fixed. It was shown that the approach of finding the surface elevation in shallow water, using shallow water theory is less complicated than the approach used for determining the same thing by determining the elevation of the free surface when the fluid is of arbitrary depth and hence let the depth tend to zero.

In chapter 8, horizontal oscillation of plates in the fluid is studied; when the fluid is of finite depth equal to the length of the wavemaker or is of infinite depth and the plate oscillates horizontally at one end of the channel, or when the plate has finite length while the fluid has infinite depth, and source and sink approach is used, or when the plate oscillates horizontally in shallow water. The surface elevation at a large distance away from the plate has been calculated for a range of values of the parameters h , K and λ . These represent the length of the plate, the capillarity parameter and the ratio of contact line speed to the variation in the contact angle respectively. The bigger the capillarity coefficient, the bigger the surface tension and hence the smaller the amplitude of the waves. The elevation at large distances away from the plate, for h smaller than or equal to 2,

increases monotonically as K increases, which is the behaviour expected. For $h = 10$ or 5 , however, when K is large, that is 0.4 , this rule does not quite hold. Since elevation at large distances has a minimum as a function of λ , when $h \geq 1$, it approaches its limit at $\lambda = 10$ from below. When $h < 1$, the limit is approached from above. The transient motion is also introduced in this chapter, and it follows that the edge condition used here does not introduce any initial singularity in either the free-surface elevation or slope at the contact line. After the transients have disappeared, the wavemaker produces a wave whose elevation at large distance from the wavemaker has the form $R \exp\{i(x - \sigma t)\}$, where $|R|$ is the amplitude of the waves which decreases monotonically as K increases. Each curve has a shallow minimum as a function of λ and approaches its limiting value as $\lambda \rightarrow \infty$ from below. When λ is finite and non-zero, there is some energy dissipation at the wavemaker which may account for the dip in the amplitude of the generated wave. The surface elevation at the wavemaker is a monotonic increasing function of λ and also decreases as K increases. When the surface elevation in shallow water is determined and compared with the results of the small finite depth, there is some discrepancy when $K = 0.1$ and λ is small. This is not unexpected, since the shallow-water limit requires $h \ll K^{1/2}$ which is hardly satisfied when $h = K = 0.1$. When $\lambda \rightarrow \infty$ there is no generated wave because then the free surface can slip freely along the wavemaker. When the edge is forced to move with the wavemaker, that is, when $\lambda = 0$, the amplitude of the generated wave is independent of the depth of the fluid and has its maximum value as a function of λ . This maximum value, as a function of K , is always less than $1 / \sqrt{2}$ and approaches that value as $K \rightarrow \infty$. The smallest value of $|R|$ (the amplitude of the wave generated by the wavemaker) as a function of K is $\sqrt{2} - 1$ as $K \rightarrow \infty$. When both the plate and the fluid are of finite depth, the surface elevation on the plate is a monotonic increasing function of λ and monotonic decreasing function of the capillarity coefficient, K .

Among the problems which was not considered to be done and is possible to do are;

a) when the fluid is of infinite depth and the cylinder is of finite height,

b) cylinders of other cross sections, rather than circles.

REFERENCES

- Abramowitz, M. and Stegun, I.A. 1970 Handbook of Mathematical functions, Dover Publications, Inc., New York.
- Benjamin, T.B. and Scott, J.C. 1979 J. Fluid Mech. **92**. 241.
- Benjamin, T.B. and Ursell, F. 1954 Proc. R. Soc. Lond. **A225**. 505.
- Case, K.M. and Parkinson, W.C. 1957 J. Fluid Mech. **2**. 172.
- Crapper, G.D. 1984 Introduction to water waves, Ellis Horwood Ltd.
- Davis, S.H. 1980 J. Fluid Mech. **98**, 225.
- Evans, D.V. 1968 Proc. Camb. Phil. Soc. **64**, 795-810.
- Evans, D.V. 1981 Ann. Rev. Fluid Mech. **13**, 157.
- Faltas, M.S. 1988 Quart. Appl. Math. **3**, 489.
- Graham-Eagle, J. 1983 Math. Proc. Camb. Phil. Soc. **94**. 553.
- Graham-Eagle, J. 1984 Gravity-capillary waves with edge constraints. D. Phil thesis, University of Oxford.
- Havelock, T.H. 1929 Phil. Mag. **8**, 569-576.
- Hocking, L.M. 1987a J. Fluid Mech. **179**. 253.
- Hocking, L.M. 1987b Wave Motion **9**, 217.

- Hocking, L.M. 1987c J. Fluid Mech. **179**, 267.
- Hocking, L.M. 1988a J. Fluid Mech. **186**, 337.
- Hocking, L.M. 1988b Wave Motion **10**, 301.
- Hocking, L.M. and Mahdmina, D. 1991 J. Fluid Mech. **224**, 217.
- Hogan, S.J. 1979 J. Fluid Mech. **91**, 167.
- Jansons, K.M. 1985 J. Fluid Mech. **154**, 1.
- Joo, S.W., Schultz, W.W. and Messiter, A.F. 1990 J. Fluid Mech. **214**, 161.
- Kagemoto, H. and Yue, D.K.P. 1986 J. Fluid Mech. **166**, 189.
- Keulegan, G.H. 1959 J. Fluid Mech. **6**, 33.
- Lamb, H. 1932 Hydrodynamics 6th edn. Cambridge University Press.
- Mahdmina, D. and Hocking, L.M. 1990 Phys. Fluids A **2**, 202.
- McCamy, R.C. and Fuchs, R.A. 1954 Tech. Memo. 69, US Army Corps of Engineers.
- Mei, C.C. 1983 The Applied Dynamics of Ocean Surfaces, Wiley, New York.
- Morse, P.M. 1948 Vibration and Sound, 2nd. ed. McGraw-Hill, New York.
- Peregrine, D.H. 1972 Flow due to a vertical plate moving in a channel. Unpublished note.
- Rhodes-Robinson, P.F. 1971 Proc. Camb. Phil. Soc. **70**, 323-337.

Roberts, A.J. 1987 Q. J. Mech. Appl. Math. **40**, 129-158.

Sneddon, I.N. 1951, Fourier Transforms, McGraw - Hill, New York.

Sommerfeld, A. 1896 Math. Ann. **47**, 317.

Thompson, Sir W. 1871, Phil. Mah. (4) xlii, 374.

Ursell, F. 1949 Q. J. Mech. Appl. Maths **2**, 218.

Ursell, F. 1952 Proc. R. Soc. Lond. **A214**. 79.

Vanden - Broeck, J.M. 1984 J. Fluid Mech. **139**. 97.

Wehausen, J.V. 1971 Ann. Rev. Fluid Mech. **3**. 237.

Yeung, R.W. 1981 Appl. Ocean Res. **3**, 119.

Young, G.W. and Davis, S.H. 1987 J. Fluid Mech. **174**, 187.